

Spring 2012

Assessing the Validity of Brain Glucose Concentration Measurement Using Microdialysis

Damon Anthony Vinciguerra
dav006@bucknell.edu

Follow this and additional works at: https://digitalcommons.bucknell.edu/masters_theses



Part of the [Chemical Engineering Commons](#)

Recommended Citation

Vinciguerra, Damon Anthony, "Assessing the Validity of Brain Glucose Concentration Measurement Using Microdialysis" (2012).
Master's Theses. 67.
https://digitalcommons.bucknell.edu/masters_theses/67

This Masters Thesis is brought to you for free and open access by the Student Theses at Bucknell Digital Commons. It has been accepted for inclusion in Master's Theses by an authorized administrator of Bucknell Digital Commons. For more information, please contact dcadmin@bucknell.edu.

I, Damon Vinciguerra, do grant permission for my thesis to be copied.

ASSESSING THE VALIDITY OF BRAIN GLUCOSE CONCENTRATION MEASUREMENT USING MICRODIALYSIS

By

Damon Vinciguerra

A Thesis

Presented to Faculty of
Bucknell University

In Partial Fulfillment of the Requirements for the degree of
Master of Science in Chemical Engineering

Approved:

Advisor- Margot Vigeant

Department Chair- Jeffrey Csernica

Committee- Erin Jablonski

Committee- James Maneval

April 2, 2012

Acknowledgements

I would like to first and foremost thank Professor Vigeant for all of her help, support, and enthusiasm. I could not have done this without her active role in my work. I would also like to thank my thesis committee Professors Jablonski and Maneval for their expertise and honest feedback. I would like to extend a further thanks to Professor Maneval who put a lot of time into helping me understand and work out the Taylor Dispersion section; that section would literally not be in here if it was not for him.

I would also like to thank Ewan McNay for all of the data and for answering any brain questions we had. Thanks also to Jeremy Dreesse, Mike Harvey and the rest of ECST for helping me wrestle with COMSOL, which I was still doing even two weeks after my defense. Thanks to the Grad office for funding my 5th year.

And of course a thank you to Nancy for all the help she has given me throughout the years (I hope you enjoy retirement, you earned it). Thanks also to Lindsay (my beautiful girlfriend) for running the final grammar edit, turns out I'm really bad, with commas. And finally thanks to my parents for raising me well, putting me through college and encouraging me every step of the way to be the best I can.

I'm outta here!

Table of Contents

3.1	Motivation	6
3.2	Microdialysis	8
3.2.1	History.....	8
3.2.2	Microdialysis Probe Used in This Project	9
3.3	Brain Physiology	10
3.4	Transport of Glucose.....	12
3.4.1	Transport model for Probe-Brain System	12
3.4.2	Transport Model for Post-Probe Tubing.....	14
3.5	Prior Work.....	15
3.5.1	Calibrating <i>In Vitro</i>	16
3.5.2	Flow Rate Based Models	16
3.5.3	Numerical Models.....	17
4.1	Finite Element Method.....	18
4.2	System Parameters and Boundary Conditions	22
4.3	Construction of Model	24
4.4	Mesh.....	24
4.5	Data Processing	25
5.1	Model Image/Drawing	26
5.1.1	Three-Dimensional (Asymmetric) Model.....	26
5.1.2	Axisymmetric Model	28
5.1.3	Presentation of Results.....	31
5.2	Mesh.....	32
5.3	Sensitivity Analysis.....	33
5.4	Temperature	35
5.5	Zero Net Flux	39
5.5.1	Validity of Model.....	39

5.5.2	Implications of ZNF.....	41
5.5.3	Time to Steady-State.....	43
5.6	Reverse Microdialysis	46
6.1	Taylor Dispersion.....	50
6.2	Velocity Profile	52
6.3	Concentration Profile	53
6.4	Convolution.....	58
6.5	Signal.....	59
6.6	Effect of Taylor Dispersion on Concentration Results	61
7.1	Validity of model	67
7.2	Comparison to Literature	69
7.3	Implications	69
7.3.1	Parameter Sensitivity	70
7.3.3	Future Work.....	70
7.4	Taylor Dispersion.....	72

List of Tables

Table 1. Physical parameters for brain-probe system.	23
Table 2. Raw data for glucose concentration sensitivity analysis of perfusate volumetric flow rate (holding all other parameters constant).	34
Table 3. Time it takes system to reach steady-state after a 0.25 mM drop in brain concentration at several levels of precision.	45
Table 4. Time it takes system to reach steady-state from start up at several levels of precision ($c_{in}=0.25$ mM).....	45
Table 5. Physical parameters for exit tubing.	61

List of Figures

Figure 1. Schematic of brain-probe system.	2
Figure 2. Zero net flux. Probe is perfused at multiple analyte concentrations (C_{in} , x-axis) and plotted against net flux of analyte across the membrane ($C_{out}-C_{in}$, y-axis). If ZNF is valid, the points can be fit by a line and the x-intercept is brain concentration.	7
Figure 3. Basic geometry for four common microdialysis designs. (A) transversal, (B) loop, (C) side-by-side and (D) concentric.	9
Figure 4. CMA 12 microdialysis probe	10
Figure 5. Diffusion of glucose (arrows) from the capillaries (red lines) to the probe (central rectangle). The white circles represent neurons and the black circles represent glial cells.	11
Figure 6. Temperature profile down the length of a metal rod.	19
Figure 7. Temperature profile down the length of a metal rod discretized into two finite elements.	20
Figure 8. Geometry of asymmetric brain-probe system. (A) overall (B) cutaway. The probe has an overall diameter of $500\text{ }\mu\text{m}$ and height of 3 mm . The probe is then broken down into the following dimensions: (a) $50\text{ }\mu\text{m}$, (b) $75\text{ }\mu\text{m}$ (c) $85\text{ }\mu\text{m}$ (d) $40\text{ }\mu\text{m}$ (e) $50\text{ }\mu\text{m}$ (f) 3 mm (g) $25\text{ }\mu\text{m}$ (h) $50\text{ }\mu\text{m}$. The bore holes near the base of the probe have a diameter of $60\text{ }\mu\text{m}$	27
Figure 9. Geometry of the two-dimensional, axisymmetric brain-probe system. The probe has an overall radius of $250\text{ }\mu\text{m}$ and height of 3 mm . The probe is then broken down into the following dimensions: (a) $85\text{ }\mu\text{m}$, (b) $40\text{ }\mu\text{m}$ (c) $50\text{ }\mu\text{m}$ (d) 3 mm (e) $25\text{ }\mu\text{m}$ (f) $50\text{ }\mu\text{m}$. The perfusate enters the model at the base of the outlet flow region.	29
Figure 10. Typical velocity profile of perfusate throughout probe using parameters in Table 1. Units are in m/s.	31
Figure 11. Typical concentration gradient throughout brain-probe system using parameters from Table 1. Units are in mM.	31
Figure 12. Sensitivity analysis. The orange boxes represent 1000% of the system parameter while the blue boxes represent 10% of the system parameter. Outlet glucose concentrations are unaffected by order of magnitude shifts in perfusate density or viscosity. The system parameters are: volumetric flow rate (V), brain width (w_B), diffusion coefficient of glucose in the brain (D_B), the membrane (DM) and the perfusate (DP), perfusate density (ρ_{oP}), and perfusate viscosity (η_{oP}).	35

Figure 13. COMSOL model used to evaluate presence of a temperature gradient. Units are in μm	36
Figure 14. Temperature profile throughout lower 14 mm of microdialysis probe. Units are in K. The first (right) 3 mm are the active region of the membrane.	38
Figure 15. Temperature profile for the annulus of the probe. The first (left) 3 mm are the active region of the membrane. The head, and therefore heat source, ends at 5 mm. The remaining 9 mm is open to ambient conditions.....	39
Figure 16. Comparison of experimental data (♦) with model results (orange). No fitting parameter is used.....	40
Figure 17. ZNF plot (using model data) for the same specimen at a brain concentration of 1.25 mM (orange) and after a concentration drop of 0.25 mM to 1.00 mM (blue).	42
Figure 18. Transient response of brain-probe system to a 0.25 mM drop in brain concentration (black) with an inlet glucose concentration of: 1.0 mM (orange), 0.75 mM (blue), 0.5 mM (red), and 0.25 mM (green).	44
Figure 19. Model geometry for reverse microdialysis. The probe itself still has an overall radius of 250 μm and height of 3 mm. The probe is then broken down into the following dimensions: (a) 85 μm , (b) 40 μm (c) 50 μm (d) 150 μm (e) 3 mm (f) 25 μm (g) 150 μm . The perfusate enters the model at the base of the outlet flow region.	47
Figure 20. Brain glucose concentration 50 μm from the probe when probe is perfused with a 100 mM glucose spike for 5 seconds. Brain starts at 0.5 mM and perfusate is reduced to 1.25mM at 6 seconds. The inset is a close-up of the first 15 seconds of the simulation.	49
Figure 21. Example model of Taylor Dispersion, for a pulse.....	51
Figure 22. Diagram of system to be examined. Diagram is not to scale.	51
Figure 23. Example of Convolution. A) signal, B) smearing function, C) result.....	59
Figure 24. Plot of actual signal (blue) compared to Boltzmann sigmoidal (orange) fit ($r^2 = 0.9996$). The data is originally found in Figure 18; a 250 s signal with one minute of dilution due time to steady-state in the probe.	60
Figure 25. Convolution results for system. Times shown are the times it takes to get from 99% of the nominal concentration to 101% of the concentration during the brain process.....	62
Figure 26. Concentrations read by analytical instrument. The graph is broken up by the dashed lines into aliquots gathered for 5 minutes. The numbers at the top (represented on the graph by blue squares) are the concentrations the analytical instrument would read if placed at the outlet of the probe. The numbers at the bottom (represented on the graph by red squares) are the concentrations the instrument would read when placed at the end of 2 m of exit tubing.	63

Figure 27. Concentrations read by analytical instrument in the case where the Vi number is 1. The graph is broken up by the dashed lines into aliquots gathered for 5 minutes. The numbers at the top (represented on the graph by blue squares) are the concentrations the analytical instrument would read if placed at the outlet of the probe. The numbers at the bottom (represented on the graph by red squares) are the concentrations the instrument would read when placed at the end of 2 m of exit tubing. 66

List of Acronyms

aECF	Artificial Extracellular fluid
ECF	Extracellular fluid
FEM	Finite element method
GMRES	General minimal residual
SEM	Scanning electron microscope
ZNF	Zero-Net-Flux

List of Symbols

a_j	Coefficient array for a trial function
B	(mM) Minimum concentration of a signal (bottom)
c	(mol) Amount of component
c_A	(mM) Concentration of component
c_B, c_c	(mM) Nominal brain concentration
c_{in}	(mM) Probe inlet concentration
c_{0B}	(mM) Initial concentration in brain
c_{0P}	(mM) Initial concentration in perfusate and membrane
c_{out}	(mM) Probe outlet concentration
$[c]$	(mM) Lowest probable concentration that analytical instrument will see
D, D_{AB}, D_P	(m ² /s) Diffusion coefficient for glucose through the perfusate
$D_B, D_{e,B}$	(m ² /s) Diffusion coefficient for glucose through brain
D_{ECF}	(m ² /s) Diffusion coefficient for free diffusion of glucose through extracellular fluid
D_{lim}	(m ² /s) Limiting diffusion coefficient for a given system
D_M	(m ² /s) Diffusion coefficient for glucose through the membrane
η, μ	(Pa s) Dynamic viscosity
f	(N) Body forces
γ	Dimensionless time variable
∇	(1/m) Gradient
h	Variable for Fourier domain
h_a	(s) Time at which the signal concentration is halfway between its minimum and maximum
h_m	(m) Height of membrane
K	(m ² /s) Dispersion coefficient
L	(m) Length of exit tubing
L_p	(m) Length of active region of probe
λ	Tortuosity of brain
m	(mM/s) Slope of concentration signal at $t = h_a$
m_{min}	(g) Minimum mass limit for an analytical device
M_W	(g/mol) Molecular weight of the analyte
η	Dimensionless radial variable, r/R
N_{Az}	(m/s ²) Average molar flux
ω_i	Mass fraction of a component in the fluid
ϕ_e	Volume fraction of extracellular fluid in brain

p	(Pa) Pressure
R	(m) Inner radius of the tubing
Re	Reynolds number, $\rho Dv/\mu$
R_{err}	Residual between trial and test function
ρ, ρ_P	(kg/m ³) Perfusate density
δ	Shifted axial coordinate, $z - \langle v_z \rangle t$
T	(mM) Maximum concentration of a signal (top)
t	(s) Time
θ	Dimensionless concentration, $c_A/c_{A,ref}$
$\langle \theta \rangle$	Dimensionless concentration averaged cross-sectionally
θ'	Dimensionless deviation concentration
φ	Axial coordinate
\vec{v}	(m/s) Velocity vector
V	(m ³ /s) Volumetric flow rate
v_z	(m/s) Velocity along the z-axis
v_z'	(m/s) Deviation velocity
$\langle v_z \rangle$	(m/s) Average velocity at a cross section
$v_{z,max}$	(m/s) Maximum velocity along the z-axis
w_a	(m) Width of annulus region
w_b	(m) Brain thickness
w_k	Test function
w_m	(m) Membrane thickness
X_A	Molar fraction of glucose in the fluid
y_a	Trial function
y_o	Boundary condition

Abstract

Brain functions, such as learning, orchestrating locomotion, memory recall, and processing information, all require glucose as a source of energy. During these functions, the glucose concentration decreases as the glucose is being consumed by brain cells. By measuring this drop in concentration, it is possible to determine which parts of the brain are used during specific functions and consequently, how much energy the brain requires to complete the function. One way to measure *in vivo* brain glucose levels is with a microdialysis probe. The drawback of this analytical procedure, as with many steady-state fluid flow systems, is that the probe fluid will not reach equilibrium with the brain fluid. Therefore, brain concentration is inferred by taking samples at multiple inlet glucose concentrations and finding a point of convergence. The goal of this thesis is to create a three-dimensional, time-dependent, finite element representation of the brain-probe system in COMSOL 4.2 that describes the diffusion and convection of glucose. Once validated with experimental results, this model can then be used to test parameters that experiments cannot access. When simulations were run using published values for physical constants (i.e. diffusivities, density and viscosity), the resulting glucose model concentrations were within the error of the experimental data. This verifies that the model is an accurate representation of the physical system.

In addition to accurately describing the experimental brain-probe system, the model I created is able to show the validity of zero-net-flux for a given experiment. A useful discovery is that the slope of the zero-net-flux line is dependent on perfusate flow rate and diffusion coefficients, but it is independent of brain glucose concentrations. The model was simplified with the realization that the perfusate is at thermal equilibrium with the brain throughout the active region of the probe. This allowed for the assumption that all model parameters are temperature independent. The time to steady-state for the probe is approximately one minute. However, the signal degrades in the exit tubing due to Taylor dispersion, on the order of two minutes for two meters of tubing. Given an analytical instrument requiring a five μL aliquot, the smallest brain process measurable for this system is 13 minutes.

1 Introduction

Brain functions, such as learning, orchestrating locomotion, recalling memory, coping with stress and processing information, all require glucose as a source of energy.¹ During these functions, there are localized drops in glucose concentration in the areas of the brain being used. By measuring the drop in glucose concentration, it is possible to determine which parts of the brain are used during specific functions and consequently, how much energy the brain requires to complete that function. One way to measure glucose levels in the brain is with a microdialysis probe. Most recently, microdialysis has been used to study animal behavior, seizures, insulin-induced hypoglycemia, transplantations, neurotransmitters and pharmacology.^{2,3}

A microdialysis probe is essentially a needle with a semipermeable membrane covering the tip. When the probe is inserted into the brain, a fluid almost identical to brain fluid, known as the perfusate, is perfused through the probe. The perfusate enters the probe at the top and flows down the center. It then passes through two small bore holes near the base of the probe into the outer annulus, which is the active region. The fluid also exits the probe at the top. The only difference between the brain fluid and the perfusate is the concentration of glucose. This creates a concentration gradient across the membrane, and glucose diffuses from the fluid of higher concentration to the fluid of

lower concentration to reduce the gradient. Figure 1 shows the case in which the concentration of glucose in the perfusate is less than that of the brain.

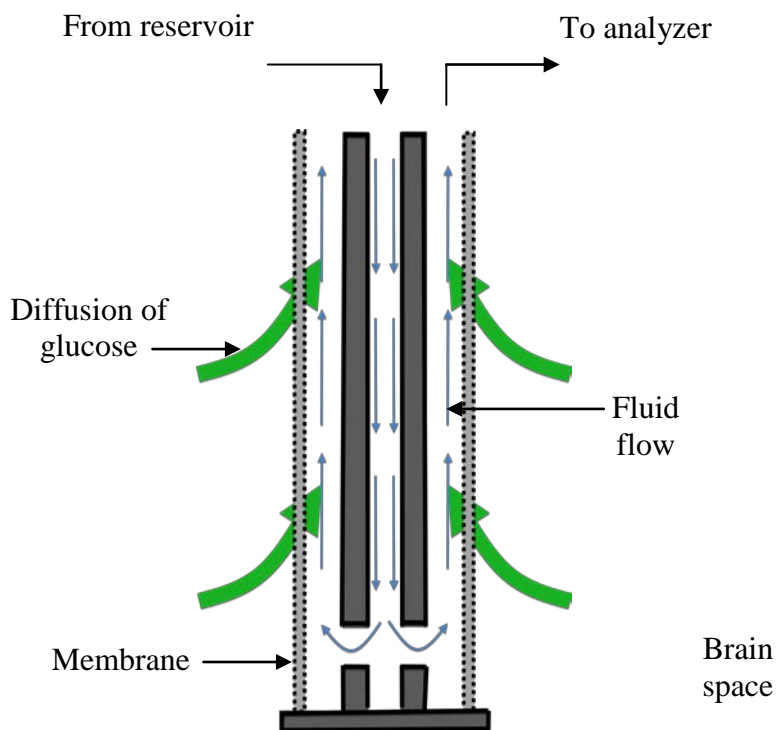


Figure 1. Schematic of brain-probe system.

The drawback of this analytical procedure, as with many steady-state fluid flow systems, is that the perfusate will exit the probe before it can reach chemical equilibrium with the brain fluid. Therefore, brain concentration is inferred by taking samples at multiple inlet glucose concentrations and finding a point of convergence. This is called the Zero-Net-Flux (ZNF) method because the brain concentration is calculated by realizing there is no net flux of glucose when the perfusate is at equilibrium with the brain fluid.⁴

A two-dimensional, axisymmetric finite element representation of a microdialysis brain-probe system was created in COMSOL 4.2. This model accurately describes the diffusion and convection of glucose in the brain-probe system. The overall goal was to use this model to validate assumptions made in the analysis of experimental results.⁵

2 Hypothesis

In the proposed work, I tested the following two hypotheses:

Current assumptions made in analyzing microdialysis data using ZNF are accurate.

Application of the ZNF method rests on several assumptions that are not experimentally assessable *in vivo*. I believe that by creating a three-dimensional finite element model of the brain-probe system I can validate all assumptions made using ZNF. I also believe that the wait time between microdialysis trails is less than 15 minutes, which is the current standard.

With a working model I can test other experimental areas previously inaccessible such as temperature dependence, parameter sensitivity and reverse microdialysis.

Dilution of signal concentration in the outlet perfusate tubing is the limiting factor in temporal resolution.

The microdialysis probe is only between two to four millimeters in length, but is followed by up to two meters of tubing before samples are collected. It is possible that Taylor dispersion significantly reduces the difference between nominal brain concentration and the concentration during an observed brain process. This is another area that is accessible by model but not *in vivo*.

3 Background

In order to understand how to create an accurate model, it is necessary to have an understanding of dialysis, mass transport and basic brain physiology. In the following sections, some of the basics of these concepts are described.

3.1 Motivation

One of the major fields of study in neurology today is the connection between glucose concentration in the brain and brain functions, such as learning and memorization.⁴ The problem that neurologists face is that brain glucose concentration cannot be measured directly. In the search for an indirect form of brain measurements, the method of microdialysis was developed. ZNF is one method used for calibrating output measurements to actual brain concentrations.⁴

When using ZNF, neurologists perfuse a microdialysis probe with a range of different glucose concentrations and record the outlet concentration. When the net change in glucose concentration through the probe is plotted against inlet concentration, a linear trend is observed. The point at which the line of best fit crosses the x-axis is the concentration of glucose in the brain, because it is at this point that there is not flux

across the probe, i.e. no concentration gradient. This concept is shown graphically in Figure 2.

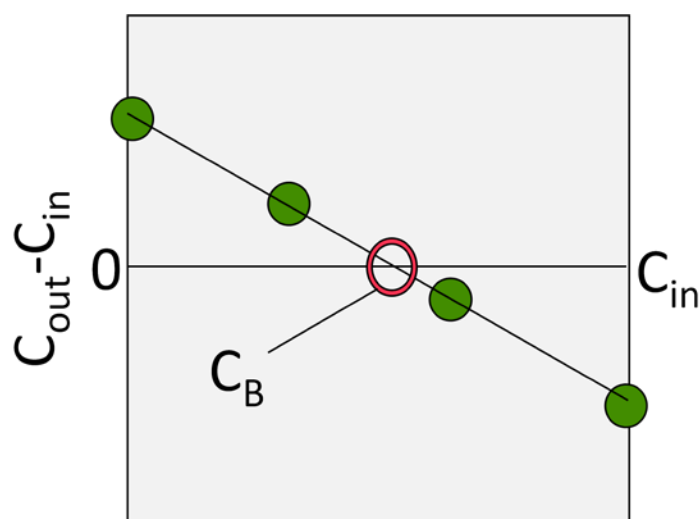


Figure 2. Zero net flux. Probe is perfused at multiple analyte concentrations (C_{in} , x-axis) and plotted against net flux of analyte across the membrane ($C_{out} - C_{in}$, y-axis). If ZNF is valid, the points can be fit by a line and the x-intercept is brain concentration.

In theory, ZNF is a reliable and efficient means of measuring brain concentration. However, the ZNF method is based on certain important transport assumptions which cannot be demonstrated experimentally due to the complexity of a living system.

By modeling the brain-probe system using finite element analysis, it will be possible to define all of the system's unknown parameters. If the model accurately predicts experimental results, then it may be inferred that ZNF assumptions are reasonable and measurements gained from ZNF readings can be assumed to be accurate.

3.2 Microdialysis

3.2.1 History

Microdialysis was first developed in the 1960s to characterize interstitial water in dog brains. One of the earliest units was a dialysis sac, in which a membrane was placed in the brain and allowed to sit for an extended period of time. It was assumed that by the time the sac was removed, the contents had come to equilibrium with the extracellular fluid (ECF) in the brain.⁶ In 1972, Delgado and Defeudis first reported the use of a probe and technique that caused significantly less tissue disruption than in previous studies.⁷ The next breakthrough in microdialysis came in 1974 when Ungerstedt and Pycock reported using “hollow fibers” to infer ECF concentrations. The hollow fibers were tubular semipermeable membranes measuring 200-300 μm in diameter.⁸ Today, the most widely-used probe is a needle with membrane covering only the tip of the unit.⁹

Within the category of membrane needle microdialysis, there are four main probe configurations (Figure 3).¹⁰ In a transversal probe, the inlet and outlet streams are on opposite sides of the membrane. This geometry is used mostly for measuring superficial brain structures. Loop, side-by-side, and concentric geometries are in a category of microdialysis called vertical probes. Vertical probes are most commonly used in research today; selecting one over the other comes down to preference.¹¹

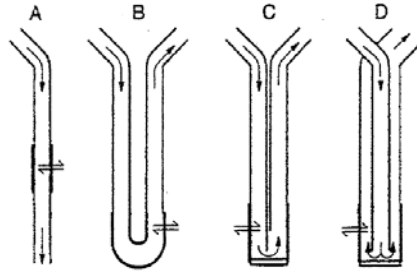


Figure 3. Basic geometry for four common microdialysis designs. (A) transversal, (B) loop, (C) side-by-side and (D) concentric.¹⁰

The majority of microdialysis probes are made of stainless steel or fused silica tubing with a 1 to 4 mm length of semipermeable membrane at the tip. Probes can either be implanted permanently or inserted temporarily into tissue or bone using a permanent guide cannula.¹⁰

3.2.2 Microdialysis Probe Used in This Project

In this project, a CMA 12 microdialysis probe (Figure 4) was modeled. This specific probe used has a concentric geometry with a stainless steel casing and a 3 mm length of 20 kDa cutoff polycarbonate membrane at the tip.⁵ While CMA reports membrane thickness to be 25 μm , many experiments have reported swelling of the membrane *in situ*. Rosenbloom *et al.* reported a membrane thickness of 40 μm using a scanning electron microscope (SEM).¹²

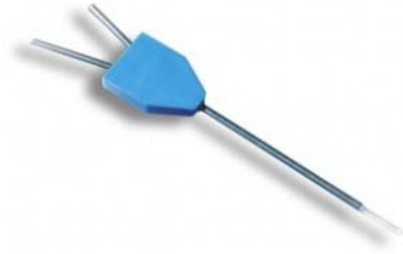


Figure 4. CMA 12 microdialysis probe¹³

3.3 Brain Physiology

While it is not within the scope of this thesis to fully explore the physiology of the brain, it is imperative to have a general grasp of related topics such as brain structure and metabolic supply.¹⁴

Brain cells produce energy necessary for functioning by metabolizing glucose found in the ECF; sufficient oxygen is needed for cells to utilize their most efficient metabolic pathway.¹⁵ Glucose is carried from the stomach to the brain in the blood stream and is transported to brain tissue via capillaries. Figure 5 is a simple diagram of the brain-probe system in which the center rectangle is the probe.² The brain itself is composed mostly of neurons (white circles) and glial cells (black circles).¹⁶ Glial cells provide structure for neurons and help regulate molecules available to neurons in the ECF.¹⁷

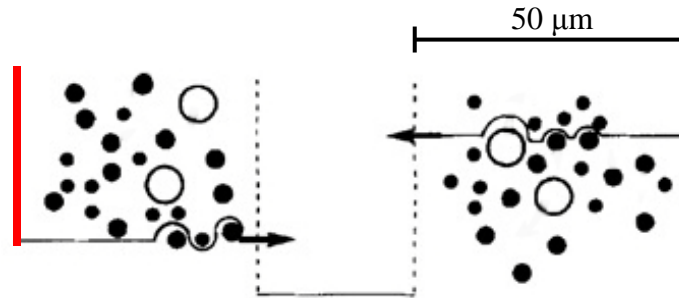


Figure 5. Diffusion of glucose (arrows) from the capillaries (red lines) to the probe (central rectangle). The white circles represent neurons and the black circles represent glial cells.²

The transport of glucose (arrows) from the capillaries (red lines) to the probe is impeded by the brain cells. As can be seen in Figure 5, glucose has to physically travel around the cells, which increases the length of the diffusion pathway. However, these cells cannot simply be considered as physical diffusion inhibitors, as neuron and glial cells are constantly consuming glucose. The amount of glucose consumed by the cells is dependent on the current neurological activity.²

Capillaries, on average, are equally spaced and evenly distributed throughout the brain. Due to the relative rates of oxygen diffusion and consumption in the brain, oxygen is almost entirely consumed by the time it reaches any distance 25 μm from the capillary. Because no cell could survive outside of 25 μm from a capillary, capillaries are always found within 50 μm of each other in healthy or normal brain tissue.¹⁴

3.4 Transport of Glucose

3.4.1 Transport model for Probe-Brain System

The transport of glucose in the brain-probe system is based on two governing differential equations: Navier-Stokes (Equation 1) and the conservation of mass (Equation 4).

$$\rho \left(\frac{\partial \vec{v}}{\partial t} + \vec{v} \cdot \nabla \vec{v} \right) = -\nabla p + \mu \nabla^2 \vec{v} + f \quad (1)$$

Navier-Stokes models the motion of a fluid and works best with laminar flow ($Re < 2000$). The first term represents the unsteady-state acceleration of the flow while the second term is convective acceleration. The third and fourth terms represent the pressure gradient and stress, respectively. The fifth encompasses external forces such as gravity and electromagnetism; these forces can be assumed to be negligible in the small brain-probe system. Navier-Stokes is used to model only the flow of the perfusate, as there is no bulk flow in the membrane and brain.

For the given microdialysis unit, the Reynolds number

$$Re = \frac{\rho w_a v}{\mu} \quad (2)$$

is on the order of 0.02, which qualifies it for Stoke's (or creeping) flow ($Re \ll 1$).¹⁸ In creep flow, the inertial terms are negligible, which allows for a much simpler differential equation

$$\rho \frac{d\vec{v}}{dt} = -\nabla p + \mu \nabla^2 \vec{v}. \quad (3)$$

Equation 3 will be used to describe the flow of perfusate through the microdialysis probe.¹⁸

The conservation of mass equation

$$\frac{dc}{dt} + \nabla \cdot (D\nabla c) = -\vec{v} \cdot \nabla c \quad (4)$$

describes the transport of material by both convection and diffusion. It will be used to simulate the diffusion of glucose from the brain, through the membrane, and into the perfusate, as well as the convection of the glucose within the perfusate. The first term represents the unsteady-state change in concentration. The second term represents the diffusion due to a concentration gradient, while the third term represents the transport due to convection.

Equation 4 is only accurate if Fickian diffusion applies to this system. Fickian diffusion assumes that diffusion is independent of the magnitude of the concentration and that there is no bulk flow of material in the brain and through the membrane. At the dilute concentrations used in this thesis, diffusion is dependent solely on the concentration gradient, not the magnitude of the concentration. Bulk flow through the pores of the membrane could occur for two reasons, extremely high concentration or pressure gradients. If the concentration gradient is too large, and diffusion therefore too fast, the glucose can actually pull water along with it through the membrane and create bulk flow. The concentration gradients in this thesis are not large enough to induce bulk flow. If the aECF is not identical to the brain composition, other ions may diffuse across

the membrane as well. However, as long as these gradients are kept small, the diffusion of glucose will be independent from the diffusion of other components.

If the pressure gradient across the membrane is too large water will be forced through the probe. The minimum pressure in the probe needed to induce flow is 6.2 kPa; this is based on the radius and length of exit tubing connecting the probe and the analytical instrument.¹⁸ Normal blood pressure in a rat brain is 17.2 kPa.¹⁹ This difference is not large enough to induce bulk flow of water.

The biggest, most consequential assumption made in this model is that the system can be described using continuum mechanics. Continuum mechanics is the analysis of materials modeled as a continuous material rather than as discrete particles. It is the assumption that this model is describing the system on a scale large enough to consider behaviors of and interactions between individual molecules negligible compared to the behavior of the material as a whole. Equations 1-4 are only valid in the field of continuum mechanics. Above, the brain is described as a non-homogenous, non-continuous material. Later this description will be adjusted in order to approximate the brain as a continuous material for use in modeling.

Boundary and initial conditions for Equations 3 and 4 are defined in Appendix A.

3.4.2 Transport Model for Post-Probe Tubing

In addition to modeling the transport of glucose from the brain to the perfusate, the transport of glucose from the probe to the detector was also modeled. When

conducting *in vivo* microdialysis, it is imperative to create an environment free from stress for the rat specimens. To achieve this, the rats need to be able to move around freely within an area, unhampered by testing equipment. For this to happen, the tubing that delivers the perfusate from the probe to the glucose detector must be of considerable length. With glucose traveling in creep flow and tubing of up to two meters in length, perfusate can take as long as an hour to reach the detector.²⁰ As perfusate flows down the tubing, glucose is diffusing both radially and linearly. If the tubing is too long or the flow rate is too small, signal strength will degrade due to Taylor dispersion. If too much dispersion occurs, the signal will be indistinguishable from nominal concentration and will therefore be undetectable. The minimum signal duration (i.e. time of thought) that can be detected by an analytical instrument will therefore be determined.

3.5 Prior Work

Due to the many uses microdialysis has in a variety of fields, it has been studied and approached both theoretically and numerically in many previous works. While this model draws on previous work, the work shown here adds further insight and development to the field of microdialysis.²¹

Lindefors and Amberg crafted a massively complex and mechanistic function that is based on *in vitro* data and detailed system parameters.²² The function is theoretically sound, but is too detailed for repeated use. A simple and quick model based on first principles and easily determined *in vivo* parameters was able to be created.

3.5.1 Calibrating *In Vitro*

The first attempts at characterizing outlet concentrations were geared towards correlating a calibration between *in vitro* and *in vivo* measurements. This approach assumed that the transport of glucose from a non-stirred beaker solution to the probe would be the same as the transport from the brain to the probe, or at least that a simple relationship existed between them.²³ Zetterström *et al.* quickly realized that the brain is significantly more complex than a solution in a beaker and that *in vivo* measurements could not be inferred from *in vitro* data.

Benveniste attempted to amend Zetterström's equations to fit empirical data.² However, Benveniste was only able to accurately represent a few substances, mainly ions. When Benveniste tried to account for molecules involved in uptake mechanisms, errors in the calculations increased. For this reason, this model describes an *in vivo* system. The brain is simplified to facilitate continuum mechanics; the model still reflects the real system close enough to produce accurate results. While Benveniste and Zetterström modeled probes of the loop design (Figure 3.B), this model describes a probe with a concentric geometry (Figure 3.D).

3.5.2 Flow Rate Based Models

An alternative approach to zero-net-flux is zero flow. In 1985, Jacobson *et al.* proposed a method based on the principal of zero flow dialysis.²⁴ This technique

involves a membrane sac filled with aECF (artificial extracellular fluid) being placed in the brain for an extended period of time, allowing the aECF to reach equilibrium with the brain.⁶ Jacobson used needle probes and recorded outlet concentrations at a variety of flow rates. He then extrapolated this data back to a flow rate of zero. The problem with this approach is the concentration has an exponential term, and therefore asymptotic, profile as the flow rate approaches zero. The ZNF system and this model are based on well-defined, linear interpolation as opposed to sensitive, asymptotic extrapolation. Jacobson's model is based on the geometry of a simple annulus.

Bungay *et al.* furthered Jacobson's work and, in doing so, developed the first model to incorporate active biological processes.²⁵ Unfortunately, Bungay's model is too detailed and requires knowledge of parameters that cannot be determined experimentally. The model is therefore based on assumptions and estimated parameters.

3.5.3 Numerical Models

As computing power increases and becomes more accessible, researchers are turning to numerical modeling to describe the microdialysis systems. Norton *et al.* and Wang *et al.* both used a modeling program called COMSOL to describe the probe.^{26,27} However, both models only described the probe *in vitro*. This paper will present the first numerical model of an *in vivo* microdialysis system. As with Jacobson, Norton's model is designed around an annular geometry, while Wang described a side-by-side probe (Figure 3.C).

4 Materials and Methods

4.1 Finite Element Method

The finite element method (FEM) was born out of the need for accurate and efficient approximate solutions. First popularized in the 1960s, FEM was used to study stresses in complex aircraft structures.²⁸ Since then, the simplicity and effectiveness of FEM has allowed it to spread to every aspect of continuum mechanics.

In a continuum mechanics problem, such as diffusion of glucose through a membrane, the domain is made up of an infinite number of values, and therefore the problem has an infinite number of unknowns.²⁸ FEM is essentially the breaking up of a single complex differential system into many simpler problems.²⁹ The overall solution domain is segmented into smaller subdomains called finite elements.³⁰ Each element is assumed to be solvable using a simple function that can accurately approximate the real system. These approximate solutions are called trial functions.³¹ Each element has a number of nodes on their boundary which act as local boundary conditions. By connecting a finite number of elements, defined by nodes and internally approximated by trial functions, a highly complex system can be easily and efficiently approximated with reasonable accuracy.²⁸

A good way to visualize FEM is by considering a simplified system, such as the linear transfer of heat through a metal rod.³⁰ The temperature profile in Figure 6 could easily be modeled by a third order function, but for the sake of the example, assume no exact solution can be found. The first step of FEM is to break the domain into subdomains and create what is called a mesh, as in Figure 7. In this example, the rod is divided into two subdomains, with a boundary across the middle of the rod. As can be seen, each element can now be approximated by a parabolic equation ($T=a_1+a_2x+a_3x^2$). If there are two parabolic equations, with two unknown constants each, there are four unknowns. In FEM, these four constants are iterated until boundary conditions are met and the approximation of the temperature profile is within a set tolerance.

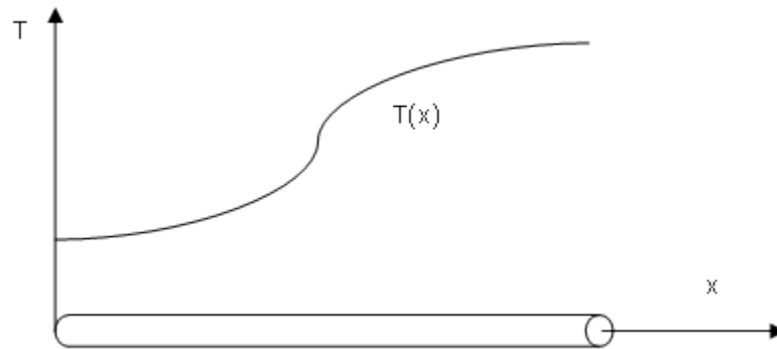


Figure 6. Temperature profile down the length of a metal rod.

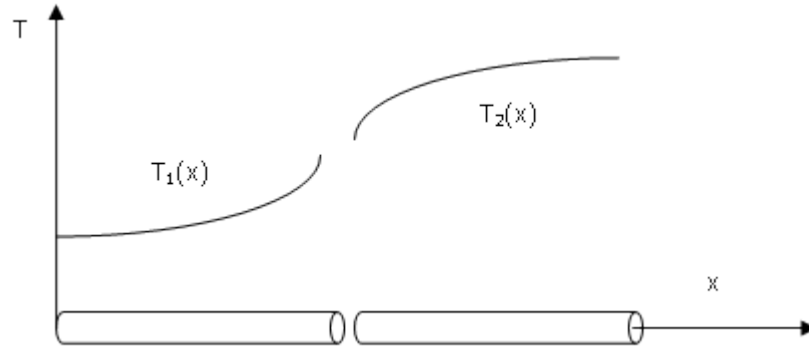


Figure 7. Temperature profile down the length of a metal rod discretized into two finite elements.

The first major decision that needs to be made is selecting the mesh, or deciding how to break up the system and is covered below. Once an appropriate mesh has been selected, a trial function has to be selected. Trial functions are usually polynomials because they are easy to integrate and differentiate.²⁸ The order of the polynomial is dependent on the number of parameters being solved for and the number of nodes on an element.

$$y_a = y_o(x) + \sum_{j=1}^N a_j x^{2(j-1)}(1 - x^2) \quad (5)$$

is a commonly used trial function, especially for profiles of symmetric shape.³¹

Next, the governing differential equation is set equal to zero and inserted into Equation 5. If Equation 5 is the analytical solution to the problem, then inserting it into the governing differential equation will produce a value of zero. However, if Equation 5 is only an approximate solution, which is usually the case, then a value will be produced that is dependent on x . This value is called the residual and is represented by R_{err} .²⁸

From this point onward, the coefficients a_j would be continually adjusted until the residual is within an allowable tolerance. However, in the residual's current state, the value is dependent on the location in the system it is being sampled; therefore, comparison between residuals would be difficult. It is therefore necessary to average the residual function. One way to carry this out is to take the inner product of the trial function with another function, called the test function.²⁸ The selection of the test function is as important as selecting the trial function as it dictates which form of the trial function is most accurate. Many methods have been derived to select appropriate test functions, the most notable being collocation, subdomain, least squares, moment, and Galerkin.²⁸

As the Galerkin method is the most commonly used method in fluid mechanics and diffusion problems, it will be the focus of this background. In this method, the test function is selected from the same family of functions as the trial function. In the case of Equation 5, a reasonable test function would be

$$w_k = (1 - x^2). \quad (6)$$

To find the inner product of two functions, they are simply multiplied and then integrated over the domain, as in

$$(R_{err}, w_k) = \int_{-x}^{+x} R w_k dx. \quad (7)$$

Now sets of coefficients can be easily compared using the residual and the trial function can be optimized. Once an accurate trial function has been established for each finite element, the elements can be put back together to form a cohesive single solution domain. For efficiency purposes, COMSOL will be used to do the computing.

4.2 System Parameters and Boundary Conditions

In reality, the path of diffusion of glucose from a blood vessel to a probe is impeded both physically and chemically by brain cells. Not all of the glucose that leaves the blood vessel makes it to the probe; some of the glucose is absorbed by brain cells. The glucose that does make it to the probe does not diffuse there in a straight line; it has to move around the brain cells (Figure 5). The diffusion path is thus influenced by tortuosity (λ). The more tortuous the paths in a material are, the longer a molecule's path is to travel from one point to another. To accurately approximate the brain as a continuous material, all of these factors can be combined with the constant of free diffusion of glucose in ECF (D_{ECF}) to produce an effective diffusion coefficient ($D_{e,B}$)

$$D_{e,B} = \frac{D_{ECF}\phi_e}{\lambda^2} \quad (8)$$

which describes the relationship between effective diffusion, free diffusion, void fraction (ϕ_e) and tortuosity.¹⁸

Equation 8 also describes the effective diffusivity in the membrane. However, because knowing the effective diffusivity is imperative for most membrane experiments, this constant has been found experimentally for a number of membranes and molecules,

including the diffusion of glucose through pores in polycarbonate. This experimental value will be used in preference to a calculated value.³²

All parameters use in this simulation are summarized in Table 1. Note that the “outer boundary” concentration is being modeled at the outer wall of a capillary. This concentration is the model’s “true” ECF glucose concentration, the concentration that ZNF is used to determine.

Table 1. Physical parameters for brain-probe system.

Variable	Expression	Value	Units	Ref
V	Volumetric flow rate of perfusate	1.67×10^{-11}	m^3/s	⁵
c_{0P}	Initial glucose concentration in perfusate/membrane	0.50	mol/m^3	⁵
c_{0B}	Initial glucose concentration in brain	1.25	mol/m^3	⁵
h_m	Height of Membrane	3.00×10^{-3}	m	⁵
c_c	Outer capillary (brain) glucose concentration	1.25	mol/m^3	⁵
w_m	Membrane thickness	4.00×10^{-5}	m	¹²
w_b	Width of brain section	5.00×10^{-5}	m	¹⁵
ρ_{0P}	Density of Perfusate	9.90×10^2	kg/m^3	³³
η_{0P}	Dynamic Viscosity of Perfusate	7.28×10^{-4}	Pa s	³³
D_P	Diffusion Coefficient of glucose in Perfusate	8.30×10^{-10}	m^2/s	³³
D_B	Diffusion Coefficient of glucose in Brain	1.16×10^{-10}	m^2/s	^{2,35}
D_M	Diffusion Coefficient of glucose in Membrane	7.62×10^{-11}	m^2/s	³²

Values for volumetric flow rate, initial perfusate/membrane and brain concentrations, membrane length, and outer boundary concentrations are the specifications and results of McNay’s research.⁵ This is the experiment used to provide a

dataset to confirm the accuracy of the simulation. The width of the membrane and brain are justified in the Background. Density, viscosity and perfusate diffusivity are calculated using the PRSV (the Stryjek-Vera modification of the Peng-Robinson equation of state) model at 38.2°C.^{33,34} The value for brain diffusivity is calculated using Equation 8 with 0.35 as the volume fraction of ECF in brain and 1.6 as the tortuosity factor.^{35,2}

4.3 Construction of Model

COMSOL 4.2, a FEM program, will be the main program used to model the brain-probe system. COMSOL stores linear equations in the form $A\mathbf{x}=\mathbf{b}$ and then uses a method called generalized minimal residual (GMRES) to solve the equations. GMRES is an iterative method which follows the general method outlined above.³⁶

4.4 Mesh

One of the most important decisions in using FEM software is selecting the mesh size. The mesh is what defines where calculations are conducted and how many degrees of freedom there will be. If a coarse mesh is selected, the solution will likely not be accurate because calculations are only taken at a few points. However, if the mesh is too fine, it will take too long for the program to compute results, and no solution will be reached. Another decision that has to be made is mesh shape. In a three-dimensional model, the mesh can take any form; however, the most common shapes are either

quadrilaterals or tetrahedra. Quadrilaterals are better suited for boxy geometries while tetrahedra are better suited for round geometries, such as spheres and cylinders. Similarly, the most common mesh shapes in two-dimensional modeling are quadrilaterals and triangles.

Therefore, once a mesh shape has been selected, a balance must be struck. The mesh must be fine enough that the solution is accurate, yet coarse enough that the computer can provide a solution in a timely manner.

4.5 Data Processing

Because most laboratories using microdialysis only record outlet glucose concentration, this is the only piece of data needed to be tracked during simulation to verify ZNF. This is accomplished by integrating the concentration of glucose over the surface of the outlet channel, generated directly by COMSOL.

5 Results

5.1 Model Image/Drawing

5.1.1 Three-Dimensional (Asymmetric) Model

A three-dimensional model of the brain-probe system, as described in the Background, was constructed using COMSOL 4.2. Three dimensions were used as a starting point because in addition to radial and axial transport, there is angular diffusion caused by the two bore holes connecting the inner cannula to the outer annulus. None of these three directional flows seemed negligible.

Figure 8 shows the overall (A) and cutaway (B) geometry of the system being modeled. The cutaway model shows the inlet perfusate channel (a), the outlet perfusate channel (c), the membrane (d), and the brain layer (e). The gap that separates the inlet and outlet channels (b), as well as the gap between the base of the flow regime and the bottom brain layer (g), are stainless steel and have no interaction with the system, so they are not modeled (i.e. an empty space). In the cutaway model, the two tubes that connect the inlet and outlet perfusate channels can be seen, as well as the layer of brain beneath the probe (h).

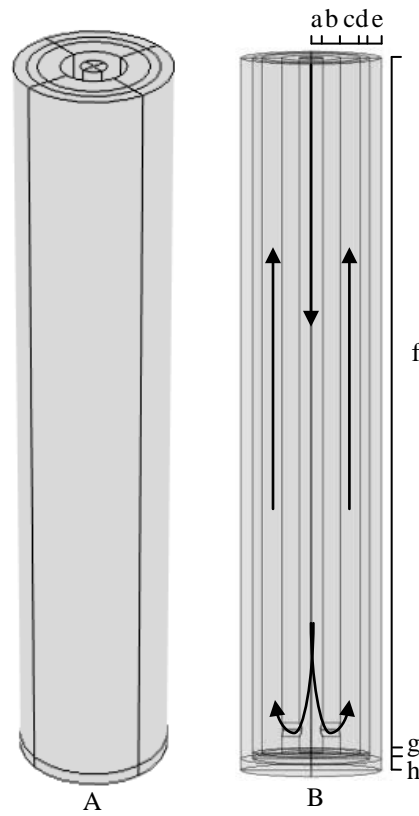


Figure 8. Geometry of asymmetric brain-probe system. (A) overall (B) cutaway. The probe has an overall diameter of 500 μm and height of 3 mm. The probe is then broken down into the following dimensions: (a) 50 μm , (b) 75 μm (c) 85 μm (d) 40 μm (e) 50 μm (f) 3 mm (g) 25 μm (h) 50 μm . The bore holes near the base of the probe have a diameter of 60 μm .

After working with the asymmetric model for some time, discrepancies were found that questioned the overall validity of the model. The largest problem is the fact

that the cross-sectional area COMSOL was calculating for inlet and outlet boundaries is incorrect. The areas calculated differ significantly from a simple hand calculation (πr^2 for the inlet and $\pi(r_o^2 - r_i^2)$ for the outlet) based on the same radii.

Further unsettling is the fact that the accuracy of this error does not improve with a finer mesh. Apparently, dimensions are not calculated using the mesh; meaning the accuracy of dimensions is therefore not dependent on how well the mesh fits the geometry. The dimensions are therefore calculated incorrectly by COMSOL at some fundamental computing level. In fact, even when a simple two-dimensional ring is examined in a separate model, the calculated area is different from both the asymmetric model and a hand calculation. This problem led me to question the accuracy of all other geometry based results, which includes outlet glucose concentration.

In addition to inaccurate geometric dimensions, the asymmetric model is inconvenient to work with. With almost 520,000 elements in the mesh, it takes nearly 10 minutes to solve it at steady-state and over 7 hours to solve it with the transient model. Due to the lack of confidence in the asymmetric model and the inconvenience of running it, a more robust means for describing and modeling the brain-probe system was sought after.

5.1.2 Axisymmetric Model

Initially, the three-dimensional asymmetric model was chosen over a radially symmetric one because it was believed that the two bore holes at the base of the probe

would cause an irregularity in the flow pattern of the active region, leading to a non-negligible amount of angular diffusion. However, the use of an axisymmetric model (Figure 9) was investigated after the geometric errors were found in the asymmetric model. By assuming that there is no significant angular diffusion, the two bore holes, and therefore the entire inlet channel, can be eliminated. To simplify things further, the inlet for the perfusate was chosen to be the bottom boundary of the active region. With these changes, the brain-probe system is still primarily the same; there is the outlet perfusate channel (a), membrane (b) and brain layer (c). There is also still a stainless steel gap (e) between the active region of the probe (d) and the bottom layer of the brain (f). All symmetric models, unless otherwise stated, have identical dimensions to the overall model and will therefore not be included in every figure.

NOTE: All further figures of probes have been rotated 90° counterclockwise; the top of the probe is to the left.

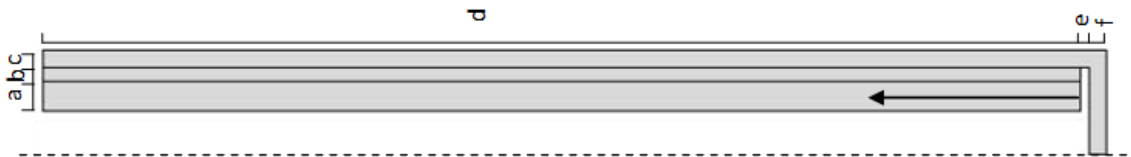


Figure 9. Geometry of the two-dimensional, axisymmetric brain-probe system. The probe has an overall radius of 250 μm and height of 3 mm. The probe is then broken down into the following dimensions: (a) 85 μm , (b) 40 μm (c) 50 μm (d) 3 mm (e) 25 μm (f) 50 μm . The perfusate enters the model at the base of the outlet flow region.

Testing of the validity of the new symmetric model was based on mass conservation and fluid flow. A mass balance was conducted on each individual domain and on the system as a whole. Overall, the system gains only 4.2 pmol/min of mass, which is less than half of the mass gain in the asymmetric model. The full mass balance can be found in Appendix B. The velocity profile in the perfusate region of the symmetric model was also examined to make sure that the skewed parabolic shape typical to annuli was conserved.

These factors show that, at the same parameters, angular diffusion at the base of the probe is negligible and that a simplified, symmetric model can produce accurate results. In addition to a higher level of confidence, the symmetric model is easy to work with. With only 8,000 elements in the mesh, the model can be solved at steady-state in less than 10 seconds.

Detailed instructions for constructing the two-dimensional steady-state brain-probe system in COMSOL can be found in Appendix C. While Appendix C is written for people with no COMSOL experience, Appendix D holds a less thorough set of instructions for people familiar with COMSOL. Appendix E has instructions for creating a probe geometry that is completely adaptable to any size probe with similar design to the CMA 12.

5.1.3 Presentation of Results

COMSOL is able to output results in a variety of different ways. The two that will be used in this project are two-dimensional renderings and line averages. Figures 10 and 11 are two-dimensional cutaways of results for the velocity and concentration profile, respectively, using the parameters in Table 1. Note that after solving the two-dimensional model, COMSOL wraps the results around the central axis to produce a three-dimensional geometry with no angular diffusion.

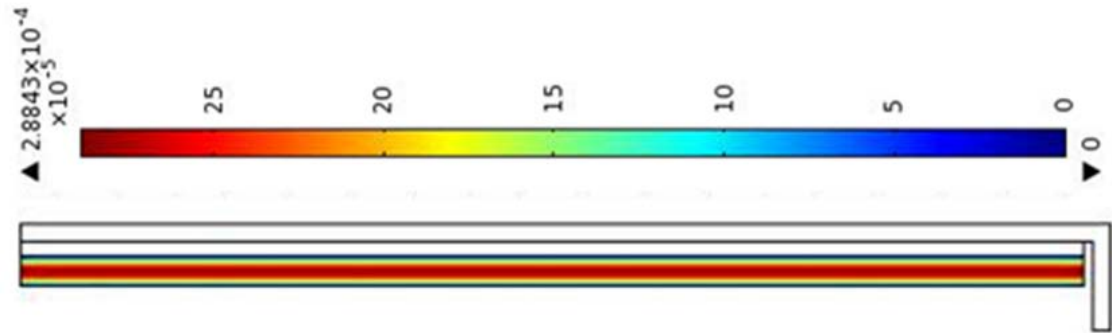


Figure 10. Typical velocity profile of perfusate throughout probe using parameters in Table 1. Units are in m/s.

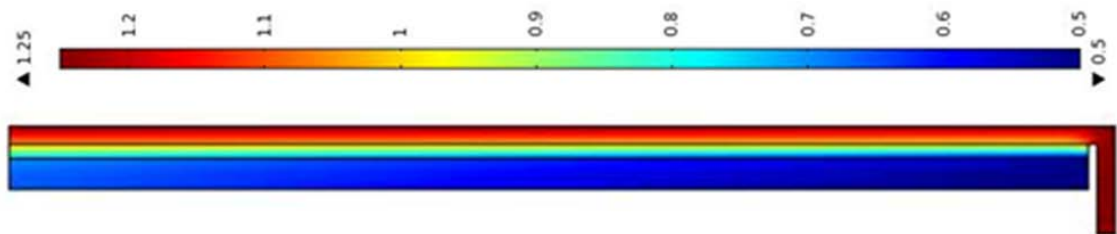


Figure 11. Typical concentration gradient throughout brain-probe system using parameters from Table 1. Units are in mM.

Another useful post-processing computation COMSOL can be used to conduct is a line average. By integrating over the outlet perfusate boundary and dividing by the length of the boundary, COMSOL can be used to calculate the concentration of glucose leaving the probe in mM.

5.2 Mesh

An extremely useful feature in COMSOL is the physics-controlled mesh sequence. The parameters chosen by this function are based on hundreds of models previously constructed in COMSOL that have similar geometries and physics packages. For this simple model, the physics-controlled mesh is able to create a mesh that supplies accurate results.

Within the physics-controlled system, a pre-defined mesh size that ranges from extremely fine to extremely coarse can be chosen. To determine which size mesh minimizes solve time while still providing an accurate solution, an iterative process was used. The model was first solved with the smallest possible mesh; the outlet glucose concentration provided by this solution was deemed the “true value”. The model was then solved with an increasingly larger mesh size until the results produced were no longer within a 95% confidence range of the true value.

For this model, COMSOL chose to construct the mesh using triangular elements. Interestingly, all of the mesh sizes were within 99.9% of the “true value”. All of the

concentration results in mM were identical out to the third decimal place. For this reason, the mesh size was based on solve time, which ranged from 101s (extremely fine) to 3s (extremely coarse). The mesh size of “Finer” (10s) was chosen because it had one of the highest ratios for number of elements to solve time.

5.3 Sensitivity Analysis

A sensitivity analysis was conducted on each of the COMSOL model constants to determine the parameters to which results are most sensitive. Each input variable was independently tested at 13 different values over a range of 10% to 1000% of the normal value. As the only experimentally measured system output, the probe outlet concentration of glucose was used as the dependent variable. This concentration was recorded for each test and graphed against parameter values to determine the sensitivity of this key result to each parameter. As an example, the sensitivity data for perfusate volumetric flow rate can be found in Table 2.

Table 2. Raw data for glucose concentration sensitivity analysis of perfusate volumetric flow rate (holding all other parameters constant).

Volumetric Flow Rate (m³/s) x10¹¹	% of Value from Normal	Outlet Glucose Concentration (mM)	% of Outlet Concentration from nominal
0.17	10	1.196	175.3
0.84	50	0.819	120.1
1.12	67	0.755	110.6
1.52	91	0.698	102.2
1.59	95	0.691	101.2
1.65	99	0.684	100.2
1.67	100	0.683	100.0
1.69	101	0.681	99.8
1.75	105	0.675	98.9
1.84	110	0.668	97.9
2.51	150	0.628	92.0
3.34	200	0.598	87.6
16.70	1000	0.522	76.4

Appendix F shows results for each of the analyses, while Figure 12 summarizes the key results. In order to validate ZNF assumptions, the COMSOL model must mimic the experimental system as closely as possible. As can be seen in Figure 12, outlet glucose concentration is most sensitive to volumetric flow rate. If volumetric flow rate is off by an order of magnitude, the concentration results can be off by as much as 75%, or 0.51 mM. Later this fact will be proven as an advantage. Figure 12 also shows that within an order of magnitude, perfusate density and viscosity have no significant effect on outlet glucose concentration.

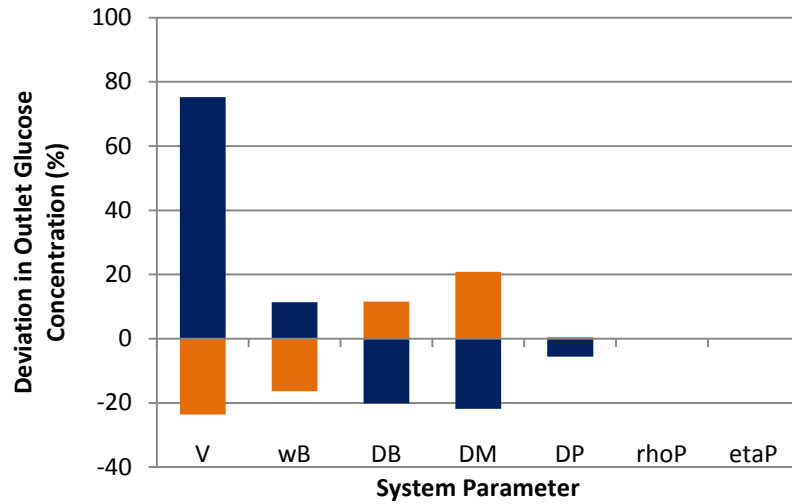


Figure 12. Sensitivity analysis. The orange boxes represent 1000% of the system parameter while the blue boxes represent 10% of the system parameter. Outlet glucose concentrations are unaffected by order of magnitude shifts in perfusate density or viscosity. The system parameters are: volumetric flow rate (V), brain width (wB), diffusion coefficient of glucose in the brain (DB), the membrane (DM) and the perfusate (DP), perfusate density (rhoP), and perfusate viscosity (etaP).

5.4 Temperature

One potential complication is the formation of a temperature gradient within the active region of the microdialysis probe. If a temperature gradient is present, the perfusate and membrane properties would vary throughout the probe. If this is the case, a

thermal package would have to be added to the model and the thermal characteristics for each parameter would have to be found.

In order to determine if a thermal solver is necessary, a new three-dimensional model, which represented the lower 14 mm of the probe, was created in COMSOL. A three-dimensional model was chosen over a two-dimensional axisymmetric model. Because there is only fluid flow and no diffusion or transport of mass across boundaries, the problems associated with the above three-dimensional model were not seen. Figure 13 shows the lower 6 mm of this model; the rest of the model is identical to the top (left) most section. It is assumed that the probe is implanted 5 mm into the head of the rat. Therefore, in addition to the 3 mm of active membrane that is in the rat head, there is a 2 mm section of non-active probe also in the head. The remaining 9 mm of the modeled probe is outside of the head and exposed to ambient conditions.

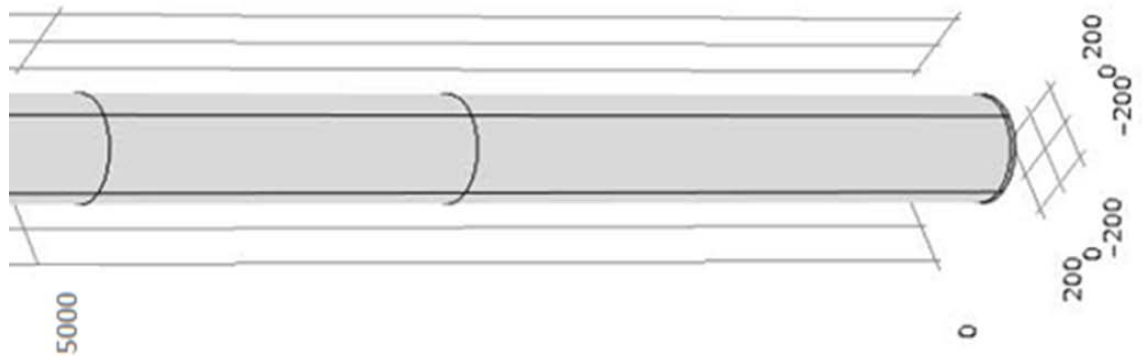


Figure 13. COMSOL model used to evaluate presence of a temperature gradient. Units are in μm .

The model is broken up into three sections to represent these three distinct temperature regions: the active region of the probe in the head, the non-active section in the rat head, and the non-active region that is not in the head. The geometry of the bottom section is identical to the three-dimensional version of the glucose model, except without the brain section. The upper two sections are a simple extension of the concentric design, the membrane being replaced with a stainless steel casing. In each section, the relevant boundary condition is the temperature of the environment. The outer surface of the membrane or stainless steel casing is therefore set to a constant temperature appropriate for that section. Because the brain is the source of heat, the domain itself did not have to be modeled and was simulated by putting the thermal boundary condition on the outer wall of the membrane. The lower two sections, which are in the head, have a boundary condition of 38.2°C, the average temperature of a rat brain.³⁷ The upper 9 mm of the probe has a boundary condition of 23°C, room temperature.

The COMSOL model was run at steady-state using creeping flow and thermal physics packages. The transport of glucose was not modeled because it is irrelevant to the thermal profile. All other parameters are identical to the ones used in the concentration model (Table 1). Results for the entire probe are shown in Figure 14.

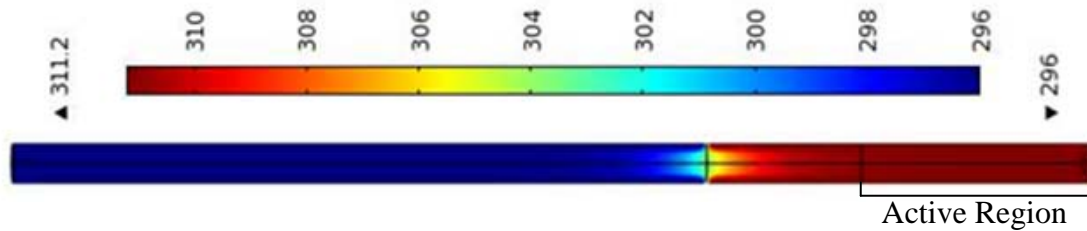


Figure 14. Temperature profile throughout lower 14 mm of microdialysis probe. Units are in K. The first (right) 3 mm are the active region of the membrane.

To get to the active region, the perfusate has to travel through the connecting tubes at the base of the probe. Figure 14 shows that by the time the perfusate reaches these connecting channels, the perfusate has reached complete thermal equilibrium with the brain and there is no temperature gradient in the active region of the perfusate flow.

To emphasize this fact, Figure 15 shows the temperature profile along the inner wall of the outer cannula from the base of the probe, including the section below the connecting tubes. As can be seen, when the perfusate leaves the active region, the temperature at the inner wall (the surface furthest from the boundary condition) is 38.0°C, which is within 99% of steady-state. With such a minute variation in temperature along the active region of the probe, it is a valid assumption to say that temperature is constant.

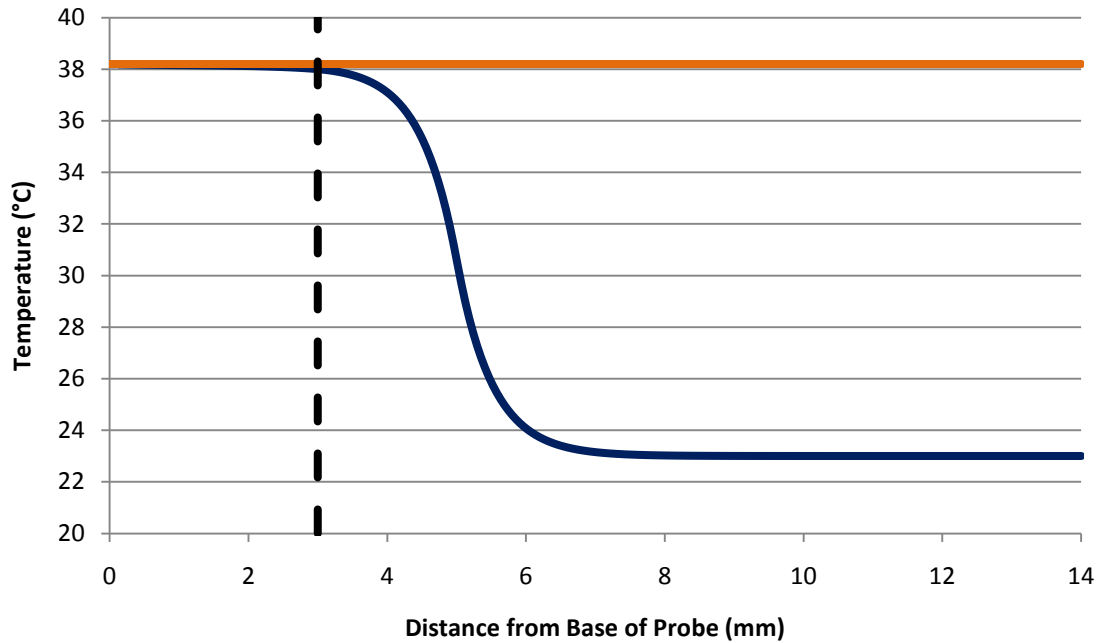


Figure 15. Temperature profile for the annulus of the probe. The first (left) 3 mm are the active region of the membrane. The head, and therefore heat source, ends at 5 mm. The remaining 9 mm is open to ambient conditions.

5.5 Zero Net Flux

5.5.1 Validity of Model

To confirm that this model accurately describes *in vivo* experiments, it was run at steady-state using the set of parameters in Table 1 that describes the experimental system run at SUNY Albany.⁵ As can be seen in Figure 16, the model accurately recreates the experimentally-determined point of ZNF, and the model's predicted data describes the

slope of the data well with an r^2 of 0.90. The line of best fit for the data only has an r^2 of 0.91.

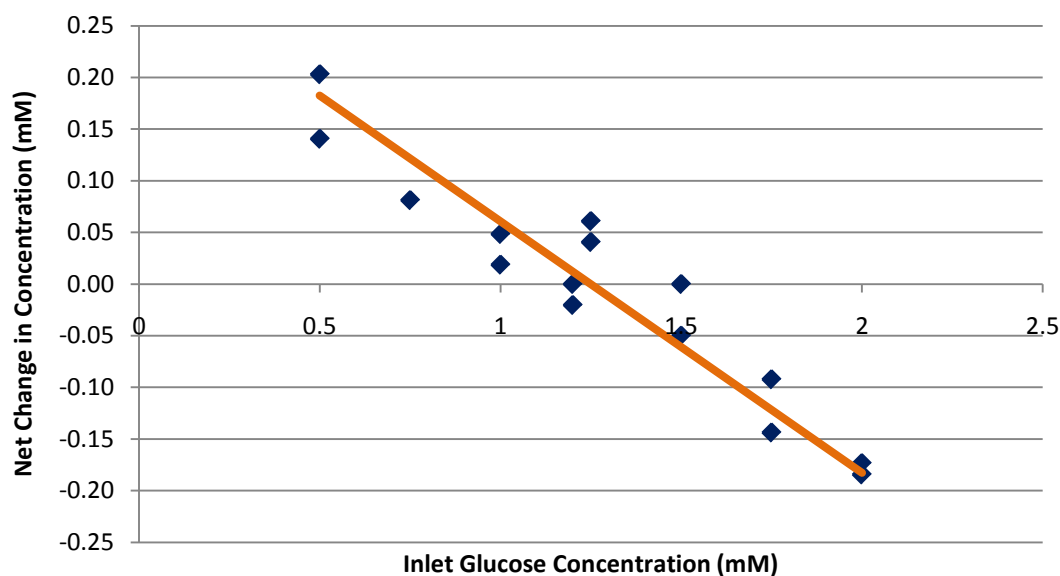


Figure 16. Comparison of experimental data (♦) with model results (orange). No fitting parameter is used.⁵

Importantly, all model parameters were based either on experimentally set parameters (flow rate, inlet concentration) or literature (diffusion coefficients, viscosity, density), using no “fitting” parameters to adjust the model. It can therefore be concluded that the evidence supports this model as an accurate representation of the brain-probe microdialysis system. Because this model was run at steady-state, the fact that the model fits the experimental data shows that assumptions made in using ZNF to analyze microdialysis data from this experiment are valid.

5.5.2 Implications of ZNF

In practice, *in vivo* experiments generate ZNF for an experimental condition and then use the slope to relate outlet concentrations. This is possible due to the fact that the slope of the ZNF line is dependent only on the volumetric flow rate and the three diffusivities. The slope is not dependent on the brain concentration or on which inlet glucose concentration is chosen. Figure 17 is the result of changing the brain glucose concentration from 1.25 mM to 1 mM while keeping all other parameters the same. This shows that the diffusivities of a given brain-probe system can be characterized with one number, the slope of the ZNF plot. The perfusate diffusivity will remain constant as long as the same aECF is used. The membrane diffusivity will not change as long as the same membrane material is used. Brain diffusivities are relatively constant throughout a species, but may change with age and disease.⁴

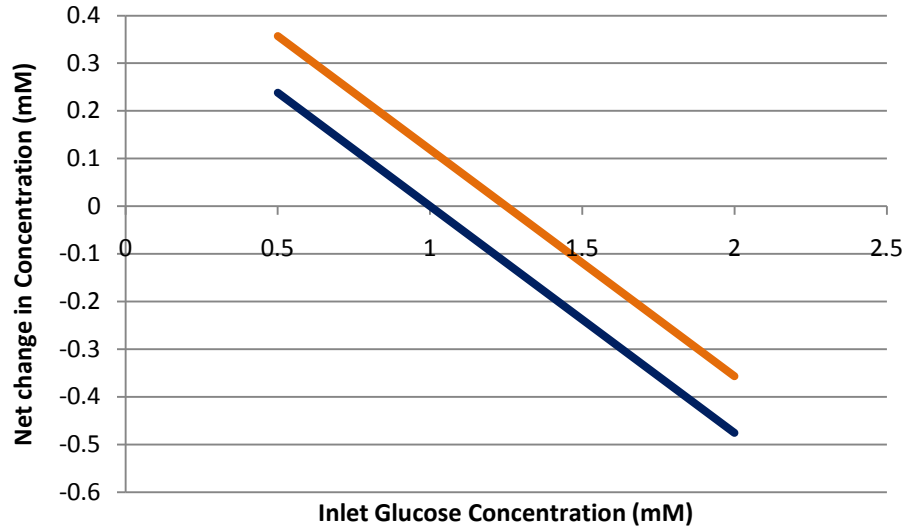


Figure 17. ZNF plot (using model data) for the same specimen at a brain concentration of 1.25 mM (orange) and after a concentration drop of 0.25 mM to 1.00 mM (blue).

Applying the concept in Figure 17 to the fact that the ZNF slope from one brain can be applied throughout a set of similar rats can be extremely useful. By realizing that when the brain concentration changes, the ZNF plot simply “shifts” to accommodate a new x-intercept, an equation can be crafted

$$c_B = c_{in} - \frac{c_{out} - c_{in}}{\text{slope}} \quad (9)$$

to quickly calculate brain concentration. To solve this equation only one set of input/output concentrations is needed, once the ZNF slope is known for the specific species. This means effectively, statistics aside, that brain glucose concentrations can be known with only one measurement.

5.5.3 Time to Steady-State

The goal of the second hypothesis was to determine the shortest brain activity, i.e. a thought, that microdialysis can measure and the limiting factor of the temporal resolution. The three factors that could be limiting are sample size, time to steady-state within the probe, and dispersion in the exit tubing.

The simplest factor to describe is sample size. One common means for measuring outlet glucose concentrations is taking an aliquot of the dialysate and running an off-line fluorometric analysis. Depending on the sensitivity of the analytical instrument, the concentration of the analyte in the dialysate and the flow rate of the perfusate, it usually takes 5 to 10 minutes to collect one sample. The best possible temporal resolution is therefore the size (divided by the flow rate) of the sample. For any further calculations, it will be assumed that outlet perfusate is collected for 5 minutes to form a large enough aliquot needed for analysis.⁴

To determine the effect of the probe on temporal resolution, a transient COMSOL model was created to determine how long the brain-probe system takes to reach steady-state, both at startup and in response to a thought. The model is identical to the one in Figure 9 except it was run as a transient model instead of at steady-state. The system simulated is initially at rest (no flow) and at 250 s, the rat has a 250 s thought. The model was run out to 750 s and the thought consumed 0.25 mM, making the brain glucose concentration 1.00 mM. Appendix G details instructions for constructing a transient model.

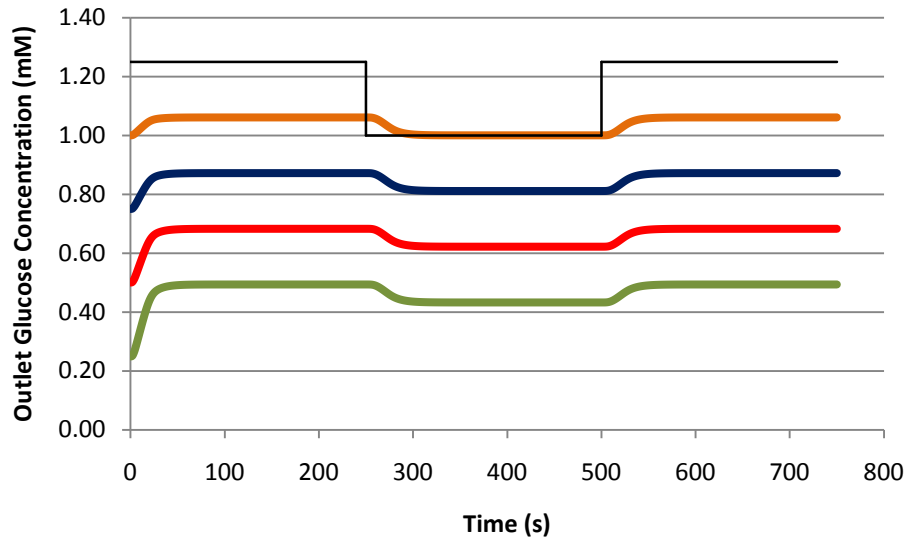


Figure 18. Transient response of brain-probe system to a 0.25 mM drop in brain concentration (black) with an inlet glucose concentration of: 1.0 mM (orange), 0.75 mM (blue), 0.5 mM (red), and 0.25 mM (green).

NOTE: The 15 s delay between the input step and the outlet slope is due to the time it takes the fluid to travel through the probe.

An interesting note is that the decrease in outlet glucose concentration when steady-state is re-achieved is independent of perfusate concentration. In the case of Figure 18, the drop in brain glucose concentration was 0.061 mM for all perfusate concentrations. This phenomenon can be attributed to the idea of a constant slope presented with Figure 17.

Table 3 shows that the closer inlet concentration is to the brain concentration, the quicker the system reaches steady-state. Therefore, the use of a perfusate with a concentration close to that of the brain will improve temporal resolution. But even

perfusate with a concentration significantly different from that of the brain still results in temporal resolution on the order of 1-2 minutes at the outlet of the probe.

Table 3. Time it takes system to reach steady-state after a 0.25 mM drop in brain concentration at several levels of precision.

Proximity to Steady-State (%)	Time to steady-state (s)	
	$C_{in} = 0.25 \text{ mM}$	$C_{in} = 1.00 \text{ mM}$
110	18	0
101	47	32
100.1	71	40
100.01	95	65
100.001	119	89

Currently, researchers are waiting 20 minutes after startup to begin taking samples. Table 4 shows that the time to steady-state for startup is similar to the reaction time to a thought. However, waiting longer than 2 minutes to start sampling is still advisable in case there are any unforeseen changes caused at startup.

Table 4. Time it takes system to reach steady-state from start up at several levels of precision ($c_{in}=0.25 \text{ mM}$).

Proximity to Steady-State (%)	Time to steady-state (s)
90	21
99	43
99.9	67
99.99	90
99.999	113

Consequently, it can be seen that the brain-probe system will regain steady-state within 1-2 minutes after any reasonable perturbation. The time for which the output is at the actual thought concentration has shrunk by one minute. So far, if the analytical device requires 5 minutes of gathering for an aliquot and system parameters are similar to those used in the transient model, no brain process lasting less than 6 minutes will be measurable. The effect of Taylor dispersion on temporal resolution will be discussed later.

5.6 Reverse Microdialysis

Another reason to accurately model microdialysis is to help develop its use as not only an analytic device, but also as a drug delivery unit. An interesting feature of the microdialysis probe is that because transport across the membrane is controlled by a concentration gradient, a perfusate can be designed so that the probe runs in “reverse”. That is, if the concentration of an analyte is higher in the perfusate than in the brain, the analyte will be transported through the membrane and into the brain. This method of drug delivery could have far-ranging implications, especially for delivering drugs that are too large to pass through the blood-brain barrier (the dense lining around capillaries).³⁸

Reverse microdialysis can be seen in Figure 16; the experimental points to the right of the x-intercept have an inlet concentration greater than the brain concentration; therefore, they have a negative net change in glucose concentration, meaning glucose was lost to the brain.

When modeling ZNF, perfusate concentrations were relatively similar to those in the brain; the maximum deviation was 0.75 mM. Drug delivery deals with adding a component at a significant concentration that is otherwise absent from the brain.^{20,39} The drug can be delivered either highly concentrated over a short period of time as a pulse or at a lower, constant concentration. It has been shown that the ZNF model works well at concentrations near the brain. However, it is a possibility at extreme concentrations, the assumptions made in the boundary conditions and homogenization of the brain could break down and provide useless data. For this reason, a separate model was created (Figure 19) which is identical to the first model except that the brain section is enlarged.

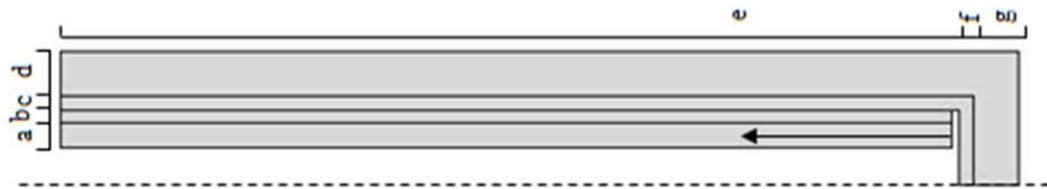


Figure 19. Model geometry for reverse microdialysis. The probe itself still has an overall radius of 250 μm and height of 3 mm. The probe is then broken down into the following dimensions: (a) 85 μm , (b) 40 μm (c) 50 μm (d) 150 μm (e) 3 mm (f) 25 μm (g) 150 μm . The perfusate enters the model at the base of the outlet flow region.

In the ZNF model, it was assumed that the brain tissue on opposite side of capillaries from the probe would not be affected by the transport of glucose to the probe because the capillaries are the source of the glucose. Drugs that are delivered using

microdialysis will most likely be too large to pass through the blood-brain barrier (BBB) and will therefore not be affected by the capillary. For this reason, the brain section needed to be extended to determine the transport of the drug throughout the entire brain. It turns out that beyond 200 μm from the probe, changes in concentration are negligible. Anything past 200 μm can effectively be viewed as “infinity” from the probe. In doing this, it is assumed that the capillary does not play a significant role in this process, specifically that the response time of the capillary to changes in brain drug concentration is much slower than action of the probe.

To ensure the model is as robust as possible, it was tested at extreme conditions. The system modeled is that of glucose delivered in a pulse to the brain. This could be used for patients severely lacking glucose and in need of fast relief. The initial concentration for glucose in the immediate region of the brain (50 μm) was set to 0.5 mM, while the outer reaches of the brain (150-200 μm) are set to the normal 1.25 mM. At $t=1\text{s}$, the inlet perfusate concentration was changed to 100 mM for a duration of 5s, at which point the concentration was held constant at 1.25 mM. All other parameters are unchanged from the ZNF simulation (Table 1).

Figure 20 shows the concentration of glucose 50 μm from the probe over time. As can be seen by the insert, the depleted region is at first serviced by the non-depleted brain immediately adjacent to the depleted region. However, after a short period, the overwhelming amount of glucose from the probe takes over and the concentration sharply increases.

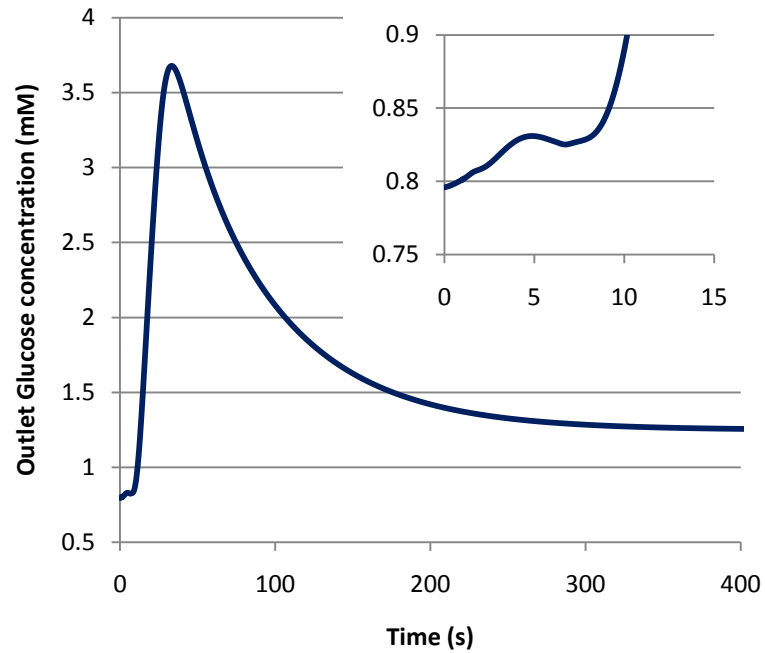


Figure 20. Brain glucose concentration 50 μm from the probe when probe is perfused with a 100 mM glucose spike for 5 seconds. Brain starts at 0.5 mM and perfusate is reduced to 1.25mM at 6 seconds. The inset is a close-up of the first 15 seconds of the simulation.

These results show that COMSOL and FEM can be used successfully to model reverse microdialysis.

6 Impact of Tubing on Temporal Resolution

It is important to determine how long a signal has to last in order to get a reading unaffected by Taylor dispersion. As stated in the Background, it was believed that the length of the exit tubing causes significant signal dilution and therefore limits the temporal resolution of results. The derivation that follows is an adaptation of G.I. Taylor's original work.⁴⁰ Before the dispersion process is derived, the basic principles of Taylor dispersion will be discussed.

6.1 Taylor Dispersion

Dispersion is the axial mixing of a fluid due to the coupling of diffusion and a radial velocity gradient. In a pipe, fluids in the center travel faster than near the walls, where velocity is zero due to no slip. One way to visualize this is by looking at the transport of a pulse, as in Figure 21. Due to no slip at the wall and no stress at the center, a parabolic flow profile is formed. If a cross-section of the tube is examined at the front of the parabolic profile, the concentration at the center is higher than at the walls. This radial concentration gradient will cause the solute to diffuse from the center radially outward towards the less concentrated, slower moving fluid. Additionally, fluid at the rear of the pulse is more concentrated at the walls, because the solute is moving slower.

This will cause solute in the rear to diffuse inward to the faster flowing fluid. The final result of this phenomenon is that the signal will spread out as it travels along the tube. Taylor dispersion is therefore the axial spreading of solute caused by a radial velocity gradient.



Figure 21. Example model of Taylor Dispersion, for a pulse.⁴¹

The system being examined (Figure 22) is a simple one. It is essentially fully laminar flow in a horizontal pipe. As described in the Background, Stoke's flow is a simplified form of Navier-Stokes, which accurately describes laminar flow. Therefore, even though the flow in the tube is technically considered creep flow, deriving Taylor dispersion as laminar flow will still provide accurate results.

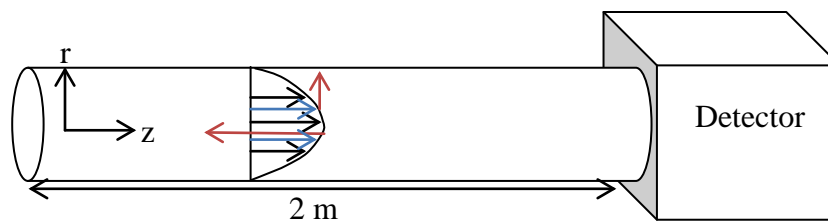


Figure 22. Diagram of system to be examined. Diagram is not to scale.

6.2 Velocity Profile

When the equations of continuity and motion are adapted to this system

$$v_z = -\frac{dp}{dz} \frac{R^2}{4\mu} \left(1 - \frac{r^2}{R^2}\right) \quad (10)$$

is derived which represent the parabolic flow profile. In developing Equation 10, it was assumed that: density, temperature, and material properties are constant, the system is at steady-state, the velocity vector is only dependent on the radial (r) coordinate but only non-zero in the axial (z) direction, no body forces exist, no slip at the walls, and no end effects. No end effect is a valid assumption because the length of the tube is so long compared to the length of the end effect zone.

Boundary conditions used to develop the flow profile are

$$\text{BC1: } v_z(r = R) = 0; \quad \text{BC2: } \left. \frac{dv_z}{dr} \right|_{r=0} = 0. \quad (11)$$

In future derivation steps, it will be helpful to note that

$$v_{z,\max} = v_z|_{r=0} = -\frac{dp}{dz} \frac{R^2}{4\mu} \quad \therefore v_z = v_{z,\max} \left(1 - \frac{r^2}{R^2}\right) \quad (12)$$

and that

$$\langle v_z \rangle = \frac{2}{R^2} \int_0^R v_z(r) r dr = -\frac{dp}{dz} \frac{R^2}{8\mu} \left(1 - \frac{r^2}{R^2}\right) = \frac{1}{2} v_{z,\max}. \quad (13)$$

Therefore

$$v_z = 2\langle v_z \rangle \left(1 - \frac{r^2}{R^2}\right) \quad (14)$$

where v_z is mass average velocity and $\langle v_z \rangle$ is the average velocity at a cross section of tubing. $v_{z,\max}$ is found at the center of the tubing where there is no stress.

6.3 Concentration Profile

Once the velocity profile was described, the species equation of continuity was adapted to the system and resulted in

$$\frac{\partial c_A}{\partial t} + v_z \frac{\partial c_A}{\partial z} = D_A \left[\frac{1}{r} \frac{\partial}{\partial r} \left(r \frac{\partial c_A}{\partial r} \right) + \frac{\partial^2 c_A}{\partial z^2} \right] \quad (15)$$

where c_A is the concentration of glucose in the fluid and D_A is the coefficient of diffusion for glucose in aECF.

In addition to the using the same geometric assumptions stated in the Velocity Profile section, it was additionally assumed that there is no reaction, that concentration is independent of angle (dependent solely on the r and z coordinates), and that the diffusion coefficient is constant.

The boundary conditions for Equation 15 are

$$\text{BC3: } c_A(t, r = 0, z) \text{ is bounded;} \quad \text{BC4: } \int_0^{2\pi} \int_0^1 c_A' r \, dr \, d\phi. \quad (16)$$

where ϕ is the angular coordinate and c_A' is a variable that will be explained below.

For this case, in which an approximation for long times are desired, it is sensible to use a coordinate system that translates with the average velocity. This new traveling variable, δ , is

$$\delta \equiv z - \langle v_z \rangle t \quad (17)$$

in which the derivative of is

$$\frac{D}{Dt} \equiv \frac{\partial}{\partial t} + \langle v_z \rangle \frac{\partial}{\partial z}. \quad (18)$$

Applied to the concentration and solved for $\partial/\partial t$

$$\frac{\partial c_A}{\partial t} = \frac{Dc_A}{Dt} - \langle v_z \rangle \frac{\partial c_A}{\partial z} \quad (19)$$

Using Equation 19 and applying it to Equation 15 along with the axially shifted coordinate in Equation 17 produces

$$\frac{Dc_A}{Dt} + v'_z \frac{\partial c_A}{\partial \delta} = D_A \left[\frac{1}{r} \frac{\partial}{\partial r} \left(r \frac{\partial c_A}{\partial r} \right) + \frac{\partial^2 c_A}{\partial \delta^2} \right] \quad (20)$$

where

$$v'_z \equiv (v_z - \langle v_z \rangle) = \langle v_z \rangle \left(1 - 2 \frac{r^2}{R^2} \right). \quad (21)$$

is the deviation velocity.

Equation 20 is then nondimensionalized using

$$\theta = c_A / c_{A,\text{ref}}; \quad \eta = r / R; \quad \xi = z / L; \quad \gamma = \langle v_z \rangle t / L \quad (22)$$

where θ , η , ξ , and γ are the dimensionless concentration, radial, axial, and time variables, respectively. $c_{A,\text{ref}}$ is an arbitrary reference concentration. The specific value of $c_{A,\text{ref}}$ is not needed because it will not be present in the solution. All variables are designed so that the entire domain is scaled to range between 0 and 1.

The result of nondimensionalizing and rearranging Equation 20 is

$$\text{Pe} \frac{R}{L} \left[\frac{D\theta}{D\gamma} + v \frac{\partial \theta}{\partial \delta} \right] = \frac{1}{\eta} \frac{\partial}{\partial \eta} \left(\eta \frac{\partial \theta}{\partial \eta} \right) + \left(\frac{R}{L} \right)^2 \frac{\partial^2 \theta}{\partial \delta^2} \quad (23)$$

where

$$v \equiv v'_z / \langle v_z \rangle = \left(1 - 2 \frac{r^2}{R^2} \right) = (1 - 2\eta^2) \quad (24)$$

and

$$\text{Pe} = \frac{\langle v_z \rangle R}{D_A}. \quad (25)$$

The Péclet number, Pe , is a dimensionless variable that relates axial convection to radial diffusion. Taylor assumed that in systems where dispersion is prevalent, $Pe \gg 1$; convection is much faster than diffusion. The Pe number for this system is 60, which is large enough for Taylor dispersion.⁴²

A decomposition of the concentration is then proposed so that

$$\theta(\eta, \xi, \gamma) = \langle \theta \rangle(\xi, \gamma) + \theta'(\eta, \xi, \gamma) \quad (26)$$

where $\langle \theta \rangle$ is the cross-sectional average of θ which is independent of r . θ' is the difference between the average concentration and the actual concentration at any point. Generally, the decomposition is made with the expectation that $\langle \theta \rangle \gg \theta'$.

Applying this decomposition to Equation 23 results in

$$Pe \frac{R}{L} \left[\frac{D\langle \theta \rangle}{D\gamma} + \frac{D\theta'}{D\gamma} + v \left(\frac{\partial \langle \theta \rangle}{\partial \delta} + \frac{\partial \theta'}{\partial \delta} \right) \right] = \frac{1}{\eta} \frac{\partial}{\partial \eta} \left(\eta \frac{\partial \theta}{\partial \eta} \right) + \left(\frac{R}{L} \right)^2 \left(\frac{\partial^2 \langle \theta \rangle}{\partial \delta^2} + \frac{\partial^2 \theta'}{\partial \delta^2} \right) \quad (27)$$

where use was made of the fact that $\langle \theta \rangle$ is independent of η .

The next step is to take the cross-sectional average of Equation 24 in order to obtain an equation for $\langle \theta \rangle$. First however, it is useful to note that two properties of the decomposition in Equation 26 are

$$\langle \langle \theta \rangle \rangle = \langle \theta \rangle \quad \text{and} \quad \langle \theta' \rangle = 0. \quad (28)$$

The cross-sectional average of Equation 27 is

$$Pe \frac{R}{L} \left[\frac{D\langle \theta \rangle}{D\gamma} + \left\langle v \frac{\partial \theta'}{\partial \delta} \right\rangle \right] = \left(\frac{R}{L} \right)^2 \left(\frac{\partial^2 \langle \theta \rangle}{\partial \delta^2} \right). \quad (29)$$

Because this derivation is interested in dispersion at long times, or long tubing, $L \gg R$.

This means that the final term in Equation 29 can be considered negligible compared to the other terms, resulting in

$$\frac{D\langle\theta\rangle}{D\gamma} = -\langle v \frac{\partial\theta'}{\partial\delta} \rangle \quad (30)$$

which shows that Taylor dispersion is due to the averaged product of deviations from the mean velocity and concentration. To solve Equation 30 for $\langle\theta\rangle$, θ' needs to be defined.

To generate an equation for θ' , subtract Equation 29 from Equation 27 to produce

$$\text{Pe} \frac{R}{L} \left[\frac{D\theta'}{D\gamma} + v \left(\frac{\partial\langle\theta\rangle}{\partial\delta} + \frac{\partial\theta'}{\partial\delta} \right) \right] = \text{Pe} \frac{R}{L} \langle v \frac{\partial\theta'}{\partial\delta} \rangle + \frac{1}{\eta} \frac{\partial}{\partial\eta} \left(\eta \frac{\partial\theta'}{\partial\eta} \right) + \left(\frac{R}{L} \right)^2 \frac{\partial^2\theta'}{\partial\delta^2}. \quad (31)$$

This equation cannot be solved analytically and must be approximated by neglecting terms based on relative magnitudes. Again, because $L \gg R$, the third term on the right-hand side of Equation 31 can be neglected. It can further be assumed that $L \gg \text{Pe}R$, therefore allowing the first term on the right-hand side to be neglected. This leaves the radial diffusion term as the predominant term on the right-hand side of Equation 31.

Even though it is assumed that $L \gg \text{Pe}R$, at least one term on the left-hand side of Equation 31 needs to be significant in order to balance out the remaining term on the right-hand side. Taylor assumed that $\langle\theta\rangle \gg \theta'$, which leaves the average axial convection term as the dominant term on the left-hand side Equation 31. These approximations reduce Equation 31 to

$$\text{Pe} \frac{R}{L} v \frac{\partial\langle\theta\rangle}{\partial\delta} = \frac{1}{\eta} \frac{\partial}{\partial\eta} \left(\eta \frac{\partial\theta'}{\partial\eta} \right). \quad (32)$$

Equation 32 can be solved for θ' by integrating twice with respect to η and applying the boundary conditions in Equation 16. The result is

$$\theta' = \frac{\text{Pe}R}{L} \frac{\partial\langle\theta\rangle}{\partial\delta} \left(\frac{\eta^2}{4} + \frac{\eta^4}{8} + \frac{1}{12} \right), \quad (33)$$

which when used in Equation 30 produces

$$\frac{D\langle\theta\rangle}{D\gamma} = \frac{\langle v_z \rangle R^2}{48D_A L} \frac{\partial^2 \langle\theta\rangle}{\partial \delta^2}. \quad (34)$$

When this equation is dimensionalized and the axially shifted coordinate system is removed

$$\frac{\partial \langle c_A \rangle}{\partial t} + \langle v_z \rangle \frac{\partial \langle c_A \rangle}{\partial z} = K \frac{\partial^2 \langle c_A \rangle}{\partial z^2} \quad (35)$$

where

$$K = \frac{R^2 \langle v_z \rangle^2}{48D_A}. \quad (36)$$

K is defined as the Taylor dispersion coefficient and has the same units as a diffusion coefficient. This fact shows that dispersion, while truly a combination of the parabolic velocity profile and radial diffusion, has the appearance of axial diffusion.

The next step is to get an explicit equation for $\langle c_A \rangle$. Equation 35 is a second order PDE with $\langle c_A \rangle$ as the only dependent variable. The equation can easily be solved using a Fourier transform. The result of this transform is

$$\frac{\partial C_A}{\partial t} + \langle v_z \rangle i2\pi h C_A = K(i2\pi h)^2 C_A \quad (37)$$

a first order ODE where h is the independent variable in Fourier space and C_A is the Fourier concentration. Solving for C_A

$$C_A = G(h) e^{(K(i2\pi h)^2 - \langle v_z \rangle i2\pi h)t} \quad (38)$$

where G(h) is the signal function, or the form of the original input function. By taking the inverse Fourier, g(z) is convolved with the inverse of the exponential term

$$\langle c_A \rangle(z) = g(z) * \frac{1}{\sqrt{4Kt_{out}\pi}} e^{-\left(\frac{z^2}{4Kt_{out}}\right)} = \frac{1}{\sqrt{4\pi Kt_{out}}} \int_{-\infty}^{\infty} g(y) e^{-\left(\frac{(z-y)^2}{4Kt_{out}}\right)} dy. \quad (39)$$

Where t_{out} is the time it takes the fluid to reach the analytical instrument. Note that the second term in the convolution has the form of a normal Gaussian distribution. The y in Equation 39 is a dummy variable used to pass one function over the other and to effectively smear them together.

Now there is an explicit equation that provides the average concentration profile of the solute as a function of axial distance, which is related proportionally to time in tubing by the average velocity. This can be used to determine at what point signals become indistinguishable from each other.

6.4 Convolution

Equation 39 is in the form of a convolution. Essentially, a convolution takes one function and rubs another function over it, causing smearing. As can be seen in Figure 23, there is a signal function (A, steps) and a smearing function (B, Gaussian curve). The signal is smeared by the Gaussian curve. The graph in Figure 23.C is the result. The output still has the same general form as the signal; however, the peaks have started to blend together. If the width of the bell curve in Figure 23.C is increased, the two individual peaks will eventually become indistinguishable from each other and no useful data will be attainable.

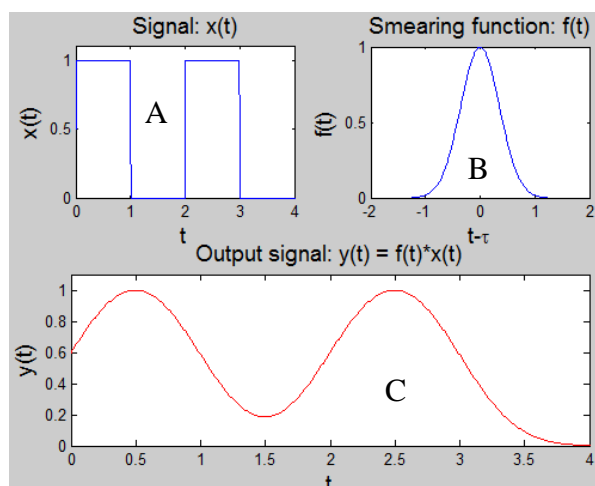


Figure 23. Example of Convolution. A) signal, B) smearing function, C) result.

6.5 Signal

For this system, the signal is the concentration profile that enters the exit tubing. Shown again in Figure 24 (originally in Figure 18), this profile was approximated by a set of Boltzmann sigmoidal equations.

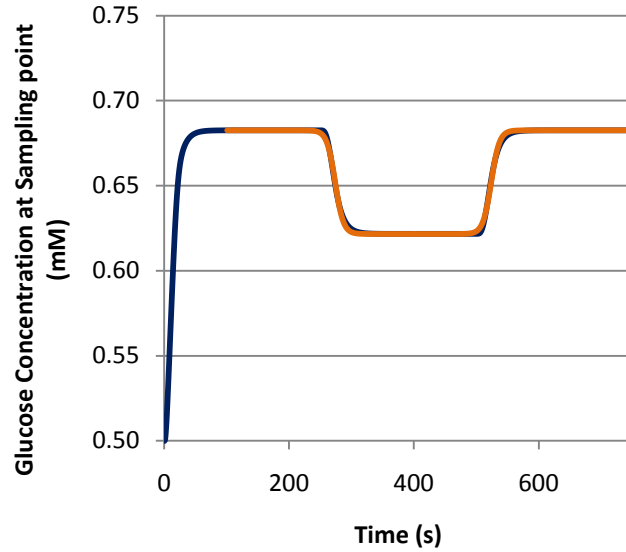


Figure 24. Plot of actual signal (blue) compared to Boltzmann sigmoidal (orange) fit ($r^2 = 0.9996$). The data is originally found in Figure 18; a 250 s signal with one minute of dilution due time to steady-state in the probe.

The Boltzmann sigmoidal

$$c_A = B + \frac{T-B}{1+e^{\left(\frac{h_a-t}{m}\right)}} \quad (40)$$

where B is the concentration during the signal (minimum), T is the nominal concentration (maximum), h_a is the time at which the concentration is halfway between B and T, and m is the slope of the curve at $t = h_a$, only encompasses one concentration change. For that reason, one sigmoidal models the drop in concentration (100 to 400s), while a second function models the concentration increase (400 to 750s). The first 100s was not modeled because the focus is on the impact dispersion has on signals, not startup.

For both the decrease and increase, the equations used are identical except the slope (m) is opposite and the half-time (h_a) is different. When compared to the COMSOL data, the Boltzmann sigmoidals fit with an r^2 of 0.9996. To fit in with Equation 39, the Boltzmann fit has to be shifted from the time domain (t) to the space domain (z). This is done by multiplying m , h , and the time domain by the average velocity in the tubing.

6.6 Effect of Taylor Dispersion on Concentration Results

Applying the adjusted Equation 40 to Equation 39 in the context of the relevant system (shown in Figure 22 and described in Table 5) and running the convolution function produces Figure 25. 1,000 seconds were added to the beginning and end of the signal so that the convolution of the ends (which MATLAB treats as a concentration of 0) does not affect the actual signal. The complete MATLAB mfile used for this model can be found in Appendix H. A second mfile was created that shows the state of the signal as it travels down the tubing. This transient version can be found in Appendix I.

Table 5. Physical parameters for exit tubing.

Variable	Expression	Value	Units
L	Length of tubing	2	m
V	Volumetric flow rate	1.67×10^{-11}	m^3/s
D	Diffusion coefficient of glucose in perfusate	8.3×10^{-10}	m^2/s
R	Inner radius of tubing	1.075×10^{-4}	m
rhoP	Dialysate density	990	kg/m^3
etaP	Dialysate kinematic viscosity	7.28×10^{-4}	Pa s
K	Dispersion coefficient	6.22×10^{-8}	m^2/s

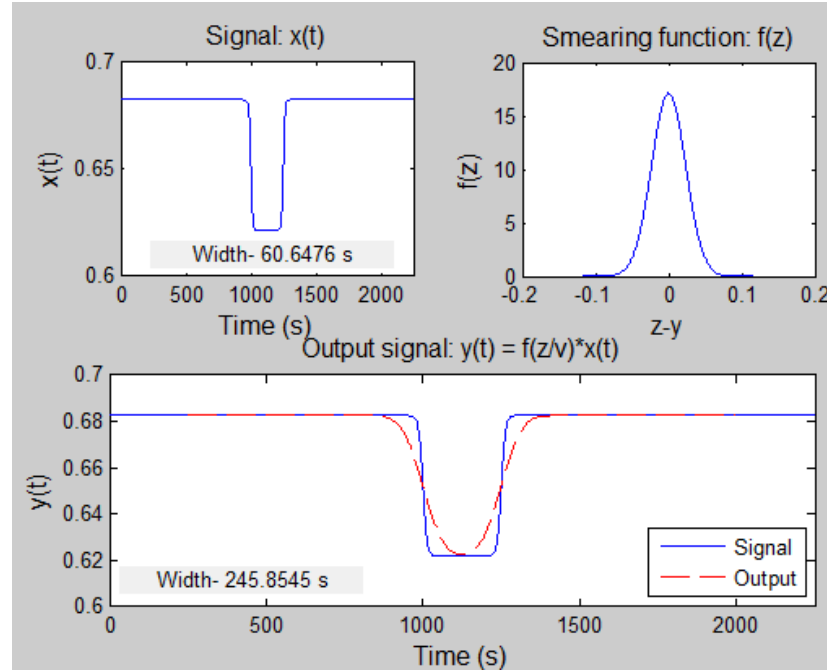


Figure 25. Convolution results for system. Times shown are the times it takes to get from 99% of the nominal concentration to 101% of the concentration during the brain process.

Figure 25 shows that by the time glucose reaches the detector, the signal (originally 250s wide) has dispersed 246 s, leaving only a 4 s duration that is at the true brain process concentration. This degradation includes time to steady-state in the probe and dispersion in the exit tubing; 185 s of the total degradation time is due to dispersion. Keeping in mind that the analytical instrument requires sampling for a duration of 300 s (five minutes), Figure 25 shows that it is impossible for an aliquot to accurately reflect the concentration during the brain function. This idea is easier seen in Figure 26 where

the output graph is separated into samples, and the concentrations both at the outlet of the probe and at the end of the exit tubing are shown.

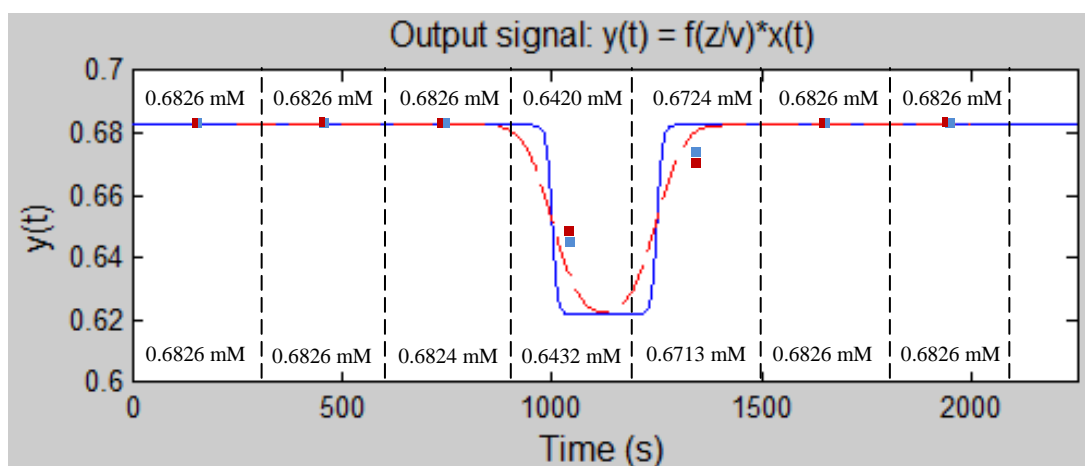


Figure 26. Concentrations read by analytical instrument. The graph is broken up by the dashed lines into aliquots gathered for 5 minutes. The numbers at the top (represented on the graph by blue squares) are the concentrations the analytical instrument would read if placed at the outlet of the probe. The numbers at the bottom (represented on the graph by red squares) are the concentrations the instrument would read when placed at the end of 2 m of exit tubing.

None of the aliquots in Figure 26 provide the true outlet glucose concentration. To procure at least one valid sample of the brain function concentration, the brain process needs to last at least as long as twice the sampling time, plus the time of dispersion due to the probe and the exit tubing. For example, if the analytical instrument requires five minutes of sampling, the probe reaches steady-state in 61 s, and the signal experiences

185 s of dispersion, the original signal needs to last longer than 846s (5 min*60 s/min * 2 samples + 61 s to steady-state + 185s of dispersion). This concept is shown more succinctly by

$$t_{signal} > 2 * t_{sample} + t_{steady-state} + t_{dispersion}. \quad (41)$$

Equation 41 can be divided through by t_{signal} to form a dimensionless group, the Vinciguerra number

$$Vi = \frac{2 * t_{sample} + t_{steady-state} + t_{dispersion}}{t_{signal}} \quad (42)$$

where

$$2 * t_{sample} = \frac{2m_{min}}{\dot{V}[c]M_W}, \quad (43)$$

$$t_{steady-state} = \frac{0.85}{\sqrt{v_z}} + 7000L_p + \frac{5 \times 10^{-5}}{\sqrt{D_{lim}}} - 45, \quad (44)$$

and

$$t_{dispersion} = 6.5 \sqrt{\frac{KL}{v_z^3}} - 50. \quad (45)$$

is produced to determine if, given a set of experimental parameters, an accurate measurement could be seen. If Vi is less than 1, then one of the aliquots taken, if sampled continuously, will contain the true glucose concentration during the brain function.

The first term in the numerator gives the time it takes to collect two aliquots based on the minimum mass limit for the analytical device (m_{min}), the volumetric flow rate through the tubing (\dot{V}), the lowest possible analyte concentration ($[c]$), and the molecular weight of the analyte (M_W). This term represents the absolute smallest aliquot that could

be read by the specified analytical instrument. If aliquots taken are larger than the minimum, this term should be replaced by the collection time for two aliquot (volume of aliquot / volumetric flow rate of perfusate).

The second term in the numerator is an approximation for the amount of signal degradation due to time to steady-state in the probe. The coefficients for this term were fit from an extensive set of data which can be found in Appendix J. This correlation is based on the velocity of the perfusate in the outlet flow region (v_z), the length of the active region of the probe (L_p), and the limiting diffusion coefficient (D_{lim}). Note that the coefficients in this term are dimensional and therefore, units for velocity, length and diffusivity have to be in m/s, m and m^2/s , respectively. The term will provide an approximation for time to steady-state accurate to within an order of magnitude for steady-state times greater than 30s

The final term in the numerator approximates the amount of signal degradation due to Taylor dispersion in the exit tubing. Again, the coefficients for this term were fit from a set of data found in Appendix J. This approximation is based on the dispersion coefficient (K), the length of the exit tubing (L), and the average velocity through the tubing (v_z). This term is accurate to within 5% for any dispersion times greater than 40 s and within 10% for times greater than 30 s.

No other dimensionless groups that relate signal length to analytical sensitivity and dispersion are apparent in literature. Figure 27 shows a brain process lasting 846 s and the associated dispersion given the same parameters used in Figure 26. The Vi

number for this case is 1, meaning that at least one of the aliquots reflects the true outlet glucose concentration, as seen in Figure 27.

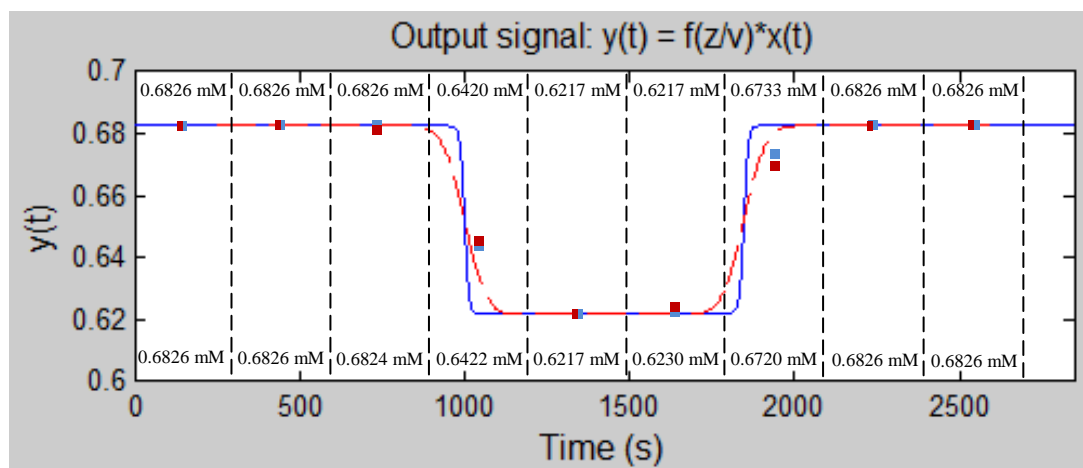


Figure 27. Concentrations read by analytical instrument in the case where the V_i number is 1. The graph is broken up by the dashed lines into aliquots gathered for 5 minutes. The numbers at the top (represented on the graph by blue squares) are the concentrations the analytical instrument would read if placed at the outlet of the probe. The numbers at the bottom (represented on the graph by red squares) are the concentrations the instrument would read when placed at the end of 2 m of exit tubing.

While Taylor dispersion in the exit tubing does not have a significant effect on the concentration read by the analytical instrument, it does increase the length of the smallest measurable thought, by more than 4 minutes in the above case.

7 Discussion

7.1 Validity of model

It was hypothesized that assumptions made in using zero-net-flux to analyze microdialysis data are accurate. The major assumption tested was that the system is able to reach steady-state. It was also hypothesized that the system takes less than 15 minutes to reach steady-state. By creating a three-dimensional finite element model of the system, it was possible to validate all assumptions.

In addition to the proof of validity given above (Figure 16 in particular), a mass balance on the model is given in Appendix B. The model has an overall relative mass imbalance of 0.60%, an acceptably small error. There are, however, some limitations to the usefulness and robustness of the model. The largest inhibiting factor for this model is the assumption made in simplifying the brain. The boundary condition is constant at the nominal brain ECF concentration, regardless of brain activity and external influences. In reality, the source of glucose is the capillaries and the concentration of glucose in the blood stream varies in time and is even dependent on brain activity. However, because I am interested solely on ECF glucose concentrations, I am able to eliminate the capillaries from the model and replace them with a boundary condition that reflects nominal ECF concentration levels.

Another limiting aspect is the fact that the reaction term is built into the effective diffusion coefficient. Coupled with the assumed boundary condition, the effective diffusion coefficient is able to accurately describe the tortuous path glucose molecules take from capillary to the probe and the consumption of glucose by brain cells. This combination works well with glucose, but could fail for other molecules that do not behave similarly. For instance, molecules that react in the ECF or molecules that do not react at all will have to be modeled differently. For the most part, they should be able to be worked into an effective diffusion coefficient, just as glucose is, but the process for deriving that coefficient may be different.

The model also has a size limitation. Just as continuum mechanics cannot properly describe molecular and atomic interactions, this model cannot describe non-continuum interactions; this is due to the homogeneous assumption of the brain. Fortunately in this aspect, the probe itself is the limiting agent and not the model. Probes can only be manufactured so small, and are therefore limited in their spatial selectivity. They cannot, for instance, measure the concentration of neurotransmitters being passed between a certain neuron. As long as microdialysis probes remain in the analytical realm of continuum mechanics, this model can provide an accurate description of the system.

Even with the three limitations found above, it has been shown that microdialysis is an accurate and efficient means for measuring brain ECF concentrations, that ZNF is a valid tool for translating microdialysis data into true concentrations, and that the finite element model presented here can properly describe a brain-probe system.

7.2 Comparison to Literature

As stated above, theoretical approaches to modeling microdialysis tended to be specific and over complicated.²¹ For this reason, results will only compared to other numerical approaches. Both Norton *et al.* and Wang *et al.* modeled an *in vitro* system and found times to steady-state of 20 s and 30 s, respectively.^{26,27} It makes sense that their time to steady-state is shorter because, as Zetterström discovered, glucose diffusion in brain tissue is much slower than in aECF.²³ If the brain domain is removed and the outer boundary of the membrane is set to nominal brain concentration, the probe can effectively be modeled as in a well-stirred beaker. Modeling the probe this way, the time to steady-state of 45 s, which is close to results from Norton *et al.* and Wang *et al.*

While Norton *et al.* modeled exit tubing dispersion in MATLAB (they also used a sigmoidal signal function), Wang *et al.* quantified the dispersion using experimental procedure. Results presented here for dispersion times are very close to those of Norton *et al.*, which helps verify the validity of this approach. Wang *et al.* only presented data from one trial, and it was in graphical form. However, when experimental parameters are estimated and entered into the MATLAB file, dispersion times are similar.²⁷

7.3 Implications

Once microdialysis, ZNF, and this model have been established, the next step is finding a use for these results.

7.3.1 Parameter Sensitivity

Prior to this model, the only sensitivity data that was available was on the analytical instruments. A detailed description of the effect that experimental parameters had on concentration results did not exist. By modeling the entire system and by being able to individually set each of these parameters, it is now possible to determine the sensitivity of results to any parameter. The sensitivity analysis is not limited to one parameter; the model allows for changing more than one parameter at a time. This is helpful in designing the experiment. For instance, from the results above, it is now apparent that it is not necessary to find the exact perfusate density; any value within reason would produce valid results.

7.3.3 Future Work

There are many areas of microdialysis still to be explored. This model will hopefully aid in opening up these fields and improving the techniques. One way to improve the robustness of the model would be to un-simplify the brain. If using COMSOL, a homogeneous brain material would still be needed for continuum mechanics. However, a reaction term could be added to the brain domain that would describe uptake of glucose into brain cells. In addition, a capillary complete with a blood-brain barrier could be created to replace the concentration boundary condition in the symmetric model. This would allow the blood glucose concentration to be the

boundary condition, which is more realistic than the outer wall of the blood-brain barrier having a constant concentration.

One of the most useful implications for reverse microdialysis is in membrane characterization. By running the probe *in vitro*, the environmental concentration is no longer an unknown because fluid medium can be specifically made. Because the external concentration is no longer an unknown, it is possible to solve for a different variable, i.e. the membrane diffusion coefficient.. Experimentally, the probe would first need to be run *in vitro* at a variety of solution and perfusate concentrations, recording the outlet concentration each time. The model can then be easily adapted to *in vitro* by removing the brain domain and setting the outer boundary of the membrane to the solution concentration (assuming a well-mixed solution). Then the model could simply be run at varying membrane diffusivities until the modeled outlet concentrations match experimental results.

The model is useful in many other “what if” scenarios. For instance, the model can be used to determine the highest flow rate possible without draining the brain glucose to a critical level. It is known that as brains get older, the nominal glucose concentration remains the same, but glucose diffusion through the brain slows down. Knowing all other data, brain diffusivities can be back-calculated using this model. The model is widely adaptable and simple to operate, and uses for the model will be far reaching.

7.4 Taylor Dispersion

The effects of Taylor dispersion were investigated due to a lack of agreement in the literature. One article concluded that dispersion was negligible, while another claimed it to be the limiting factor in temporal resolution.^{26,27} The two papers had consistent results but differing perspectives. Norton *et al.* was looking at large, long-lasting signals, while Wang *et al.* was trying to precisely describe the short transient period during concentration changes.

In the case presented here, time to steady-state degrades the signal nearly as much as dispersion in the tubing, 60 s to 104 s, respectively. When working with awake, freely-moving rats and long exit tubing is necessary, Taylor dispersion should not be ignored.

The mfile was run at increasingly shorter tube lengths to determine at what point dispersion is negligible. Even with a tube length of 0.1 m (a customary length for anaesthetized rats), the signal is still degraded 12 s by dispersion. This could be considered negligible for large scale brain functions, but as microdialysis techniques improve and as researchers want to look at shorter and shorter brain functions, even dispersion in short tubes will have to be considered.

8. Conclusion

In this thesis, I created a model based on first principles and well-founded parameters that accurately describes a real microdialysis system. With this model, I was able to show the validity of ZNF and the accompanying assumptions. I was also able to prove that the ZNF slope is independent of brain concentration, a feature that is helpful in practice. Furthermore, I determined that it takes approximately one minute for the probe to reach steady-state after both startup and an environmental change. The model allowed me to determine the sensitivity of results to each individual parameter, values that were inaccessible experimentally. Using a separate model, I was able to show that the perfusate is in thermal equilibrium with the brain throughout the active region of the probe.

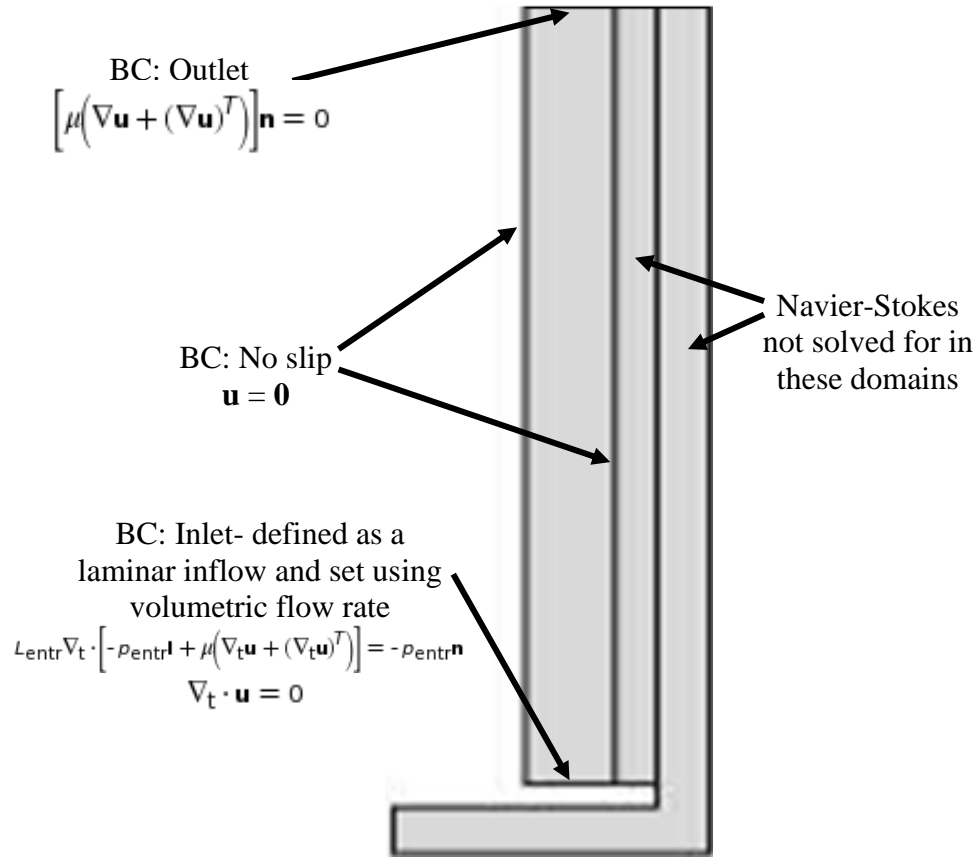
I quantified the extent of Taylor dispersion in probe exit tubing. For a two meter tube, a common length for testing awake specimens, the dispersion time is around two minutes. Signal degradation should not be thought of in the typical limiting factor sense because the three factors that affect necessary signal time are additive, not competitive. The sensitivity of the analytical instrument, the time to steady-state in the probe, and the amount of dispersion in the tubing all compound to increase the length of the shortest measurable thought. I designed a dimensionless number to help quantify this concept.

Bibliography

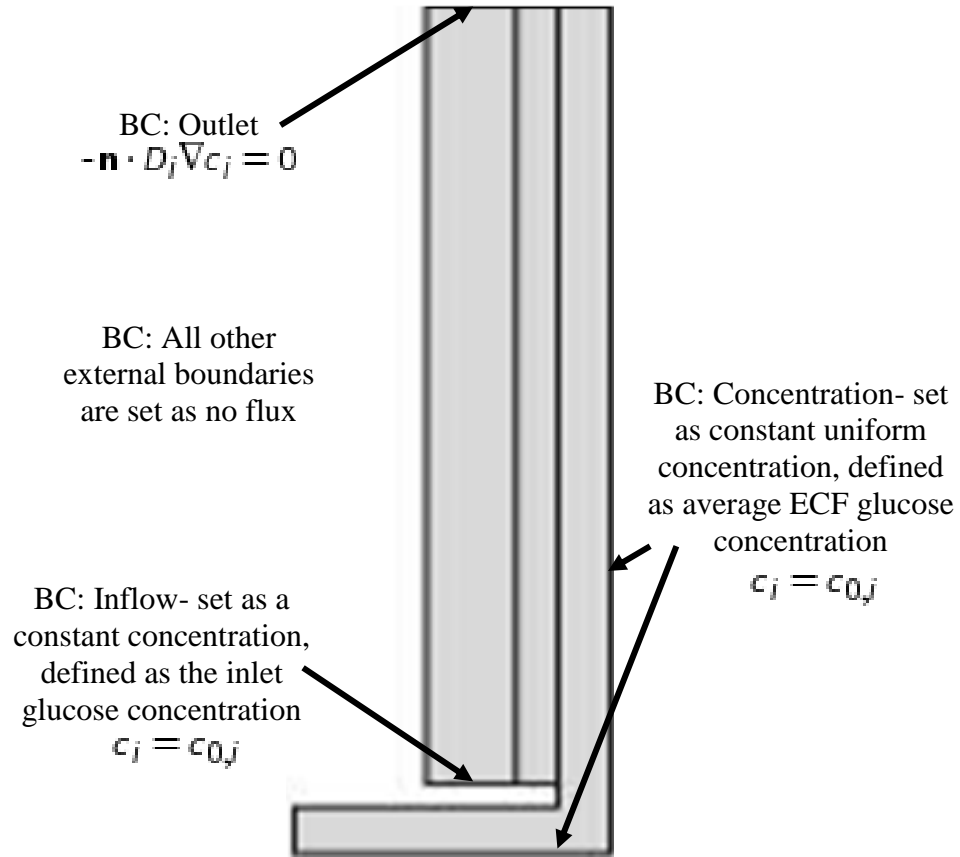
- ¹ Dienel, G. A., Hertz, L. (2001). Glucose and Lactate Metabolism during Brain Activation. *Journal of Neuroscience Research*, 66, 824-838.
- ² Benveniste, H. (1989). Brain Microdialysis. *Journal of Neuroscience*, 52 (6), 1667-1677.
- ³ Parkin, M. C., Hopwood, S. E., Strong, A. J., Boutelle, M. G. (2003). Resolving dynamic changes in brain metabolism using biosensors and on-line microdialysis. *Trends in Analytical Chemistry*, 22 (9), 487-497.
- ⁴ McNay, E. C., Gold, P. E. (1999). Extracellular Glucose Concentrations in the Rat Hippocampus Measured by Zero-Net-Flux: Effects of Microdialysis Flow Rate, Strain, and Age. *Journal of Neurochemistry*, 72 (2), 785-795.
- ⁵ McNay, E. C., Sherwin, R. S. (2004). From artificial cerebro-spinal fluid (aCSF) to artificial extracellular fluid (aECF): microdialysis perfusate composition effects on in vivo brain ECF glucose measurements. *Journal of Neuroscience Methods*, 132, 35-43.
- ⁶ Bito, L., Davson, H. Levin, E. Murray, M., Snier, N. (1966). The Concentrations of Free Amino Acids and other Electrolytes in Cerebrospinal Fluid, in vivo Dialysate of Brian, and Blood Plasma of the Dog. *Journal of Neurochemistry*, 13 (11), 1057-1067.
- ⁷ Delgado, J. M. R., Defeudis, F. V. (1972). Dialytrode for long-term intracerebral perfusion in awake monkeys. *Archives Internationales de Pharmacodynamie et de Therapie*, 198 (1), 7-21.
- ⁸ Ungreterstedt, U., Pycoc, C., (1974), Functional correlates of dopamine neurotransmission. *Bulletin der Schweizerischen Akademie der Medizinischen Wissenschaften*, 30 (1-3), 44-55.
- ⁹ Heinemann, L. (2003). Continuous Glucose Monitoring by Means of the Microdialysis Technique: Underlying Fundamental Aspects. *Diabetes Technology & Therapeutics*, 5 (4), 545-561.
- ¹⁰ Chaurasia, C. S. (1999). In vivo microdialysis sampling: theory and applications. *Biomedical Chromatography*, 13 (5), 317-332.
- ¹¹ de Lange, E. C., de Boer, A. G., Breimer, D. D. (1998). Intercerebral microdialysis. In W. M. Pardridge, *Introduction to Blood-Brain Barrier*. Cambridge: Cambridge University Press. 94-112.
- ¹² Rosenbloom, A. J., Sipe, D. M., Weedn, V. W. (2005). Microdialysis of proteins: Performance of CMA/20 probe. *Journal of Neuroscience Methods*, 148, 147-153.
- ¹³ *CMA Microdialysis*. (n.d.). Retrieved 2010, from <http://www.microdialysis.se/>

- ¹⁴ Pardridge, W. M. (2005). The Blood-Brain Barrier: Bottleneck in Brain Drug Development. *The Journal of the American Society for Experimental NeuroTherapeutics*, 2, 3-14.
- ¹⁵ Masamoto, K., Kershaw, J., Ureshi, M., Takizawa, N., Kobayashi, H., Tanishita, K., Kanno, I. (2007). Apparent diffusion time of oxygen from blood to tissue in rat cerebral cortex: implication for tissue oxygen dynamics during brain functions. *Journal of Applied Physiology*, 103, 1352-1358.
- ¹⁶ Stolzrnburg, J., Reichenbach, A., Neumann, M. (1989). Size and Density of Glial and Neuronal Cells within the Cerebral Neocortex of Various Insectivorian Species. *Glia*, 2 (2), 78-84.
- ¹⁷ Barres, B. A. (2008). The Mystery and Magic of Glia: A Perspective on Their Roles in Health and Disease. *Neuron*, 60 (3), 430-440.
- ¹⁸ McCabe, W. L., Smith, J. C., Harriott, P. (2005). Unit Operations in Chemical Engineering. New York: McGraw-Hill.
- ¹⁹ Sakima A, Teruya H, Yamazato M, Matayochi R, Mauratani H, Fukiyama K. (1998). Prolonged NOS inhibition in the brain elevates blood pressure in normotensive rats. *The American Journal of Physiology*. 275,410-417.
- ²⁰ McNay, Ewan. Personal Communication, 2011.
- ²¹ Kehr, J. (1993). A survey on quantitative microdialysis: theoretical models and practical implications. *Journal of Neuroscience Methods*, 48, 251-264.
- ²² Lindefors, N., Amberg, G., Ungerstedt, U. (1989). Intracerebral microdialysis. I. Experimental studies of Diffusion Kinetics. *Journal of Pharmacological Methods*, 22, 141-156.
- ²³ Zetterström, T., Vernet, L., Ungerstedt, U., Tossman, U., Jonzon, B., Fredholm, B. B. (1982). Purin Levels in the Intact Rat Brain. Studies with an Implanted Perfused Hollow Fibre. *Neuroscience Letters*, 29, 111-15.
- ²⁴ Jacobson, I., Sandberg, M., Hamberger, A. (1985). Mass transfer in brain dialysis devices a new method for the estimation of extracellular amino acids concentration. *Journal of Neuroscience Methods*, 15, 263-268.
- ²⁵ Bungay, P.M., Morrison, P.F., Dedrick R.L. (1990). Steady-state theory for quantitative microdialysis of solutes and water in vivo and in vitro. *Life Science*, 46, 105-119.
- ²⁶ Norton, L. W., Yuan, F., Reichert, W. M. (2007). Glucose Recovery with Bare and Hydrogel-Coated Microdialysis Probes: Experiment and Simulation of Temporal Effects. *Analytical Chemistry*, 79, 445-452.
- ²⁷ Wang, M., Roman, F. T., Schultz, K., Jennings, C., Kennedy, T. (2008). Improved Temporal Resolution for in Vivo Microdialysis by Using Segmented Flow. *Analytical Chemistry*. 80, 5607-5615.
- ²⁸ Huebner, K. H., Thornton, E. A., Byrom, T. G. (1995). *The Finite Element Method for Engineers*. New York: Wiley-Interscience.

- ²⁹ Rao, S. S. (1982). *The Finite Element Method in Engineering*. Oxford: Pergamon.
- ³⁰ Ottosen, N., & Petersson, H. (1992). *Introduction to the Finite Element Method*. Great Britain: Prentice Hall.
- ³¹ Rice, R. G., Do, D. D. (1995). *Applied Mathematical and Modeling for Chemical Engineers*. New York: Wiley-Interscience.
- ³² Buttler, T., Nilsson, C., Gorton, L., Marko-Varga, G., & Laurell, T. (1996). Membrane characterization and performance of microdialysis probes intended for use as bioprocess sampling units. *Journal of Chromatography A*, 725, 41-56.
- ³³ Aspen Tech HYSYS. Burlington, Massachusetts.
- ³⁴ Peng, D., Robinson, D. B. (1976), A New Two-Constant Equation of State. *Industrial & Engineering Chemistry Fundamentals*, 15 (1), 59-64.
- ³⁵ Dykstra, K. H., Hsiao, J. K., Morrison, P. F., Bungay, P. M., Mefford, I. N., Scully, M. M., Dedrick, R. L. (1992). Quantitative examination of tissue concentration profiles associated with microdialysis. *J. Neurochemistry*. 58 (3), 931-940.
- ³⁶ COMSOL Multiphysics 4.2, see <http://www.comsol.com/>
- ³⁷ Matin, G. E., Papp, N. L. (1979). Effect on core Temperature of Restraint after peripherally and Centrally Injected Morphine in the Sprague-Dawley Rat. *Pharmacology, Biochemistry & Behavior*, 10, 313-315.
- ³⁸ Muller, M. (2000). Microdialysis in clinical drug delivery studies. *Advanced Drug Delivery Reviews*, 45, 255-269.
- ³⁹ Duva, M. A., Tomkins, E. M., Moranda, L. M., Kaplan, R., Sukhaseum, A., Jimenez, A., Stanley, B. G. (2001). Reverse microdialysis of N-methyl-D-aspartic acid into the lateral hypothalamus of rats: effects on feeding and other behaviors. *Brain Research*, 921 (1-2), 122-132.
- ⁴⁰ Leal, L. G. (2007). *Advanced Transport Phenomena*. Cambridge: Cambridge University Press. Pp166-175.
- ⁴¹ Taylor Dispersion Technique, *Complex Fluids*, 2009. Web. Feb 2011. <<http://www.fisica.unam.mx/liquids/taylor.php>>.
- ⁴² Ananthakrishnan, V., Gill, W. N., Barduhn, A. J. (1965). *AIChE Journal*, 11, 1063-1072.



Boundary conditions for Stokes Creep Flow (Equation 3).
Model is not shown to scale.



Boundary conditions for Conservation of Mass Equation (Equation 4).
Model is not shown to scale.

Mass Balance

Mass balance conducted on each subdomain (normal mesh)				negative flux is toward the center or down					
Values calculated are either r or z fluxes, depending on boundary				positive flux is up and outward					
2-D									
Perfusate				Membrane					
Boundary Areas (m ²)	Inlet	Inner Wall	Outlet	Membrane	Boundary Areas (m ²)	Bottom	Perfusate	Top	Brain
cOP (mM)	Flux (mol/m ² s)				cOP (mM)	Flux (mol/m ² s)			
0.5	9.36E-05	-2.91E-09	1.28E-04	-7.67E-07	0.5	3.27E-08	-7.67E-07	3.21E-09	-6.48E-07
1	1.87E-04	-9.71E-10	1.99E-04	-2.56E-07	1	1.09E-08	-2.56E-07	1.07E-09	-2.16E-07
1.25	2.34E-04	3.58E-18	2.35E-04	1.25E-15	1.25	-7.46E-17	1.25E-15	1.68E-18	1.05E-15
1.5	2.81E-04	9.71E-10	2.70E-04	2.56E-07	1.5	-1.09E-08	2.56E-07	-1.07E-09	2.16E-07
2	3.75E-04	2.91E-09	3.42E-04	7.67E-07	2	-3.27E-08	7.67E-07	-3.21E-09	6.48E-07
Flux for cOP = 0.5 mM									
mol/s	8.37E-12	6.86E-15	1.14E-11	3.03E-12	Flux for cOP = 0.5 mM				
pmol/s	8.374	0.007	11.440	3.035	mol/s	1.89E-15	3.03E-12	1.86E-16	3.05E-12
pmol/min	502.4	0.4	686.4	182.1	pmol/s	0.002	3.035	0.000	3.054
Flux Direction	In	Out	Out	In	pmol/min	0.1	182.1	0.0	183.3
Total Mass Balance (pmol/min)				-2.3	Total Mass Balance (pmol/min)				
					1.3				

Brain								
Boundary Areas (m ²)	Membrane	Top	Casing	Out Bottom	Bottom	Center	Top Bottom	In Bottom
cOP (mM)	Flux (mol/m ² s)			Flux (mol/m ² s)				
0.5	-6.48E-07	4.34E-09	-5.51E-07	-6.46E-08	1.85E-08	9.83E-11	1.31E-08	-1.77E-07
1	-2.16E-07	1.45E-09	-1.84E-07	-2.15E-08	6.15E-09	3.28E-11	4.38E-09	-5.90E-08
1.25	1.05E-15	2.28E-18	9.16E-16	1.40E-17	-3.91E-18	-2.19E-20	-2.73E-18	2.37E-17
1.5	2.16E-07	-1.45E-09	1.84E-07	2.15E-08	-6.15E-09	-3.28E-11	-4.38E-09	5.90E-08
2	6.48E-07	-4.34E-09	5.51E-07	6.46E-08	-1.85E-08	-9.83E-11	-1.31E-08	1.77E-07
Flux for cOP = 0.5 mM								
mol/s	3.05E-12	3.75E-16	3.14E-12	6.08E-15	5.22E-15	0.00E+00	2.58E-15	6.95E-15
pmol/s	3.054	0.000	3.140	0.006	0.005	0.000	0.003	0.007
pmol/min	183.3	0.0	188.4	0.4	0.3	0.0	0.2	0.4
Flux Direction	Out	Out	In	In	In	Out	Out	Out
Total Mass Balance (pmol/min)				5.2				

Mass Balance

%RIB	0.602%
------	--------

For those not familiar with COMSOL 4.2 Creating a CMA-12 Brain-Probe System

Open COMSOL 4.2

From the **Model Wizard** window, select **2D axisymmetric** and press **next** (light blue arrow)

From the **Add Physics** tree, select **Fluid Flow>Single-Phase Flow>Creeping Flow (spf)**

Click the **Add Selected** button at the bottom (light blue plus sign)

From the **Add Physics** tree, select **Chemical Species Transport>Transport of Diluted Species (chds)**

Press the **Add Selected** button, then press **next**

From the **Studies** tree, select **Preset Studies for Selected Physics>Stationary**

Press **Finish** (checkered flag) to start modeling

In the **Model Builder** window, right-click **Global Definitions** and choose **Parameters**

Go to the **Settings** window for **Parameters**

In the **Parameters** table, enter the following settings (the name column is case sensitive)

Name	Expression	Description (optional)
V	1.67e-11 [m ³ /s]	Volumetric flow rate, perfusate
rhoP	990 [kg/m ³]	Density, perfusate
etaP	7.28e-4 [kg/(m*s)]	Dynamic viscosity, perfusate
c0P	0.5 [mol/m ³]	Initial concentration, perfusate
c0B	1.25 [mol/m ³]	Initial concentration, brain
cC	1.25 [mol/m ³]	Concentration in sampling fluid
DP	8.3e-10 [m ² /s]	Diffusion coefficient, perfusate
DM	7.62e-11 [m ² /s]	Diffusion coefficient, membrane
DB	1.16e-10 [m ² /s]	Diffusion coefficient, brain

(If you intend to make any more models in the future, it may be beneficial to save your parameters as a text file. You can do this by selecting the **Save to file** button (looks like a floppy disk) located under the parameters table.)

Modeling the System

From the **Model Builder** window, select **Geometry 1**

In the **Settings** window for Geometry, change the **Length Unit** from **m** to **μm**

From the **Model Builder** window, right-click **Geometry 1** and choose **Rectangle**

In the **Settings** window for Rectangle, enter the following dimensions:

Width: 85

Height: 3000

Base: Corner

r: 125

z: 0

For those not familiar with COMSOL 4.2

From the **Model Builder** window, right-click **Geometry 1** and choose **Rectangle**
In the **Settings** window for Rectangle, enter the following dimensions:

Width: 40
Height: 3000
Base: Corner
r: 210
z: 0

From the **Model Builder** window, right-click **Geometry 1** and choose **Rectangle**
In the **Settings** window for Rectangle, enter the following dimensions:

Width: 50
Height: 3025
Base: Corner
r: 250
z: -25

From the **Model Builder** window, right-click **Geometry 1** and choose **Rectangle**
In the **Settings** window for Rectangle, enter the following dimensions:

Width: 300
Height: 50
Base: Corner
r: 0
z: -75

From the **Model Builder** window, right-click **Geometry 1** and choose **Boolean Operation>Union**

In the **Graphics** window, left-click on the right most rectangle (**r3**) (the domain should turn red) and then right-click the same rectangle (the domain should turn blue and is now added to the **Input objects** list in the **Settings** window). Repeat this step for **r4**, the lowest rectangle.

The **Input objects** list should now contain: **r3** and **r4**

Uncheck the **Keep interior boundaries** box

From the **Model Builder** window, select **Form Union**

In the **Settings** window for Finalize, select **Build Selected** (the light blue skyscraper with red box, near the top)

In the **Model Builder** window, minimize the **Geometry 1** menu (white downward arrow head next to **Geometry 1**)

You now have a 2D representation of the brain-probe system that will produce accurate results. The inner (left most) rectangle is the perfusate domain. Fluid will come in from the bottom and exit to top. The middle rectangle is the membrane. And the backwards-L-

For those not familiar with COMSOL 4.2

shaped domain is the brain. When solving, COMSOL will “wrap” this 2D section around the $r=0$ axis (red dashed line) to form a 3D cylinder. We can use the 2D axisymmetric model because the system is angle independent. Now you will assign domain and boundary conditions to the geometry.

Perfusate Settings

From the **Model Builder** window, select **Creeping Flow**

In the **Settings** window, use the control button on your keyboard to simultaneously select the following **Domains**: 1, 3

Press the **Remove from Selection** button (light blue minus sign to the right of the selection field)

*You may have to scroll the **Settings** window over to see the button.*

In the **Settings** window, under **Physical Model**, change **Compressibility** to **Incompressible flow**

Expand the **Creeping Flow** menu by clicking the rightward facing arrow next to **Creeping Flow**

From the **Model Builder** window, select **Creeping Flow>Fluid Properties 1**

In the **Settings** window, change **Density** to **User defined** and enter “rhoP” into the edit field (*do not include the quotation marks*)

In the **Settings** window, change **Dynamic viscosity** to **User defined** and enter “etaP” into the edit field

You have just assigned conditions of incompressible creep fluid flow to the probe. We do not do this for the other parts of the model because the brain and membrane do not contain fluid flow. The next step is assigning the boundary conditions governing the flow of the perfusate.

From the **Model Builder** window, right-click **Creeping Flow** and select **Inlet**

In the **Graphics** window, left-click the bottom boundary of **r1** (the perfusate domain) and then right-click

In the **Settings** window, the **Boundary Selection** list should now contain: 5

In the **Settings** window, under **Boundary Conditions**, change **Boundary Condition** to **Laminar inflow**

Under **Laminar Inflow**, select **Flow rate** and then enter “V” into the V_0 edit field

Enter “0” into the L_{entr} edit field and select the box next to **Constrain endpoints to zero**

From the **Model Builder** window, right-click **Creeping Flow** and select **Outlet**

In the **Graphics** window, left-click the top boundary of **r1** (the perfusate domain) and the right-click it

In the **Settings** window, the **Boundary Selection** list should now contain: 6

Minimize the **Creeping Flow** menu

For those not familiar with COMSOL 4.2

Expand the **Transport of Diluted Species** menu

From the **Model Builder** window, right-click **Convection and Diffusion 1** and select **Rename**

F2 is the shortcut key for renaming an item.

Change the name to **Perfusate** and press **OK**

In the **Settings** window, under **Model Inputs**, change the **Velocity field** to **Velocity Field (spf/fp1)**

In the **Settings** window, under **Diffusion**, enter “DP” into the **Diffusion coefficient** edit field

From the **Model Builder** window, right-click **Initial Values 1** and select **Rename**

Change the name to **Initial Perf/Memb Values** and press **OK**

In the **Settings** window, under **Initial**, enter “c0P” into the **Concentration** edit field

From the **Model Builder** window, right-click **Transport of Diluted Species** and select **Inflow**

In the **Graphics** window, left-click the bottom boundary of **r1** (the perfusate domain) and then right-click

In the **Settings** window, the **Boundary Selection** list should now contain: 5

In the **Settings** window, under **Concentration**, enter “c0P” into the **c_{0,c}** edit field

From the **Model Builder** window, right-click **Transport of Diluted Species** and select **Outflow**

In the **Graphics** window, left-click the top boundary of **r1** (the perfusate domain) and the right-click it

In the **Settings** window, the **Boundary Selection** list should now contain: 6

Membrane Settings

From the **Model Builder** window, right-click **Transport of Diluted Species** and select **Convection and Diffusion**

From the **Model Builder** window, right-click **Convection and Diffusion 2** and select **Rename**

Change the name to **Membrane** and press **OK**

In the **Graphics** window, left-click the middle rectangle (**r2**) and then right-click it

In the **Settings** window, the **Boundary Selection** list should now contain: 3

In the **Settings** window, under **Diffusion**, enter “DM” into the **Diffusion coefficient** edit field

Brian Settings

From the **Model Builder** window, right-click **Transport of Diluted Species** and select **Convection and Diffusion**

From the **Model Builder** window, right-click **Convection and Diffusion 3** and select **Rename**

Change the name to **Brain** and press **OK**

In the **Graphics** window, left-click the backwards-L-shaped domain and then right-click it

In the **Settings** window, the **Boundary Selection** list should now contain: 1

In the **Settings** window, under **Diffusion**, enter “DB” into the **Diffusion coefficient** edit field

From the **Model Builder** window, right-click **Transport of Diluted Species** and select **Initial Values**

From the **Model Builder** window, right-click **Initial Values 2** and select **Rename**

Change the name to **Initial Brain Values** and press **OK**

In the **Graphics** window, left-click the backwards-L-shaped domain and then right-click it

In the **Settings** window, the **Boundary Selection** list should now contain: 1

In the **Settings** window, under **Initial**, enter “c0B” into the **Concentration** edit field

From the **Model Builder** window, right-click **Transport of Diluted Species** and select **Concentration**

In the **Graphics** window, alternatively left- and right-click the two right most and the lowest boundary and then right-click them (*the second right most boundary is small and at the bottom*)

In the **Settings** window, the **Boundary Selection** list should now contain: 2, 13 and 14

In the **Settings** window, under **Concentration**, select the box next to **Species c** and enter “cC” into the $c_{0,c}$ edit field

Minimize the **Transport of Diluted Species** menu

Mesh

Now you have set up all the physics governing the system. Next, a mesh must be created which COMSOL will solve the equations over and then solve the problem. Fortunately, COMSOL has suggested meshes for certain physics and geometries. The suggestion works for our case and is the default mesh; so you do not have to do anything.

From the **Model Builder** window, select **Mesh 1**

In the **Settings** window, make sure the **Sequencing type** reads **Physics-controlled mesh** and the **Element size** is **Normal**

For those not familiar with COMSOL 4.2

Solving

From the **Model Builder** window, right-click **Study 1** and select **Parametric Sweep**

In the **Settings** window, select the **Add** button (light blue plus sign)

Select **c0P (Initial concentration, perfusate)** from the list and press **OK**

In the **Parameter Values** edit field, enter the inlet concentrations you are using for the ZNF method, separating each concentration by a space

For example, entering: “0.5 1 1.5 2” will tell COMSOL to run the model 4 times with each run having one of the following inlet concentrations: 0.5 mM, 1.0 mM, 1.5 mM and 2.0 mM

From the toolbar, select **Compute** (green equal sign)

Postprocessing

COMSOL should automatically produce both 2D and 3D solutions which can be found in the Results tab in the Model Builder. If they are not automatically produced, follow the below directions as examples of possible result graphics.

To see the 2D velocity profile:

From the **Model Builder** window, right-click **Results** and select **2D Plot Group**

From the **Model Builder** window, right-click **2D Plot Group 1** and select **Rename**

Change the name to **Velocity** and press **OK**

From the **Model Builder** window, right-click **Velocity** and select **Surface**

In the **Settings** window, select **Plot** (rainbow and pencil at top)

Minimize the **Velocity** menu

To see the 3D velocity profile:

From the **Model Builder** window, right-click **Results** and select **3D Plot Group**

From the **Model Builder** window, right-click **3D Plot Group 1** and select **Rename**

Change the name to **Velocity** and press **OK**

From the **Model Builder** window, right-click **Velocity** and select **Surface**

In the **Settings** window, select **Plot** (rainbow and pencil at top)

Minimize the **Velocity** menu

For those not familiar with COMSOL 4.2

To see the 2D concentration profile:

From the **Model Builder** window, right-click **Results** and select **2D Plot Group**
 From the **Model Builder** window, right-click **2D Plot Group 1** and select **Rename**
 Change the name to **Concentration** and press **OK**
 From the **Model Builder** window, right-click **Concentration** and select **Surface**
 In the **Settings** window, under **Expression**, select **Replace Expression** (green and orange triangles)
 Select **Transport of Diluted Species>Species c>Concentration (c)**
 In the **Settings** window, select **Plot** (rainbow and pencil at top)
 Minimize the **Concentration** menu

To see the 3D concentration profile:

From the **Model Builder** window, right-click **Results** and select **3D Plot Group**
 From the **Model Builder** window, right-click **3D Plot Group 1** and select **Rename**
 Change the name to **Concentration** and press **OK**
 From the **Model Builder** window, right-click **Concentration** and select **Surface**
 In the **Settings** window, under **Expression**, select **Replace Expression** (green and orange triangles)
 Select **Transport of Diluted Species>Species c>Concentration (c)**
 In the **Settings** window, select **Plot** (rainbow and pencil at top)
 Minimize the **Concentration** menu

To change which value of c_0P is shown (for any graphic):

From the **Model Builder** window, select **Concentration**
 In the **Settings** window, under **Data**, select the desired **c_0P** from the **Parameter Value** drop down menu
 In the **Settings** window, select **Plot** (rainbow pencil near top)

To find the concentration of glucose at the outlet of the Perfusate:

From the **Model Builder** window, right-click **Results>Derived Values** and select **Average>Line Average**
 In the **Graphics** window, left-click the top boundary of **r1** (the perfusate domain) and the right-click it
 In the **Settings** window, the **Boundary Selection** list should now contain: 6
 In the **Settings** window, under **Expression**, select **Replace Expression** (green and orange triangles)
 Select **Transport of Diluted Species>Species c>Concentration (c)**
 Select **Evaluate (New Table)** (orange equal sign at top)

Appendix D

88

For those familiar with COMSOL 4.2

Creating a CMA-12 Brain Probe

Space Dimension: **2D axisymmetric**

Physics: **Creeping Flow (spf), Transport of Diluted Species (chds)**

Study: **Stationary (Preset for Selected Physics)**

Parameters

Add these under global definitions

Name	Expression	Description (optional)
V	1.67e-11 [m ³ /s]	Volumetric flow rate, perfusate
rhoP	990 [kg/m ³]	Density, perfusate
etaP	7.28e-4 [kg/(m*s)]	Dynamic viscosity, perfusate
c0P	0.5 [mol/m ³]	Initial concentration, perfusate
c0B	1.25 [mol/m ³]	Initial concentration, brain
cC	1.25 [mol/m ³]	Concentration in sampling fluid
DP	8.3e-10 [m ² /s]	Diffusion coefficient, perfusate
DM	7.62e-11 [m ² /s]	Diffusion coefficient, membrane
DB	1.16e-10 [m ² /s]	Diffusion coefficient, brain

Geometry

Length Unit: **μm**

Geometries:

Perfusate (r1)	Membrane (r2)	Side of Brain (r3)	Bottom of Brain (r4)
Shape: rectangle	Shape: rectangle	Shape: rectangle	Shape: rectangle
Width: 85	Width: 40	Width: 50	Width: 300
Height: 3000	Height: 3000	Height: 3025	Height: 50
Base: Corner	Base: Corner	Base: Corner	Base: Corner
r: 125	r: 210	r: 250	r: 0
z: 0	z: 0	z: -25	z: -75

Create a **Boolean Union** between **r3** and **r4**. Do NOT keep **Interior Boundaries**

Finalize the geometry with **Form a Union**

Physics

Creeping Flow (domain 2):

Compressibility: **Incompressible flow**

Fluid Properties:

Density: **User defined:** “rhoP”

Dynamic viscosity: **User defined:** “etaP”

Inlet (boundary 5):

Boundary Condition: **Laminar Inflow**

Laminar Inflow: **Flow rate**

Flow rate: “V”

Entrance length: “0”

Constrain endpoints to zero: \checkmark

Outlet (boundary 6):

Boundary Condition: **Pressure, no viscous stress**

Pressure: “0”

Transport of Diluted Species (domains 1,2,3)

Convection: \checkmark

Convection and Diffusion 1:

Velocity field: **Velocity field (spf/fp1)**

Diffusion coefficient: **User defined:** “DP”

Initial Values 1:

Concentration: “c0P”

Inflow 1 (boundary 5):

c_{0,c}: “c0P”

Outflow 1 (boundary 6)

Convection and Diffusion 2 (domain 3):

Velocity field: “0” r

“0” z

Diffusion coefficient: **User defined:** “DM”

Convection and Diffusion 3 (domain 1):

Velocity field: “0” r

“0” z

Diffusion coefficient: **User defined:** “DB”

Initial Values 2 (domain 1):

Concentration: “c0B”

Concentration 1 (boundaries 2,13,14):

Species c: \checkmark

c_{0,c}: “cC”

For those familiar with COMSOL 4.2

Mesh

Sequence type: **Physics-controlled mesh**

Element size: **Normal**

Solving

If using model for ZNF, use a **Parametric Sweep** to vary **c0P**

Postprocessing

COMSOL should automatically plot 2D and 2D results for both velocity and concentration.

To determine outlet analyte concentration:

Select the following boundary: 6

Create a **Line Average** from **Results>Derived Values>Averages**

Change the **Expression** to **Transport of Diluted Species>Species c>Concentration (c)**

.

Creating a Microdialysis Probe

This is to be used when you are working with a probe that has the same basic structure as the CMA-12 but different dimensions, ie. a CMA-10

These instructions are to be used in conjunction with another instruction. Start in the other instructions, set up the basic physics, and when you get to the Parameters section, start here.

Parameters

Add these under global definitions. The following values are for a CMA-12 probe and should be adjusted for the appropriate system.

Name	Expression	Description (optional)
V	1.67e-11 [m ³ /s]	Volumetric flow rate, perfusate
rhoP	990 [kg/m ³]	Density, perfusate
etaP	7.28e-4 [kg/(m*s)]	Dynamic viscosity, perfusate
c0P	0.5 [mol/m ³]	Initial concentration, perfusate
c0B	1.25 [mol/m ³]	Initial concentration, brain
cC	1.25 [mol/m ³]	Concentration in sampling fluid
DP	8.3e-10 [m ² /s]	Diffusion coefficient, perfusate
DM	7.62e-11 [m ² /s]	Diffusion coefficient, membrane
DB	1.16e-10 [m ² /s]	Diffusion coefficient, brain
wa	8.5e-5 [m]	Width of annulus, active region of probe
hM	.003 [m]	Membrane height
off	1.25e-4 [m]	Distance inner wall of annulus if from center of probe
wM	4e-5 [m]	Membrane width

Geometry

Length Unit: μm

Geometries:

Perfusate (r1)	Membrane (r2)	Side of Brain (r3)	Bottom of Brain (r4)
Shape: rectangle	Shape: rectangle	Shape: rectangle	Shape: rectangle
Width: wa	Width: wM	Width: wB	Width: off+wa+wM+wB
Height: hM	Height: hM	Height: wB+base	Height: wB
Base: Corner	Base: Corner	Base: Corner	Base: Corner
x: off	x: off+wa	x: off+wa+wM	x: 0
y: 0	y: 0	y: -base	y: -base-wB

Create a **Boolean Union** between **r3** and **r4**. Do NOT keep **Interior Boundaries**

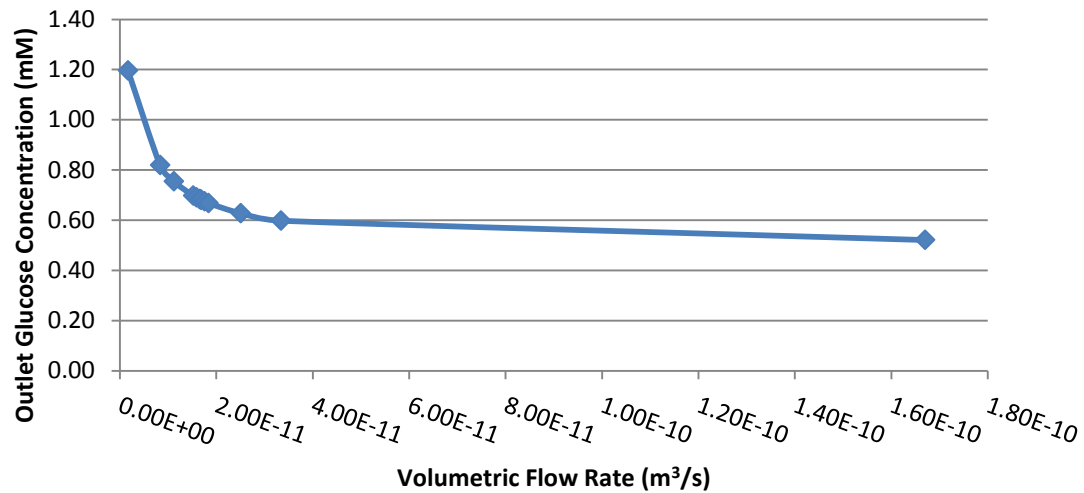
Finalize the geometry with **Form a Union**

Now continue with the other instructions starting at Perfusate Settings

Sensitivity Data

In all analyses, $C_{in} = 0.5 \text{ mM}$
Sensitivity of Outlet Glucose Concentration to:

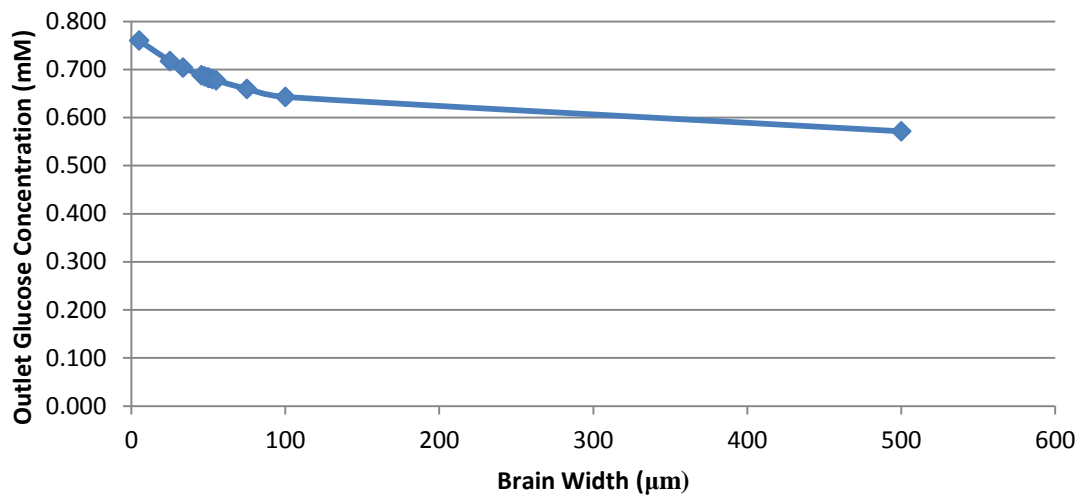
Inlet Flow Rate			
% off norm	V (m ³ /s)	Co (mM)	% c off norm
10	1.67E-12	1.196371648	175.3
50	8.35E-12	0.819496487	120.1
67	1.12E-11	0.754872636	110.6
91	1.52E-11	0.697953383	102.2
95	1.59E-11	0.690837086	101.2
99	1.65E-11	0.684213152	100.2
100	1.67E-11	0.682628216	100.0
101	1.69E-11	0.681070261	99.8
105	1.75E-11	0.675095027	98.9
110	1.84E-11	0.668157966	97.9
150	2.51E-11	0.627697607	92.0
200	3.34E-11	0.598220227	87.6
1000	1.67E-10	0.521500262	76.4



Sensitivity Data

In all analyses, $C_{in} = 0.5 \text{ mM}$
Sensitivity of Outlet Glucose Concentration to:

Brain Width			
% off norm	wB (μm)	Co (mM)	% c off norm
10	5.0	0.760106855	111.4
50	25.0	0.71727512	105.1
67	33.5	0.703741017	103.1
91	45.5	0.687821859	100.8
95	47.5	0.685466335	100.4
99	49.5	0.68318767	100.1
0	50.0	0.682628223	100.0
101	50.5	0.682095834	99.9
105	52.5	0.679913196	99.6
110	55.0	0.677261851	99.2
150	75.0	0.659318232	96.6
200	100.0	0.642652459	94.1
1000	500.0	0.571224998	83.7

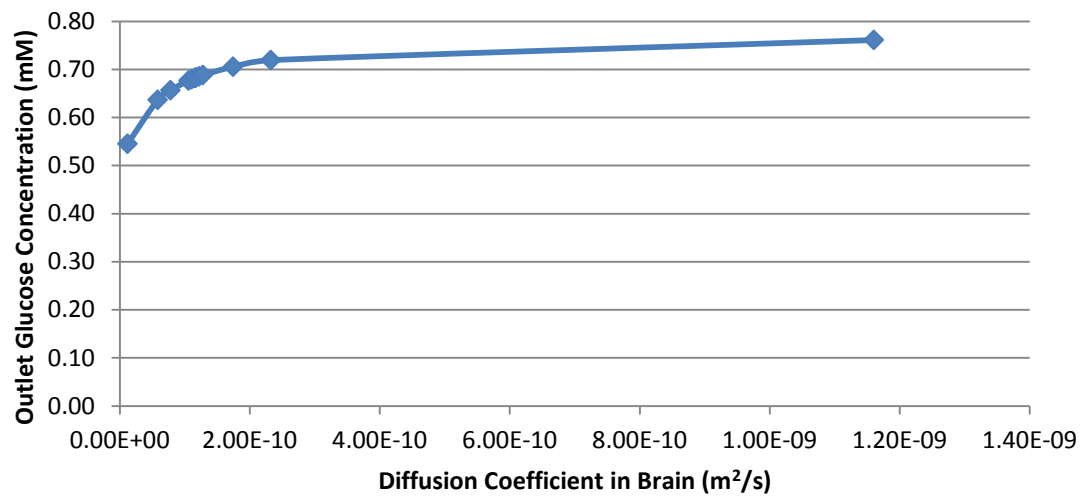


Sensitivity Data

In all analyses, $C_{in} = 0.5 \text{ mM}$
Sensitivity of Outlet Glucose Concentration to:

Diffusion Coefficient in Brain

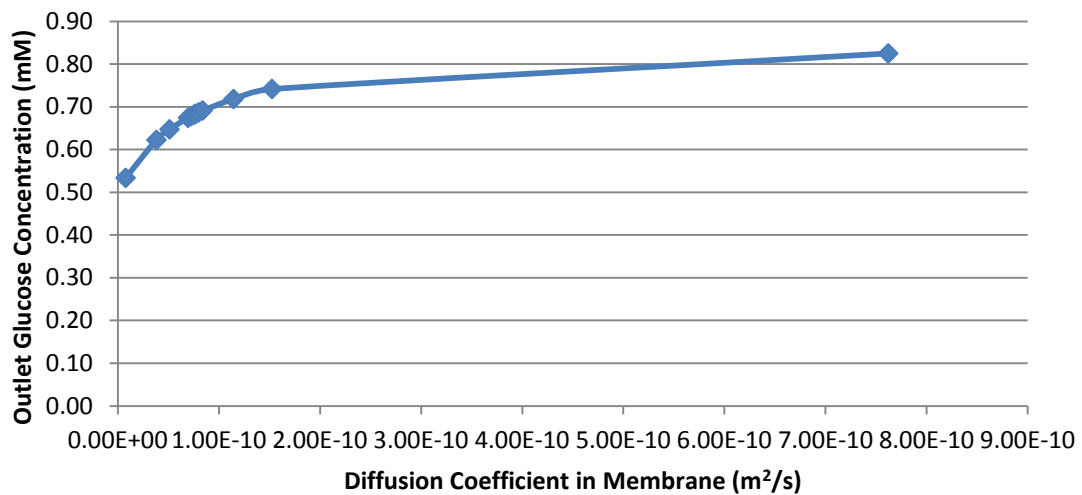
% off norm	$D_B \text{ (m}^2\text{/s)}$	$C_o \text{ (mM)}$	% c off norm
10	1.16E-11	0.545311844	79.9
50	5.80E-11	0.636711234	93.3
67	7.77E-11	0.656719474	96.2
91	1.06E-10	0.67676442	99.1
95	1.10E-10	0.679460428	99.5
99	1.15E-10	0.68201167	99.9
0	1.16E-10	0.682628216	100.0
101	1.17E-10	0.683236593	100.1
105	1.22E-10	0.685591572	100.4
110	1.28E-10	0.688369632	100.8
150	1.74E-10	0.705589725	103.4
200	2.32E-10	0.719357181	105.4
1000	1.16E-09	0.761218841	111.5



Sensitivity Data

In all analyses, $C_{in} = 0.5 \text{ mM}$
Sensitivity of Outlet Glucose Concentration to:

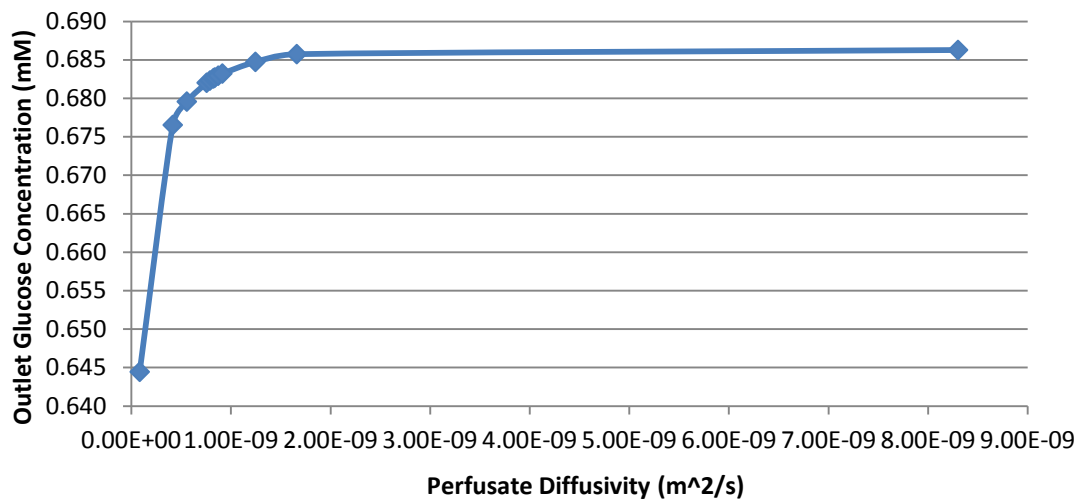
Diffusion Coefficient in Membrane			
% off norm	$D_M (\text{m}^2/\text{s})$	$C_o (\text{mM})$	% c off norm
10	7.62E-12	0.53357684	78.2
50	3.81E-11	0.622428341	91.2
67	5.11E-11	0.647126927	94.8
91	6.93E-11	0.674121608	98.8
95	7.24E-11	0.67804422	99.3
99	7.54E-11	0.6816836	99.9
0	7.62E-11	0.682629269	100.0
101	7.70E-11	0.683564803	100.1
105	8.00E-11	0.686985485	100.6
110	8.38E-11	0.691129452	101.2
150	1.14E-10	0.718040094	105.2
200	1.52E-10	0.741566103	108.6
1000	7.62E-10	0.824792021	120.8



Sensitivity Data

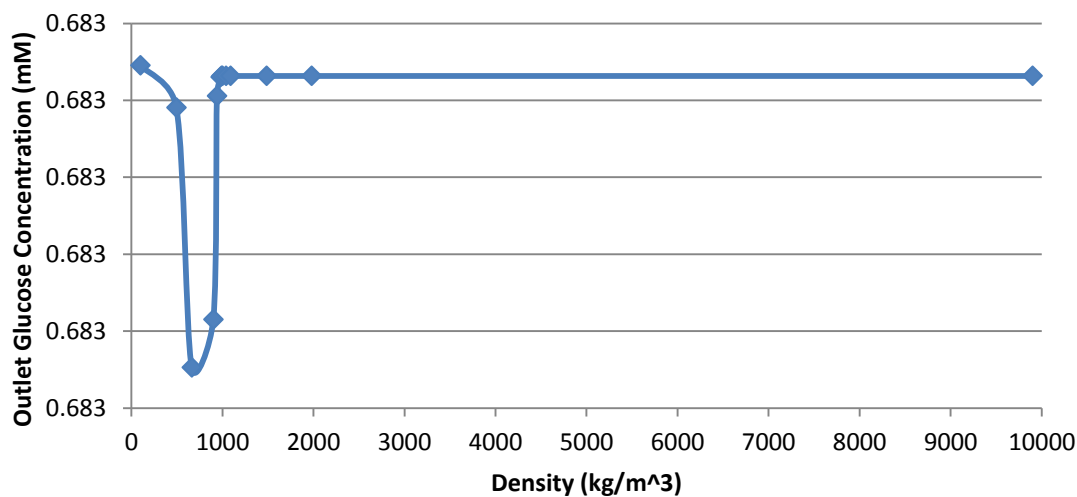
In all analyses, $C_{in} = 0.5 \text{ mM}$
Sensitivity of Outlet Glucose Concentration to:

Diffusion Coefficient in Perfusate			
% off norm	$D_p \text{ (m}^2/\text{s)}$	$C_o \text{ (mM)}$	% c off norm
10	8.30E-11	0.644430147	94.4
50	4.15E-10	0.676519387	99.1
67	5.56E-10	0.679560704	99.6
91	7.55E-10	0.682005735	99.9
95	7.89E-10	0.68229671	100.0
99	8.22E-10	0.682564558	100.0
0	8.30E-10	0.682628216	100.0
101	8.38E-10	0.682690626	100.0
105	8.72E-10	0.682928469	100.0
110	9.13E-10	0.683201525	100.1
150	1.25E-09	0.684721967	100.3
200	1.66E-09	0.68573044	100.5
1000	8.30E-09	0.68626844	100.5



In all analyses, $C_{in} = 0.5 \text{ mM}$
Sensitivity of Outlet Glucose Concentration to:

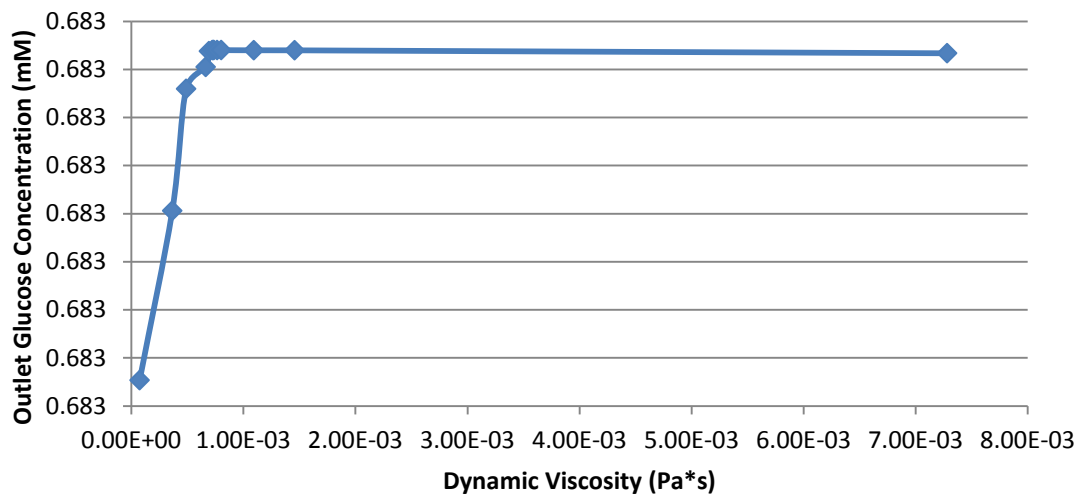
Perfusate Density			
% off norm	rhoP (kg/m ³)	Co (mM)	% c off norm
10	99.0	0.682628223	100.0
50	495.0	0.682628195	100.0
67	663.3	0.682628026	100.0
91	900.9	0.682628058	100.0
95	940.5	0.682628203	100.0
99	980.1	0.682628215	100.0
0	990.0	0.682628216	100.0
101	999.9	0.682628216	100.0
105	1039.5	0.682628216	100.0
110	1089.0	0.682628216	100.0
150	1485.0	0.682628216	100.0
200	1980.0	0.682628216	100.0
1000	9900.0	0.682628216	100.0



Sensitivity Data

In all analyses, $C_{in} = 0.5 \text{ mM}$
Sensitivity of Outlet Glucose Concentration to:

Perfusate Viscosity			
% off norm	etaP (Pa*s)	Co (mM)	% c off norm
10	7.28E-05	0.682628216	100.0
50	3.64E-04	0.682628216	100.0
67	4.88E-04	0.682628216	100.0
91	6.62E-04	0.682628216	100.0
95	6.92E-04	0.682628216	100.0
99	7.21E-04	0.682628216	100.0
0	7.28E-04	0.682628216	100.0
101	7.35E-04	0.682628216	100.0
105	7.64E-04	0.682628216	100.0
110	8.01E-04	0.682628216	100.0
150	1.09E-03	0.682628216	100.0
200	1.46E-03	0.682628216	100.0
1000	7.28E-03	0.682628216	100.0



Creating a Transient CMA-12 Brain-Probe System

For those not familiar with COMSOL 4.2

Open COMSOL 4.2

From the **Model Wizard** window, select **2D axisymmetric** and press **next** (light blue arrow)

From the **Add Physics** tree, select **Fluid Flow>Single-Phase Flow>Creeping Flow (spf)**

Click the **Add Selected** button at the bottom (light blue plus sign)

From the **Add Physics** tree, select **Chemical Species Transport>Transport of Diluted Species (chds)**

Press the **Add Selected** button, then press **next**

From the **Studies** tree, select **Preset Studies for Selected Physics>Time Dependent**

Press **Finish** (checkered flag) to start modeling

In the **Model Builder** window, right-click **Global Definitions** and choose **Parameters**

Go to the **Settings** window for **Parameters**

In the **Parameters** table, enter the following settings (the name column is case sensitive)

Name	Expression	Description (optional)
V	1.67e-11 [m ³ /s]	Volumetric flow rate, perfusate
rhoP	990 [kg/m ³]	Density, perfusate
etaP	7.28e-4 [kg/(m*s)]	Dynamic viscosity, perfusate
c0P	0.5 [mol/m ³]	Initial concentration, perfusate
c0B	1.25 [mol/m ³]	Initial concentration, brain
cC	1.25 [mol/m ³]	Concentration in sampling fluid
DP	8.3e-10 [m ² /s]	Diffusion coefficient, perfusate
DM	7.62e-11 [m ² /s]	Diffusion coefficient, membrane
DB	1.16e-10 [m ² /s]	Diffusion coefficient, brain

(If you intend to make any more models in the future, it may be beneficial to save your parameters as a text file. You can do this by selecting the **Save to file** button (looks like a floppy disk) located under the parameters table.)

In the **Model Builder** window, right-click **Global Definitions** and choose

Functions>Piecewise

From the **Model Builder** window, right-click **Piecewise 1 (pw1)** and select **Rename**
F2 is the shortcut key for renaming an item.

Change the name to **Vstep** and press **OK**

From the **Model Builder** window, select **Vstep (pw1)**

In the **Settings** window, under **Function**, enter “Vstep” into the **Function name** edit field

In the **Settings** window, under **Parameters**, enter “t” into the **Argument** edit field

In the **Settings** window, under **Parameters**, change **Smoothing** to **Continuous Function**

In the **Settings** window, under **Parameters**, enter “0.01” into the **Relative Size of Transition Zone** edit field

In the **Settings** window, under **Parameters**, enter the following into the **Intervals** table

Start	End	Function
0	0.01	0
0.01	1000	V

This creates the initial ramping up of the perfusate flow.

In the **Model Builder** window, right-click **Global Definitions** and choose

Functions>Piecewise

From the **Model Builder** window, right-click **Piecewise 2 (pw2)** and select **Rename**

Change the name to **cBstep** and press **OK**

From the **Model Builder** window, select **cBstep (pw2)**

In the **Settings** window, under **Function**, enter “cBstep” into the **Function name** edit field

In the **Settings** window, under **Parameters**, enter “t” into the **Argument** edit field

In the **Settings** window, under **Parameters**, change **Smoothing** to **Continuous Function**

In the **Settings** window, under **Parameters**, enter “0.01” into the **Relative size of transition zone** edit field

In the **Settings** window, under **Parameters**, enter the following into the **Intervals** table

Start	End	Function
0	250	c0B
250	500	1
500	1000	c0B

This creates a step function in the brain concentration. The “dip” constitutes a thought, i.e. more glucose is being consumed.

Modeling the System

From the **Model Builder** window, select **Geometry 1**

In the **Settings** window for Geometry, change the **Length Unit** from **m** to **μm**

From the **Model Builder** window, right-click **Geometry 1** and choose **Rectangle**

In the **Settings** window for Rectangle, enter the following dimensions:

Width: 85

Height: 3000

Base: Corner

r: 125

z: 0

From the **Model Builder** window, right-click **Geometry 1** and choose **Rectangle**
In the **Settings** window for Rectangle, enter the following dimensions:

Width: 40
Height: 3000
Base: Corner
r: 210
z: 0

From the **Model Builder** window, right-click **Geometry 1** and choose **Rectangle**
In the **Settings** window for Rectangle, enter the following dimensions:

Width: 50
Height: 3025
Base: Corner
r: 250
z: -25

From the **Model Builder** window, right-click **Geometry 1** and choose **Rectangle**
In the **Settings** window for Rectangle, enter the following dimensions:

Width: 300
Height: 50
Base: Corner
r: 0
z: -75

From the **Model Builder** window, right-click **Geometry 1** and choose **Boolean Operation>Union**

In the **Graphics** window, left-click on the right most rectangle (**r3**) (the domain should turn red) and then right-click the same rectangle (the domain should turn blue and is now added to the **Input objects** list in the **Settings** window). Repeat this step for **r4**, the lowest rectangle.

The **Input objects** list should now contain: **r3** and **r4**
Uncheck the **Keep interior boundaries** box

From the **Model Builder** window, select **Form Union**

In the **Settings** window for Finalize, select **Build Selected** (the light blue skyscraper with red box, near the top)

In the **Model Builder** window, minimize the **Geometry 1** menu (white downward arrow head next to **Geometry 1**)

You now have a 2D representation of the brain-probe system that will produce accurate results. The inner (left most) rectangle is the perfusate domain. Fluid will come in from the bottom and exit to top. The middle rectangle is the membrane. And the backwards-L-shaped domain is the brain. When solving, COMSOL will “wrap” this 2D section

around the $r=0$ axis (red dashed line) to form a 3D cylinder. We can use the 2D axisymmetric model because the system is angle independent. Now you will assign domain and boundary conditions to the geometry.

Perfusate Settings

From the **Model Builder** window, select **Creeping Flow**

In the **Settings** window, use the control button on your keyboard to simultaneously select the following **Domains**: 1, 3

Press the **Remove from Selection** button (light blue minus sign to the right of the selection field)

*You may have to scroll the **Settings** window over to see the button.*

In the **Settings** window, the **Domain Selection** list should now contain: 2

In the **Settings** window, under **Physical Model**, change **Compressibility** to **Incompressible flow**

Expand the **Creeping Flow** menu by clicking the rightward facing arrow next to Creeping Flow

From the **Model Builder** window, select **Creeping Flow>Fluid Properties 1**

In the **Settings** window, change **Density** to **User defined** and enter “rhoP” into the edit field (*do not include the quotation marks*)

In the **Settings** window, change **Dynamic viscosity** to **User defined** and enter “etaP” into the edit field

You have just assigned conditions of incompressible creep fluid flow to the probe. We do not do this for the other parts of the model because the brain and membrane do not contain fluid flow. The next step is assigning the boundary conditions governing the flow of the perfusate.

From the **Model Builder** window, right-click **Creeping Flow** and select **Inlet**

In the **Graphics** window, left-click the bottom boundary of **r1** (the perfusate domain) and then right-click

In the **Settings** window, the **Boundary Selection** list should now contain: 5

In the **Settings** window, under **Boundary Conditions**, change **Boundary Condition** to **Laminar inflow**

Under **Laminar Inflow**, select **Flow rate** and then enter “Vstep(t)” into the **V₀** edit field
The entry will remain orange, that is OK.

Enter “0” into the **L_{entr}** edit field and select the box next to **Constrain endpoints to zero**

From the **Model Builder** window, right-click **Creeping Flow** and select **Outlet**

In the **Graphics** window, left-click the top boundary of **r1** (the perfusate domain) and the right-click it

In the **Settings** window, the **Boundary Selection** list should now contain: 6

Minimize the **Creeping Flow** menu

Expand the **Transport of Diluted Species** menu

From the **Model Builder** window, right-click **Convection and Diffusion 1** and select **Rename**

Change the name to **Perfusate** and press **OK**

In the **Settings** window, under **Model Inputs**, change the **Velocity field** to **Velocity Field (spf/fp1)**

In the **Settings** window, under **Diffusion**, enter “DP” into the **Diffusion coefficient** edit field

From the **Model Builder** window, right-click **Initial Values 1** and select **Rename**

Change the name to **Initial Perf/Memb Values** and press **OK**

In the **Settings** window, under **Initial**, enter “c0P” into the **Concentration** edit field

From the **Model Builder** window, right-click **Transport of Diluted Species** and select **Inflow**

In the **Graphics** window, left-click the bottom boundary of **r1** (the perfusate domain) and then right-click

In the **Settings** window, the **Boundary Selection** list should now contain: 5

In the **Settings** window, under **Concentration**, enter “c0P” into the **c_{0,c}** edit field

From the **Model Builder** window, right-click **Transport of Diluted Species** and select **Outflow**

In the **Graphics** window, left-click the top boundary of **r1** (the perfusate domain) and the right-click it

In the **Settings** window, the **Boundary Selection** list should now contain: 6

Membrane Settings

From the **Model Builder** window, right-click **Transport of Diluted Species** and select **Convection and Diffusion**

From the **Model Builder** window, right-click **Convection and Diffusion 2** and select **Rename**

Change the name to **Membrane** and press **OK**

In the **Graphics** window, left-click the middle rectangle (**r2**) and then right-click it

In the **Settings** window, the **Boundary Selection** list should now contain: 3

In the **Settings** window, under **Diffusion**, enter “DM” into the **Diffusion coefficient** edit field

Brian Settings

From the **Model Builder** window, right-click **Transport of Diluted Species** and select **Convection and Diffusion**

From the **Model Builder** window, right-click **Convection and Diffusion 3** and select **Rename**

Change the name to **Brain** and press **OK**

In the **Graphics** window, left-click the backwards-L-shaped domain and then right-click it

In the **Settings** window, the **Boundary Selection** list should now contain: 1

In the **Settings** window, under **Diffusion**, enter “DB” into the **Diffusion coefficient** edit field

From the **Model Builder** window, right-click **Transport of Diluted Species** and select **Initial Values**

From the **Model Builder** window, right-click **Initial Values 2** and select **Rename**

Change the name to **Initial Brain Values** and press **OK**

In the **Graphics** window, left-click the backwards-L-shaped domain and then right-click it

In the **Settings** window, the **Boundary Selection** list should now contain: 1

In the **Settings** window, under **Initial**, enter “c0B” into the **Concentration** edit field

From the **Model Builder** window, right-click **Transport of Diluted Species** and select **Concentration**

In the **Graphics** window, alternatively left- and right-click the two right most and the lowest boundary and then right-click them (*the second right most boundary is small and at the bottom*)

In the **Settings** window, the **Boundary Selection** list should now contain: 2, 13 and 14

In the **Settings** window, under **Concentration**, select the box next to **Species c** and enter “cBstep(t)” into the $c_{0,c}$ edit field

The entry will remain orange, that is OK.

Minimize the **Transport of Diluted Species** menu

Mesh

Now you have set up all the physics governing the system. Next, a mesh must be created which COMSOL will solve the equations over and then solve the problem. Fortunately, COMSOL has suggested meshes for certain physics and geometries. The suggestion works for our case and is the default mesh; so you do not have to do anything.

From the **Model Builder** window, select **Mesh 1**

In the **Settings** window, make sure the **Sequencing type** reads **Physics-controlled mesh** and the **Element size** is **Normal**

Solving

In the **Settings** window, under **Study Settings**, enter “range(0,1,750)” into the **Times** edit field

From the toolbar, select **Compute** (green equal sign)

Postprocessing

COMSOL should automatically produce both 2D and 3D solutions which can be found in the Results tab in the Model Builder. If they are not automatically produced, follow the below directions as examples of possible result graphics.

To see the 2D velocity profile:

From the **Model Builder** window, right-click **Results** and select **2D Plot Group**

From the **Model Builder** window, right-click **2D Plot Group 1** and select **Rename**

Change the name to **Velocity** and press **OK**

From the **Model Builder** window, right-click **Velocity** and select **Surface**

In the **Settings** window, select **Plot** (rainbow and pencil at top)

Minimize the **Velocity** menu

To see the 3D velocity profile:

From the **Model Builder** window, right-click **Results** and select **3D Plot Group**

From the **Model Builder** window, right-click **3D Plot Group 1** and select **Rename**

Change the name to **Velocity** and press **OK**

From the **Model Builder** window, right-click **Velocity** and select **Surface**

In the **Settings** window, select **Plot** (rainbow and pencil at top)

Minimize the **Velocity** menu

To see the 2D concentration profile:

From the **Model Builder** window, right-click **Results** and select **2D Plot Group**
 From the **Model Builder** window, right-click **2D Plot Group 1** and select **Rename**
 Change the name to **Concentration** and press **OK**
 From the **Model Builder** window, right-click **Concentration** and select **Surface**
 In the **Settings** window, under **Expression**, select **Replace Expression** (green and orange triangles)
 Select **Transport of Diluted Species>Species c>Concentration (c)**
 In the **Settings** window, select **Plot** (rainbow and pencil at top)
 Minimize the **Concentration** menu

To see the 3D concentration profile:

From the **Model Builder** window, right-click **Results** and select **3D Plot Group**
 From the **Model Builder** window, right-click **3D Plot Group 1** and select **Rename**
 Change the name to **Concentration** and press **OK**
 From the **Model Builder** window, right-click **Concentration** and select **Surface**
 In the **Settings** window, under **Expression**, select **Replace Expression** (green and orange triangles)
 Select **Transport of Diluted Species>Species c>Concentration (c)**
 In the **Settings** window, select **Plot** (rainbow and pencil at top)
 Minimize the **Concentration** menu

To change which value of c0P is shown (for any graphic):

From the **Model Builder** window, select **Concentration**
 In the **Settings** window, under **Data**, select the desired **c0P** from the **Parameter Value** drop down menu
 In the **Settings** window, select **Plot** (rainbow pencil near top)

To find the concentration of glucose at the outlet of the Perfusate:

From the **Model Builder** window, right-click **Results>Derived Values** and select **Average>Line Average**
 In the **Graphics** window, left-click the top boundary of **r1** (the perfusate domain) and the right-click it
 In the **Settings** window, the **Boundary Selection** list should now contain: 6
 In the **Settings** window, under **Expression**, select **Replace Expression** (green and orange triangles)
 Select **Transport of Diluted Species>Species c>Concentration (c)**
 Select **Evaluate (New Table)** (orange equal sign at top)

Modeling Taylor Dispersion in MATLAB

```
%Damon Vinciguerra Thesis Taylor Dispersion
clc
clear all
close all
home

%% General Parameters
V = 1.67e-11; % m^3/s, Volumetric flow rate of dialysate
L = 2; % m, Length of tubing
R = 0.0001075; % m, inner radius of tubing
eta = 7.28e-4; % Pa*s, viscosity of perfusate
D = 8.3e-10; % m^2/s, diffusivity of glucose through
perfusate
vzavg = V/(pi*R^2); % m/s, Velocity of dialysate

K = D+((R*vzavg)^2)/(48*D); % m^2/s, mass transfer coefficient
Re = vzavg*2*R*990/eta; % Reynolds number
Per = R*vzavg/D; % Peclet number, radial
Pea = L*vzavg/K; % Peclet number, axial

%% Domains - Boltzmann Sigmoidal
ex = 1000; % s, Excess on ends to cushion test
tth = 250; % s, Duration of thought
tfin = ex + tth + ex; % s, Total time of simulation
ts = 100000; % Time steps
tD = linspace(0,tfin/2+1,ts/2); % s, Domain for concentration drop
dt = tD(2)-tD(1);
tI = linspace(tfin/2+dt,tfin,ts/2); % s, Domain for concentration
increase
t = [tD tI];
Dt50 = ex ; % s, Time at which drop is half way between T
and B
It50 = ex + tth; % s, Time at which increase is half way
between B and T

z1 = Dt50*vzavg;
z2 = It50*vzavg;
tout=L/vzavg;

%% Signal - Boltzmann Sigmoidal Approximation
T = 0.6826; % mM, Upper limit (Normal dialysate
concentration)
B = 0.6217; % mM, Lower limit (Affected dialysate
concentration)
m = 6.6; % mM/s, slope at t50

xD = B+((T-B)./(1+exp((Dt50-tD)./(-m)))); % mM, Signal for drop
xI = B+((T-B)./(1+exp((It50-tI)./m))); % mM, Signal for
dincrease
x = [xD xI];

subplot(2,2,1)
```

Modeling Taylor Dispersion in MATLAB

```

plot(t,x)
ylabel('x(t)', 'FontSize',12)
xlabel('Time (s)', 'FontSize',12)
title('Signal: x(t)', 'FontSize',12)
axis([0 tfin .6 .7])

%% Smearing function: (1/sqrt(4*pi*k*t))*exp(L)
sig2 = 2.*K.*tout; % Square of standard deviation
sig = sqrt(sig2); % Standard deviation
Ng = 1001;
N = (Ng-1)/2;
dy = 10*sig/Ng; % Number of points to trace out the curve (+/-
5*sig)

zf = dy*(-N:N); % time base for smearing
function
f = exp(-((-zf).^2)./(2.*sig2))./(sqrt(2.*pi.*sig2)); % smearing
function, Normal Distribution

subplot(2,2,2)
plot(zf,f)
xlabel('z-y', 'FontSize',12)
ylabel('f(z)', 'FontSize',12)
title('Smearing function: f(z)', 'FontSize',12)

%% Compute convolution - Boltzmann Sigmoidal
Nz = round(vzavg*tfin/dy);
zz = dy*(0:Nz);
mz = m*vzavg; % mM/m, slope at t50

zzD = zz(1:floor(end/2));
zzI = zz(floor(end/2)+1:end);
xsD = B+((T-B)./(1+exp((z1-zzD)./-mz))); % mM, Signal for drop
xsI = B+((T-B)./(1+exp((z2-zzI)./mz))); % mM, Signal for
dincrease
xs = [xsD xsI];

xc = conv(xs,f,'full'); % Convolution of signal with smearing
function
tc = dy*(0:length(xc)-1);
tau = dy*length(f)/2; % offset for filter width

g = (tc-tau)./vzavg;
y = xc/max(xc)*max(x);

subplot(2,1,2)
plot(t,x,'b',g(2*N:end-(2*N-1)),y(2*N:end-(2*N-1)), '--r')
axis([0 tfin .6 .7])
ylabel('y(t)', 'FontSize',12)
xlabel('Time (s)', 'FontSize',12)
title('Output signal: y(t) = f(z/v)*x(t)', 'FontSize',12)
legend('Signal', 'Output', 'Location', 'SouthEast')

```

```

%% Width of dispersion in signal
er = 0.1; % Allowable deviation from steady state

if min(x) < B + (T-B)*er
    sigD = T;
    k = 0;
    while sigD > T - (T-B)*er
        k = k + 1;
        sigD = xD(k);
    end
    tDsT = tD(k);

    while sigD > B + (T-B)*er
        k = k + 1;
        sigD = xD(k);
    end
    tDsB = tD(k);

    wsig = tDsB - tDsT; % Width of signal change
    disp(['width of signal- ', num2str(wsig), ' s (', num2str(wsig/60), '
min)'])
else
    sigD = T;
    k = 0;
    while sigD > T - (T-B)*er
        k = k + 1;
        sigD = xD(k);
    end
    tDsT = tD(k);
    tDsB = tfin/2;

    wsig = tDsB - tDsT; % Width of signal change
    disp(['width of signal- ', num2str(wsig), ' s (', num2str(wsig/60), '
min)'])
end
%% Width of Output
if min(y(2*N:end-(2*N-1))) < B + (T-B)*er
    testD = T;
    k = 2*N;
    while testD > T - (T-B)*er
        k = k + 1;
        testD = y(k);
    end
    tDoT = g(k);

    while testD > B + (T-B)*er
        k = k + 1;
        testD = y(k);
    end
    tDoB = g(k);

```

Modeling Taylor Dispersion in MATLAB

```

wout = tDoB - tDoT; % Width of output
disp(['Width of Output- ', num2str(wout), ' s (', num2str(wout/60), '
min)'])
else
    testD = T;
    k = 2*N;
    while testD > T - (T-B)*er
        k = k + 1;
        testD = y(k);
    end
    tDoT = g(k);
    tDoB = tfin/2;

    wout = tDoB - tDoT; % Width of output
    disp(['Width of Output- ', num2str(wout), ' s (', num2str(wout/60), '
min)'])
end
%% Extent of Broadening
disp(' ')
disp(['Increase in width- ', num2str(wout-wsig), ' s (', num2str((wout-
wsig)/60), ' min)'])

%% Describing Broadenings
mTextBox = uicontrol('style','text');
set(mTextBox, 'String', ['Width- ', num2str(wsig), '
s'], 'Position', [99, 256, 150, 17], 'FontSize', 10)
nTextBox = uicontrol('style','text');
set(nTextBox, 'String', ['Width- ', num2str(wout), '
s'], 'Position', [80, 55, 150, 17], 'FontSize', 10)

%% Fitting Output
[coefffD, rD] = fit(g(2*N:floor(end/2)), y(2*N:floor(end/2)), 'a + (b -
a) ./ (1 + exp((h - x)/m))', 'start', [0.62 0.68 1100 -6.6]);
[coefffI, rI] = fit(g(floor(end/2)+1:end-(2*N-1)), y(floor(end/2)+1:end-
(2*N-1)), 'a + (b - a) ./ (1 + exp((h - x)/m))', 'start', [0.62 0.68 1900
6.6]);

```

Plotting Dispersion Along Length of Tubing in MATLAB

```
%Damon Vinciguerra Thesis Taylor Dispersion
clc
clear all
close all
home

%% General Parameters
V = 1.67e-11; % m^3/s, Volumetric flow rate of dialysate
R = 0.0001075; % m, inner radius of tubing
eta = 7.28e-4; % Pa*s, viscosity of perfusate
D = 8.3e-10; % m^2/s, diffusivity of glucose through
perfusate
vzavg = V/(pi*R^2); % m/s, Velocity of dialysate

K = D+((R*vzavg)^2)/(48*D); % mass transfer coefficient
Re = vzavg*2*R*990/eta; % Reynolds number
Per = R*vzavg/D; % Peclet number, radial

%% Domains - Boltzmann Sigmoidal
ex = 1000; % s, Excess on ends to cushion test
tth = 250; % s, Duration of thought
tfin = ex + tth + ex; % s, Total time of simulation
ts = 100000; % Time steps
tD = linspace(0,tfin/2+1,ts/2); % s, Domain for concentration drop
dt = tD(2)-tD(1);
tI = linspace(tfin/2+dt,tfin,ts/2); % s, Domain for concentration
increase
t = [tD tI];
Dt50 = ex ; % s, Time at which drop is half way between T
and B
It50 = ex + tth; % s, Time at which increase is half way
between B and T

z1 = Dt50*vzavg;
z2 = It50*vzavg;

%% Signal - Boltzmann Sigmoidal Approximation
T = 0.6826; % mM, Upper limit (Normal dialysate
concentration)
B = 0.6217; % mM, Lower limit (Affected dialysate
concntration)
m = 6.6; % mM/s, slope at t50

xD = B+((T-B)./(1+exp((Dt50-tD)./-m))); % mM, Signal for drop
xI = B+((T-B)./(1+exp((It50-tI)./m))); % mM, Signal for
dincrease
x = [xD xI];

%%
o = 0;
for L = 0.01:0.01:2
    o = o + 1;
```

Plotting Dispersion Along Length of Tubing in MATLAB

```

%% Smearing function:  $(1/\sqrt{4\pi kt}) \cdot \exp(L/vz_{avg})$ 
tout=L/vzavg;
sig2 = 2.*K.*tout;           % Square of standard deviation
sig = sqrt(sig2);           % Standard deviation
Ng = 1001;
N = (Ng-1)/2;
dy = 10*sig/Ng;           % Number of points to trace out the curve (+/-
5*sig)

zf = dy*(-N:N);           % time base for
smearing function
f = exp(-((-zf).^2)./(2.*sig2))./sqrt(2.*pi.*sig2);           % smearing
function, Normal Distribution

%% Compute convolution - Boltzmann Sigmoidal
Nz = round(vzavg*tfin/dy);
zz = dy*(0:Nz);
mz = m*vzavg;           % mM/m, slope at t50

zzD = zz(1:floor(end/2));
zzI = zz(floor(end/2)+1:end);
xsD = B+((T-B)./(1+exp((z1-zzD)./mz)));           % mM, Signal for
drop
xsI = B+((T-B)./(1+exp((z2-zzI)./mz)));           % mM, Signal for
dincrease
xs = [xsD xsI];

xc = conv(xs,f,'full');           % Convolution of signal with
smearing function
tc = dy*(0:length(xc)-1);
tau = dy*length(f)/2;           % offset for filter width

g = (tc-tau)./vzavg;
y = xc/max(xc)*max(x);

%% Width of Dispersion
er = 0.001;           % Allowable deviation from steady
state

if min(y(2*N:end-(2*N-1))) < B + (T-B)*er
    testD = T;
    k = 2*N;

    while testD > T - (T-B)*er
        k = k + 1;
        testD = y(k);
    end
    tDoT = g(k);

    while testD > B + (T-B)*er
        k = k + 1;

```

Plotting Dispersion Along Length of Tubing in MATLAB

```

testD = y(k);
end
tDoB = g(k);

wdis(o) = tDoB - tDoT;           % Width of output
else
testD = T;
k = 2*N;
while testD > T - (T-B)*er
    k = k + 1;
    testD = y(k);
end
tDoT = g(k);

wdis(o) = tfin/2 - tDoT;
end

%% Width of Readable Signal
if min(y(2*N:end-(2*N-1))) < B + (T-B)*er
    testS = T;
    k = 2*N;

    while testS > B + (T-B)*er
        k = k + 1;
        testS = y(k);
    end
    tSoU = g(k);
    k = k + 1;

    while testS < B + (T-B)*er
        k = k + 1;
        testS = y(k);
    end
    tSoB = g(k);

    wsig(o) = tSoB - tSoU;       % Width of output
else
    wsig(o) = 0;
end

%% Plotting
plot(t,x,'--b',g(2*N:end-(2*N-1)),y(2*N:end-(2*N-1)),'r')
axis([0 tfin .6 .7])
ylabel('Concentration (mM)','FontSize',12)
xlabel('Time (s)','FontSize',12)
title('Comparison of Output (-) to Signal (- -)','FontSize',12)
format short
nTextBox = uicontrol('style','text');
set(nTextBox,'String',['Distance Along Tube- ',num2str(L,3),' m',
'Width of Deviation- ',num2str(wsig(o)/60),' min'],
'Position',[200,55,180,34],'FontSize',10)
drawnow
end

```


Plotting Dispersion Along Length of Tubing in MATLAB

```
title('Comparison of Output to Signal','FontSize',12)
legend('Signal','Output')

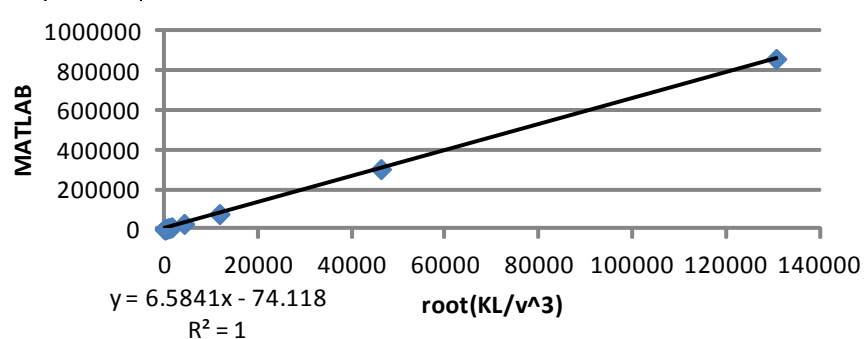
figure(2)
plot(0.005:0.005:1,wsig./tth)
title('Width of True Signal Concentration over Tube Length')
xlabel('Length of Tubing (%)')
ylabel('Width of Signal (% of initial)')

figure(3)
plot(0.005:0.005:1,wdis)
title('Dispersion of Signal "Step" over Length of Tubing')
xlabel('Length of Tubing (%)')
ylabel('Extent of Broadening (s)')
```

Appendix J

115

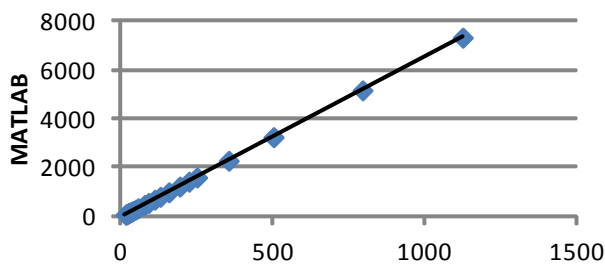
Data for the Vinciguerra number

	Fitting Dispersion Time			
Change	Varying V			
	root(KL/v^3)	MATLAB (s)	Approximation (s)	Error
/1000	130600	859829.6813	848850	-1%
/500	46179	303969.4128	300113.5	-1%
/200	11692	76748.5314	75948	-1%
/100	4145	27170.9758	26892.5	-1%
/50	1481.5	9693.9621	9579.75	-1%
/40	1068.6	6975.5339	6895.9	-1%
/30	705.9237	4586.9504	4538.50405	-1%
/20	402.0771	2586.355	2563.50115	-1%
/10	172.2414	1073.3724	1069.5691	0%
/5	91.8576	546.7489	547.0744	0%
/2	51.5636	283.2164	285.1634	1%
Nominal	35.5131	179.6789	180.83515	1%
*1.5	29.0834	138.6134	139.0421	0%
*2	25.154	114.1767	113.501	-1%
*5	15.8862	58.2856	53.2603	-9%
*10	11.231	33.1067	23.0015	-31%
*20	7.9411	17.7541	1.61715	-91%
*30	6.4838	12.0651	-7.8553	-165%
*40	5.6151	9.1429	-13.50185	-248%
*50	5.0223	7.3781	-17.35505	-335%
*100	3.5513	3.7038	-26.91655	-827%
*200	2.5112	1.8434	-33.6772	-1927%
*500	1.5882	0.74472	-39.6767	-5428%
*1000	1.123	0.3528	-42.7005	-12203%
	Line of best fit for highlighted data			
	slope	6.491702447		
	y-intercept	-47.58237584		
	r-squared	0.999866556		
				

Appendix J

116

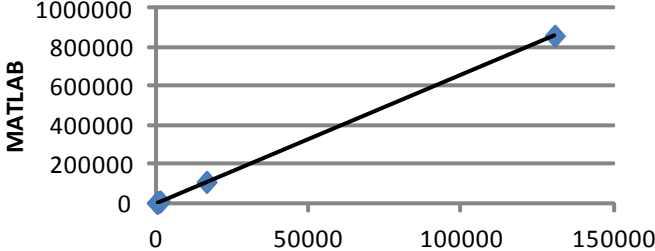
Data for the Vinciguerra number

Change	Fitting Dispersion Time			
	Varying Dp			
	root(KL/v^3)	MATLAB (s)	Approximation (s)	Error
/1000	1123	7333.5959	7249.5	-1%
/500	794.0978	5168.0614	5111.6357	-1%
/200	502.2316	3246.5162	3214.5054	-1%
/100	355.1315	2277.4571	2258.35475	-1%
/50	251.1164	1592.6579	1582.2566	-1%
/40	224.6057	1418.1205	1409.93705	-1%
/30	194.5149	1220.013	1214.34685	0%
/20	158.8222	985.025	982.3443	0%
/10	112.31	680.3912	680.015	0%
/5	79.4312	465.709	466.3028	0%
/2	50.308	274.8694	277.002	1%
Nominal	35.7525	181.3065	182.39125	1%
*1.5	29.4342	141.0439	141.3223	0%
*2	25.7818	117.8387	117.5817	0%
*5	18.3715	73.0282	69.41475	-5%
*10	17.2241	66.14	61.95665	-6%
*20	20.1039	83.3603	80.67535	-3%
*30	23.5308	103.9178	102.9502	-1%
*40	26.7159	123.928	123.65335	0%
*50	29.6309	142.3915	142.60085	0%
*100	41.4505	218.1099	219.42825	1%
*200	58.4582	328.3564	329.9783	0%
*500	92.3589	548.7221	550.33285	0%
*1000	130.6007	801.0696	798.90455	0%
	Line of best fit for highlighted data			
	slope	6.47294151		
	y-intercept	-48.21067885		
	r-squared	0.999913226		
				
y = 6.5747x - 54.345 R ² = 1				

Appendix J

117

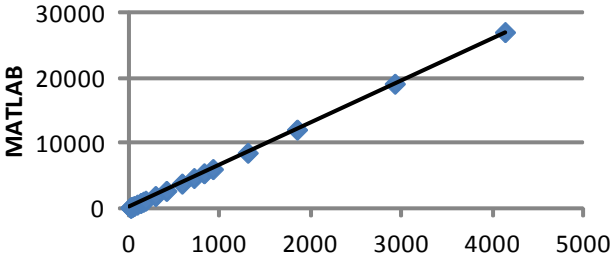
Data for the Vinciguerra number

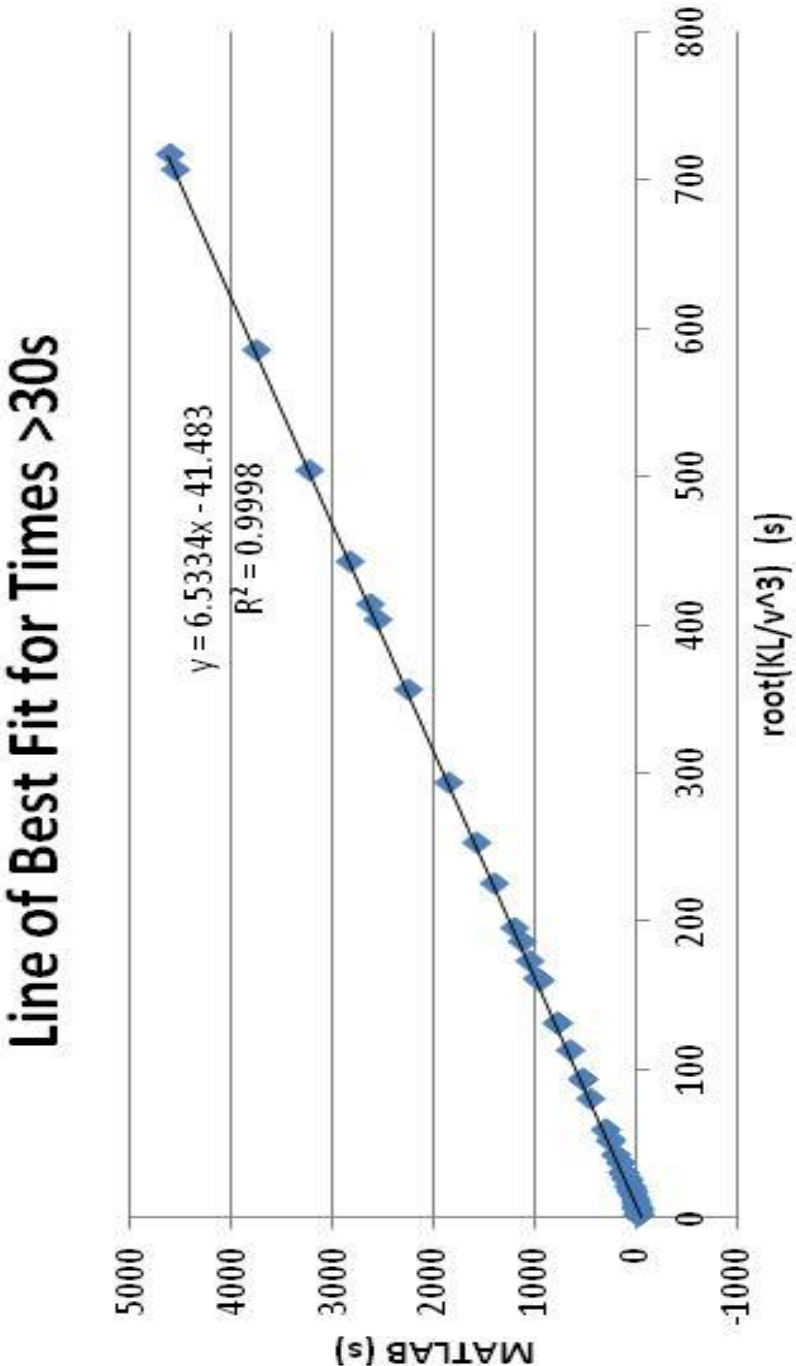
	Fitting Dispersion Time			
Change	Varying R			
	root(KL/v^3)	MATLAB (s)	Approximation (s)	Error
/1000		-		
/500		-		
/200		-		
/100		-		
/50		-		
/40		-		
/30		-		
/20	0.0166	0.013884	-49.8921	-359450%
/10	0.1311	0.020063	-49.14785	-245068%
/5	1.0457	0.33116	-43.20295	-13146%
/2	16.3269	60.9197	56.12485	-8%
Nominal	130.6007	801.6732	798.90455	0%
*1.5	440.7684	2841.864	2814.9946	-1%
*2	1044.8	6818.4451	6741.2	-1%
*5	16324	107414.894	106056	-1%
*10	130600	859798	848850	-1%
*20		-		
*30		-		
*40		-		
*50		-		
*100		-		
*200		-		
*500		-		
*1000		-		
	Line of best fit for highlighted data			
	slope	6.58374287		
	y-intercept	-41.17147965		
	r-squared	0.999999993		
	 <p>$y = 6.5839x - 57.029$ $R^2 = 1$</p>			

Appendix J

118

Data for the Vinciguerra number

	Fitting Dispersion Time			
Change	Varying L			
	root(KL/v^3)	MATLAB (s)	Approximation (s)	Error
/1000	4.13	5.6983	-23.155	-506%
/500	5.8406	10.5501	-12.0361	-214%
/200	9.2349	24.1517	10.02685	-58%
/100	13.0601	43.3256	34.89065	-19%
/50	18.4697	74.1218	70.05305	-5%
/40	20.6498	87.0355	84.2237	-3%
/30	23.8443	106.7504	104.98795	-2%
/20	29.2032	140.1012	139.8208	0%
/10	41.2996	217.7352	218.4474	0%
/5	58.4064	327.8266	329.6416	1%
/2	92.3487	550.5992	550.26655	0%
Nominal	130.6007	801.6732	798.90455	0%
*1.5	159.9526	993.0704	989.6919	0%
*2	184.6973	1158.8906	1150.53245	-1%
*5	292.0321	1862.636	1848.20865	-1%
*10	412.9958	2659.0186	2634.4727	-1%
*20	584.0642	3785.2736	3746.4173	-1%
*30	715.3296	4639.3733	4599.6424	-1%
*40	825.9915	5378.0388	5318.94475	-1%
*50	923.4866	6019.9124	5952.6629	-1%
*100	1306	8538.2952	8439	-1%
*200	1847	12099.8264	11955.5	-1%
*500	2920.3	19166.3746	18931.95	-1%
*1000	4130	27130.2003	26795	-1%
	Line of best fit for highlighted data			
	slope	6.571225023		
	y-intercept	-55.80755791		
	r-squared	0.999997394		
	 <p>$y = 6.5819x - 56.31$ $R^2 = 1$</p>			



Appendix J

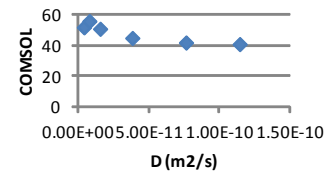
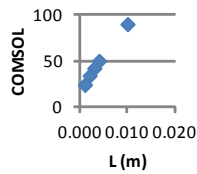
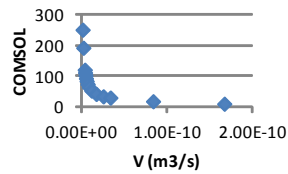
120

Data for the Vinciguerra number

Fitting Time to Steady-State in Probe

Data

V			L		D		
Change	V (m3/s)	COMSOL (s)	L (m)	COMSOL (s)	Change	D (m2/s)	COMSOL (s)
/50	1.67E-14	-	0.010	90	/30	2.54E-12	-
/20	8.35E-13	252	0.004	50	/20	3.81E-12	52
/10	1.67E-12	193	0.003	42	/10	7.62E-12	56
/5	3.34E-12	121	0.002	34	/5	1.52E-11	51
/4.5	3.71E-12	112	0.001	24	/2	3.81E-11	45
/4	4.18E-12	103			Nominal	7.62E-11	42
/3.5	4.77E-12	93			*1.5	1.14E-10	41
/3	5.57E-12	84			*2	1.52E-10	40
/2.5	6.68E-12	74			*5	3.81E-10	39
/2	8.35E-12	64			*10	7.62E-10	38
/1.5	1.11E-11	53			*20	1.52E-09	38
Nominal	1.67E-11	42			*30	2.29E-09	38
*1.5	2.51E-11	34			*40	3.05E-09	38
*2	3.34E-11	30			*50	3.81E-09	38
*5	8.35E-11	18			*100	7.62E-09	37
*10	1.67E-10	10			*200	1.52E-08	37
					*500	3.81E-08	37
					*1000	7.62E-08	36



121

Multilinear Regression										
All three parameters (L, v _z , D) and assessed individually										
Real Time	Data from above				Processed for MATLAB				Results	
COMSOL (s)	V (m ³ /s)	L (m)	D (m ² /s)	1/root(v _z)	L	1/root(D)	Constant	Approximation (s)	Deviation	
V	252	8.35E-13	0.003	7.62E-11	327.3135068	0.003	114557.23	1	2.60E+02	3%
	193	1.67E-12	0.003	7.62E-11	231.4456002	0.003	114557.23	1	1.78E+02	-8%
	121	3.34E-12	0.003	7.62E-11	163.6567534	0.003	114557.23	1	1.21E+02	0%
	112	3.71111E-12	0.003	7.62E-11	155.2584286	0.003	114557.23	1	1.14E+02	2%
	103	4.175E-12	0.003	7.62E-11	146.3790502	0.003	114557.23	1	1.06E+02	3%
	93	4.77143E-12	0.003	7.62E-11	136.9250636	0.003	114557.23	1	9.81E+01	5%
	84	5.56667E-12	0.003	7.62E-11	126.7679761	0.003	114557.23	1	8.95E+01	7%
	74	6.68E-12	0.003	7.62E-11	115.7228001	0.003	114557.23	1	8.01E+01	8%
	64	8.35E-12	0.003	7.62E-11	103.505619	0.003	114557.23	1	6.97E+01	9%
	53	1.11333E-11	0.003	7.62E-11	89.63849553	0.003	114557.23	1	5.79E+01	9%
	42	1.67E-11	0.003	7.62E-11	73.18952512	0.003	114557.23	1	4.39E+01	5%
	34	2.505E-11	0.003	7.62E-11	59.75899702	0.003	114557.23	1	3.25E+01	-4%
	30	3.34E-11	0.003	7.62E-11	51.75280952	0.003	114557.23	1	2.57E+01	-14%
	18	8.35E-11	0.003	7.62E-11	32.73135068	0.003	114557.23	1	9.55E+00	-47%
10	1.67E-10	0.003	7.62E-11	23.14456002	0.003	114557.23	1	1.40E+00	-86%	
L	90	1.67E-11	0.01	7.62E-11	73.18952512	0.01	114557.23	1	9.29E+01	3%
	50	1.67E-11	0.004	7.62E-11	73.18952512	0.004	114557.23	1	5.09E+01	2%
	34	1.67E-11	0.002	7.62E-11	73.18952512	0.002	114557.23	1	3.69E+01	9%
	24	1.67E-11	0.001	7.62E-11	73.18952512	0.001	114557.23	1	2.99E+01	25%
D	56	1.67E-11	0.003	7.62E-12	73.18952512	0.003	362261.78	1	5.63E+01	1%
	51	1.67E-11	0.003	1.524E-11	73.18952512	0.003	256157.76	1	5.10E+01	0%
	45	1.67E-11	0.003	3.81E-11	73.18952512	0.003	162008.39	1	4.63E+01	3%
	41	1.67E-11	0.003	1.143E-10	73.18952512	0.003	93535.59	1	4.29E+01	5%
	40	1.67E-11	0.003	1.524E-10	73.18952512	0.003	81004.20	1	4.23E+01	6%
	39	1.67E-11	0.003	3.81E-10	73.18952512	0.003	51231.55	1	4.08E+01	5%
	38	1.67E-11	0.003	7.62E-10	73.18952512	0.003	36226.18	1	4.00E+01	5%
	38	1.67E-11	0.003	1.524E-09	73.18952512	0.003	25615.78	1	3.95E+01	4%
	38	1.67E-11	0.003	2.286E-09	73.18952512	0.003	20915.19	1	3.93E+01	3%
	38	1.67E-11	0.003	3.048E-09	73.18952512	0.003	18113.09	1	3.91E+01	3%
	38	1.67E-11	0.003	3.81E-09	73.18952512	0.003	16200.84	1	3.90E+01	3%
	37	1.67E-11	0.003	7.62E-09	73.18952512	0.003	11455.72	1	3.88E+01	5%
	37	1.67E-11	0.003	1.524E-08	73.18952512	0.003	8100.42	1	3.86E+01	4%
	37	1.67E-11	0.003	3.81E-08	73.18952512	0.003	5123.16	1	3.85E+01	4%
	36	1.67E-11	0.003	7.62E-08	73.18952512	0.003	3622.62	1		